Functional characterization and analysis of the *ARABIDOPSIS CRINKLY 4* promoter

Inaugural-Dissertation

zur Erlangung des Doktorgrades
der Mathematisch-Naturwissenschaftlichen Fakultät
der Heinrich-Heine-Universität Düsseldorf

vorgelegt von

Adrian Hülsewede

aus Duisburg

Düsseldorf, Januar 2016

aus dem Institut für Entwicklungsgenetik

der Heinrich-Heine-Universität Düsseldorf

Gedruckt mit der Genehmigung der
Mathematisch-Naturwissenschaftlichen Fakultät der

Heinrich-Heine-Universität Düsseldorf

Referent: Professor Dr. Rüdiger Simon

Korreferent: Professor Dr. Michael Feldbrügge

Tag der mündlichen Prüfung:

This thesis is part of a manuscript in preparation.

Index

1 Introduction

1.1 Meristems

Postembryonic Growth and development of seed plants (*Spermatophytina*) depend on the activity of meristems which are undifferentiated (meristematic) small cells located in defined zones of the plant body (Nägeli et al., 1858). The two primary meristems of *Arabidopsis thaliana* are located at opposing poles of the seedling and are established during embryogenesis (Barton and Poethig, 1993; Dolan et al., 1993). Because of their position they are often referred to as apical meristems. From the shoot apical meristem (SAM) all above ground tissues, such as stem, leaves and inflorescences are formed, while the root apical meristem (RAM) gives rise to the root system (Dolan et al., 1993; Leyser and Furner, 1992). Meristems contain stem cells, which can divide indefinitely during the whole lifespan of the organism and are controlled by signals coming from the stem cell niche. The stem cell niche can be defined as the entire amount of cells communicating with the stem cells to maintain them in an undifferentiated state and influencing their fate (Schofield, 1977). Since a stem cell niche is based on signaling molecules such as transcription factors and phytohormones, it is not necessarily a defined physical location but rather a microenvironment. This microenvironment can also be created *in vitro* to transform differentiated cells into stem cell-like callus cells, from which a complete plant can be regenerated (Nagata and Takebe, 1971; Steward et al., 1958).

In the apical meristems of *A. thaliana*, organizing centers are adopting many functions of the stem cell niche. In the SAM the organizing center consists of cells located below the stem cells and in the RAM the organizing center is located within the stem cell pool (Figure 1 A + B). Although different in their organization they both control stem cell fate through similar mechanisms, partly involving related genes. In the SAM cell to cell communication occurs between the organizing center and the stem cell pool, thereby balancing the stem cell amount and preventing stem cell consumption or stem cell over-proliferation (see chapter 1.2) (Figure 1 A). In the RAM however, no communication feedback from the stem cells to the organizing center was discovered so far, but differentiated cells of the root tip are communicating with their stem cells (see chapter 1.6) (Figure 1B). Thus stem cell maintenance, at least in the distal part of the root, is achieved by signals from the organizing center and by signals coming from differentiated daughter cells. Asymmetric cell division is a further feature of stem cells. This division gives rise to a new stem cell and to a daughter cell, which may directly differentiate or further divide a finite number of times before differentiation (Stahl and Simon, 2005) (Figure 1C). The latter cell is referred to as transit amplifying cell. Differentiation is generally accompanied by cell enlargement, change of gene expression and cell specialization (Kadereit et al., 2014).

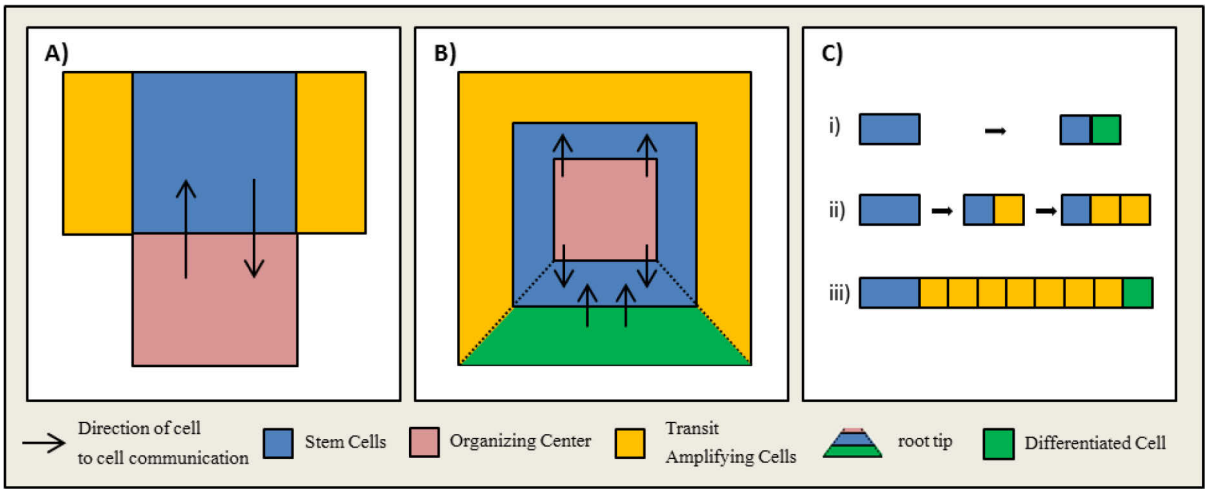

Figure 1 Communication within the apical meristems of *A. thaliana* and scheme of asymmetric cell division

A) In the SAM, communication between the organizing center (pink) and the stem cell pool (blue) is bi-directional. Transit amplifying cells (yellow) seem not to be involved in stem cell maintenance.

B) In the RAM, the organizing center signals to its surrounding stem cells. This signaling seems to be uni-directional. The stem cells in the root tip (colored trapeze) additionally receive signals from their distal daughter cells.

C) i) When a stem cell undergoes asymmetric cell division, one daughter cell remains as a stem cell whereas the other daughter cell will differentiate (green). ii + iii) Often this will not happen directly after cell division, but after several rounds of further mitotic divisions. These daughter cells are referred to as transit amplifying cells.

1.2 Organization of the SAM and factors controlling stem cell homeostasis (principles)

After germination of *A. thaliana*, the SAM can be found between the two cotyledons of the seedling. From this meristem the first postembryonic leafs and all other above ground organs will develop. The SAM is a dome shaped structure of undifferentiated small cells in which different zones and layers can be appointed (Figure 2) (Leyser and Furner, 1992). The first two cell layers (L1 and L2) are named tunica and are dividing preferentially anticlinal (Satina et al., 1940; Schmidt, 1924). The third layer (L3) is referred to as corpus and cell divisions occurs in anticlinal, periclinal and oblique orientation. The slowly dividing stem cells are located in the central zone and can undergo asymmetric cell division. Descendants of transit amplifying cells are displaced to the peripheral zone where they form organ primordia and eventually differentiate. In a longitudinal section, the organizing center is located proximal to the central zone. Stem cells of the central zone are expressing *CLAVATA 3* (*CLV3*), encoding a small signaling peptide which is processed from a 96 amino acids (aa) long preproprotein containing a signal sequence which directs the protein to the apoplast (Sharma et al., 2003). The mature CLV3 glycopeptide consists of 13 aa and is post-translationally arabinosylated (Ohyama et al., 2009). CLV3 acts non cell autonomously through its receptors CLAVATA1 (CLV1), CLAVATA2-CORYNE (CLV2-CRN) and RECEPTOR-LIKE PROTEIN KINASE 2 (RPK2) to repress stem cell proliferation [reviewed in (Barton, 2010)] by repressing the homeodomain transcription factor *WUSCHEL* (*WUS*) on transcriptional

level (Brand et al., 2000; Müller et al., 2006; Reddy and Meyerowitz, 2005). *WUS* is expressed in the organizing center and directly promotes *CLV3* expression in the stem cells, thereby providing a feedback loop (Daum et al., 2014; Mayer et al., 1998). Thus, WUS, which is promoting stem cell proliferation, activates its own repression through the CLAVATA-pathway in a negative feedback loop (Figure 3).

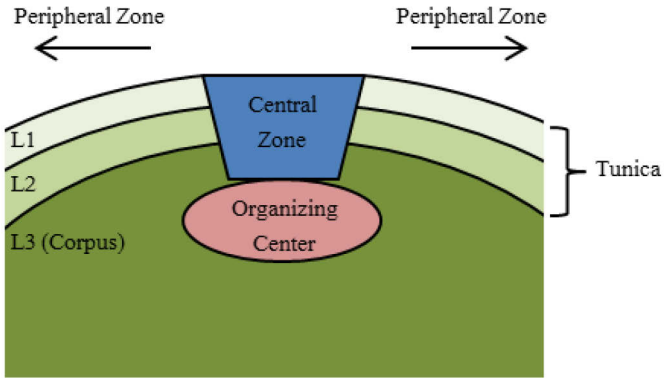

Figure 2 Organization of the SAM (scheme of a longitudinal section)
Stem cells are located in the central zone (blue) and its descendants are displaced to the peripheral zone (arrows) where they form organ primordia. The organizing center (pink) is located proximal to the central zone. The first two outer cell layers (L1 and L2) are referred to as tunica and the tissue proximal to L2 is referred to as L3 which builds the corpus.

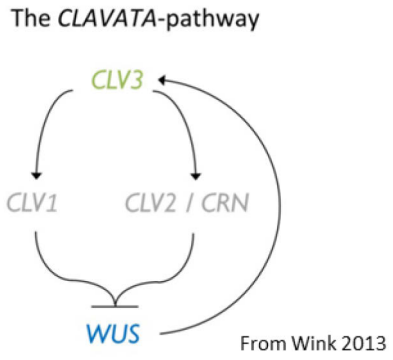

Figure 3 The CLAVATA-pathway
The CLAVATA-pathway controls stem cell maintenance in the SAM. CLV3, a small secreted peptide expressed in the central zone moves to the organizing center where it is signaling, through its receptors CLV1 and CLV2/CRN, to repress *WUS*. The transcription factor WUS moves to the central zone to directly promote *CLV3* expression. Picture taken from Wink 2013.

1.3 Organization of the RAM

During germination of *A. thaliana,* the embryonic root, referred to as radicula, penetrates through the seed coat and grows along the gravitation axis towards the soil. The different tissues of the root concentrically surround the central cylinder (stele, consisting of: vasculature, procambium and the pericycle) and are referred to (from the inside to the outside) as, endodermis, cortex and epidermis or rhizodermis [reviewed in (Stahl and Simon, 2005)]. The RAM, giving rise to these tissues, is located at the tip of the growing root (Figure 4). It can be divided into 3 zones through which the new daughter cells transit on their way to differentiation (Dolan et al., 1993): First, the meristematic zone, where the stem cells (in the RAM referred to as initials) are located, rapid cell division of the newly produced daughter cells takes place and which is overlaid by the root cap. Second, the elongation zone, where growth of the root mainly relies on elongation of the young daughter cells, and third, the differentiation zone, where the cells acquire final cell fate, e.g. epidermis cells differentiate to root hair and non-root hair cells. Depending on the relative position towards the quiescent center (QC) on the proximal-distal

axis, the meristematic zone can be further divided into the proximal root meristem (PRM) and the distal root meristem (DRM). The PRM consists of the initials and their daughter cells proximal to the QC, which will differentiate into the ground tissue (endodermis and cortex) and into the stele (pericycle, phloem, xylem and procambium). The DRM consists of the initials and their daughter cells producing the root cap (columella and lateral root cap). The epidermis of the root is derived from stem cells of the distal root meristem located distolateral to the organizing center. These initials are producing two different tissues and are referred to as lateral root cap (LRC)/ epidermis initials. Whereas from periclinal divisions the LRC is formed which belongs to the DRM, from anticlinal divisions the epidermis is produced which belongs to the PRM.

The initials of the root meristem concentrically surround the four cells of the organizing center, which is referred to as quiescent center (QC) (Figure 4). The QC signals to its surrounding initials to maintain them in an undifferentiated state (Van den Berg et al., 1997). Each stem cell gives rise to a specific type of cell, depending on the relative position of the stem cells towards each other and the QC (Dolan et al., 1993). Although the tissues of the root are arranged in cell files and each cell file can be traced back to a single type of initial, the fate of a cell is determined by signals from the neighboring cells and tissues rather than its clonal origin (van den Berg et al., 1995). This indicates a complex regulatory signaling network, which controls the balance between stem cell maintenance and differentiation, and also specifies the identity of the stem cell daughter cells.

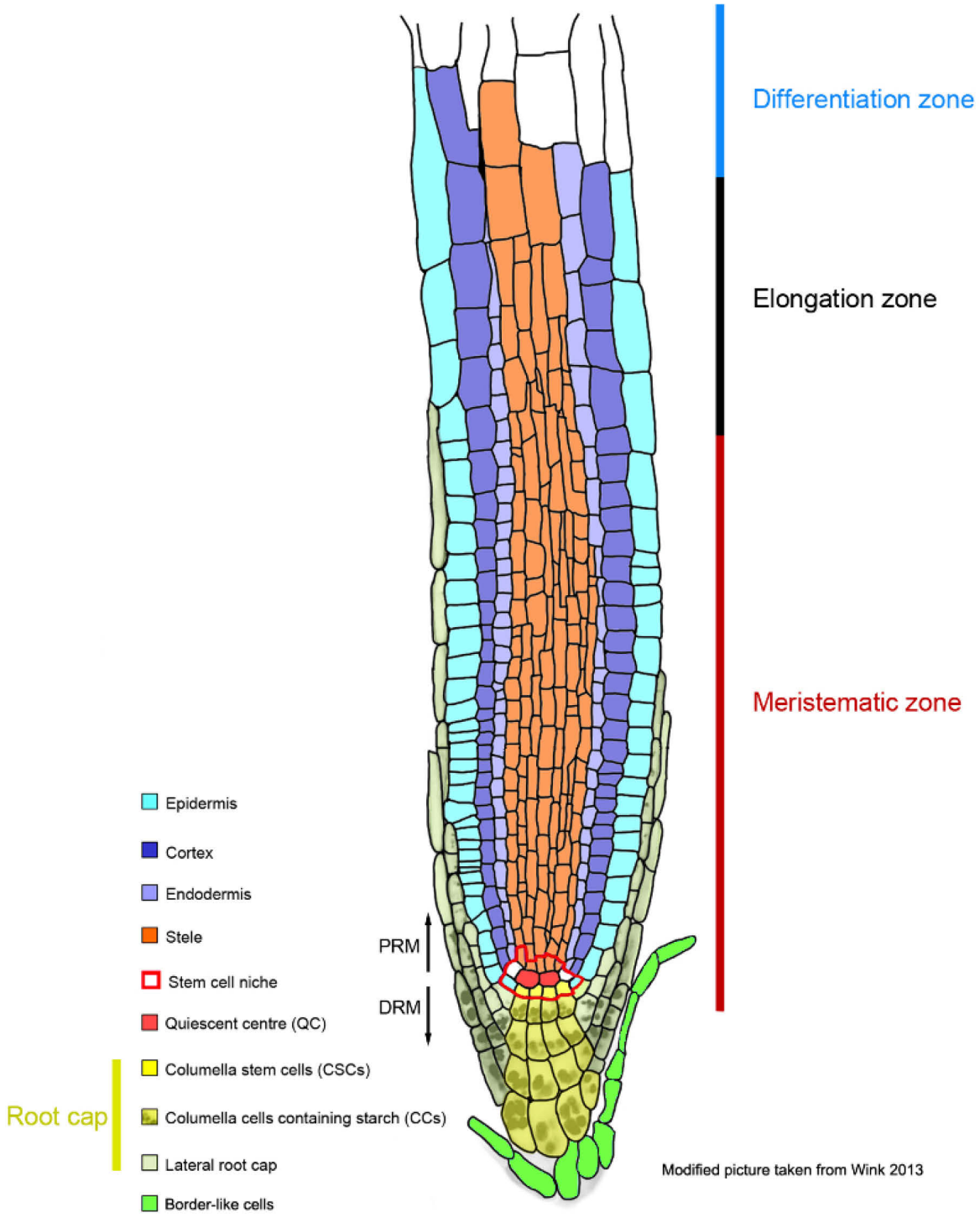

Figure 4 Organization of the RAM

The RAM can be divided into 3 zones: First the meristematic zone (red bar) with its stem cell niche (outlined in red), second the elongation zone (black bar) and third the differentiation zone (blue bar). The meristematic zone can be further divided into the proximal root meristem (PRM) containing all cells proximal to the QC and the distal root meristem (DRM) containing all cells distal to the QC. The proximal root meristem is organized in concentric layers, which are referred to as (from the outside to the inside): lateral root cap (grey), epidermis (cyan), cortex (dark blue), endodermis (light blue) and the stele (orange). Distal to the QC (red) the columella stem cells (yellow) are located which will differentiate into columella cells (yellow with grey dots) before undergoing terminal differentiation into border-like cells (green). The root cap consists of the columella stem cells, the columella cells and the LRC. A color-coded figure legend can be found on the left side of the picture with the cells contributing to the root cap marked with a yellow bar. This modified picture was taken from: Wink 2013 (Wink, 2013).

1.4 Development of the distal RAM during embryogenesis

In contrast to the majority of seed plants, embryogenesis in *A. thaliana* follows always the same predictable pattern, which allows to identify genetic components involved in this highly regulated process (Jürgens et al., 1994; Mansfield and Briarty, 1991). To discriminate between the different time points of development, embryogenesis is sectioned in different stages based on the morphology of the embryo (Figure 5) [reviewed in (Colette et al., 2015)]. After fertilization of the zygote, an asymmetric cell division separates a small apical cell from a larger basal cell (1-cell stage). From the apical cell almost the entire embryo will develop, whereas from the basal cell the extra embryonic suspensor is derived. The suspensor is a temporary organ connecting the developing embryo with maternal tissues before it undergoes apoptosis later in development (Zhao et al., 2013). The apical cell divides tree times giving rise to a bulbous structure of 8 small cells which in total have the same size of the former apical cell at the 1-cell stage (Yoshida et al., 2014). This time point is referred to as octant stage and differential expression of homeodomain transcription factors from the WUSCHEL RELATED HOMEOBOX (WOX) family in the upper and lower 4 cells are marking the apical and basal domain of the proembryo. In the dermatogen stage inner and outer tissues (protoderm) are specified and the uppermost suspensor cell is determined as the hypophysis, which is from now on part of the embryo. Thus a cell from the extra embryonic structure is integrated into the developing embryo. This is achieved by rerouting auxin flux via the AUXIN RESPONSE FACTOR 5 (ARF5)/MONOPTEROS (MP) / IAA12/BODENLOS (BDL) / PIN-FORMED 1 (PIN1) module from the basal embryo domain into the suspensor cells, resulting in the expression of specific target genes regulating cell identity [reviewed in (Colette et al., 2015)]. At the same time point MP promotes the expression of TARGET OF MONOPTEROS 7 (TMO7), which translocates to the uppermost suspensor cell and acts together with auxin to specify the hypophysis [reviewed in (Colette et al., 2015)]. The hypophysis then initiates expression of *WUSCHEL RELATED HOMEOBOX 5* (*WOX5*) and will subsequently divide into a small lens shape cell and a bigger basal cell. After this asymmetric cell division the expression of *WOX5* is only retained in the lens shaped cell, which will develop into the QC. The basal daughter cell however will give rise to the columella cells [reviewed in (Colette et al., 2015)]. The asymmetric division of the hypophysis is controlled through the transcription factors NO TRANSMITTING TRACT (NTT), WIP DOMAIN Protein 4 (WP4) and WP5, which are acting redundantly downstream of MP. Triple mutants of these genes fail to perform this asymmetric division and consequently lack a QC, eventually leading to non-viable seedlings without a root (Crawford et al., 2015). WOX genes play important roles in pattern formation during embryogenesis and the expression of *WOX5* in the hypophysis and of *WUS* in the precursor cells of the SAM are considered as early meristem markers (Haecker et al., 2004; Sarkar et al., 2007).

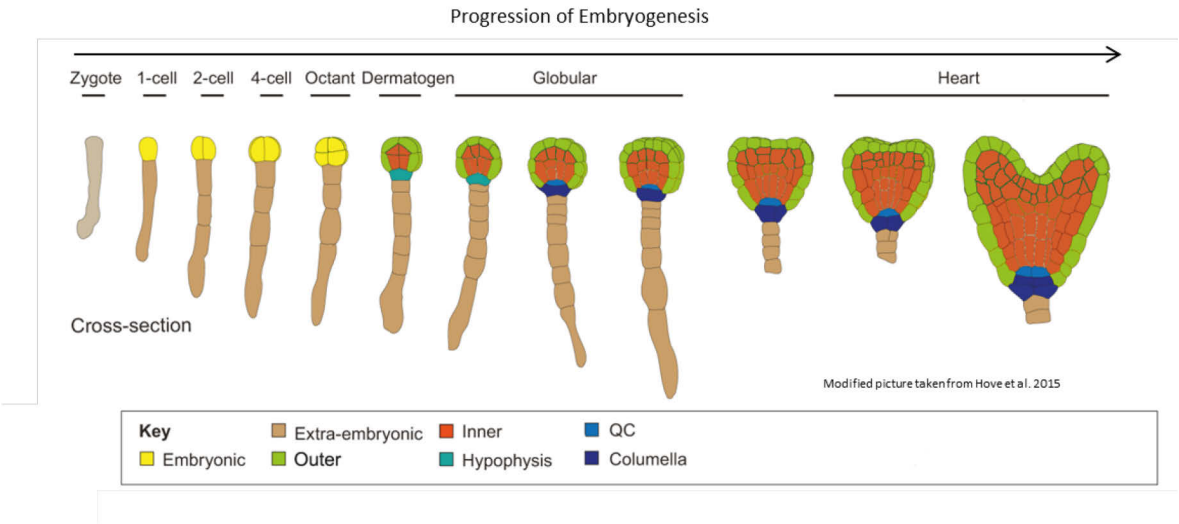

Figure 5 Development of the distal RAM during embryogenesis

After fertilization of the egg cell, the resulting zygote (grey) divides asymmetrically forming a small apical cell (yellow) and a larger basal cell (brown). The apical cell will divide 3 times (2-cell stage, 4-cell stage and octant stage) and then form in the dermatogen stage inner (orange) and outer (green) tissues. In this stage also the hypophysis (cyan) is specified, which will give rise to QC (light blue) and columella cells (dark blue) in the mid to late globular stage. At the beginning of the heart stage, columella cells are dividing anticlinal to form additional columella layers. A color-coded figure legend can be found at the bottom of the picture.

1.5 Functions and organization of the root cap

The evolution of roots allowed the vascular land plants to grow bigger and to conquer new ecological niches as they were now able to actively penetrate the soil to get access to water and nutrients. The root system is also anchoring the plant, providing stabilization of the whole plant body. In seed plants, the root cap (calyptra) serves as a root-soil-interface and is essential for root function. It protects the root and its stem cell niche, by reducing friction through secreting a lubricant consisting of mucilage and detached border-like cells (Bengough and McKenzie, 1997). It is also needed to guide the root along the gravitation axis, as it can perceive gravitation by specialized cells containing large starch granules referred to as statoliths (Blancaflor et al., 1998). Changes of the root position in relation to the gravitation axis leads to redistribution of auxin and to asymmetric root growth which eventually results in root bending and to a change of the growth direction (Abas et al., 2006). After direct contact of the root tip with impenetrable objects such as stones, the root reacts with a redirection of growth to bypass the obstacle. For this thigmonastic movement, the root cap was shown to play an important role (Massa and Gilroy, 2003). Taken together the root cap is serving as a signaling center or as Darwin wrote as the “brain” of the plants: “It is hardly an exaggeration to say that the tip of the radicle […] acts like the brain of one of the lower animals” (Darwin and Darwin, 1880). The root cap consists of the columella (CC) and the columella stem cells (CSC), which are both bracketed by the lateral root cap (LRC) and the LRC/epidermis initial. The most distal CCs and LRC cells are referred to as border-like cells, which are periodically released from the root. Because of this, CSCs and the LRC/epidermis initials have to divide frequently to provide new CCs and LRC cells. The border-

like cells are still living after detachment and have an active metabolism. They can even be cultured to produce callus tissue *in vitro* and represent the most differentiated cells of the root cap (Bennett et al., 2010; Hawes et al., 1991). Because of the stereotype divisions of the CSCs and the predictable fate of its daughter cells, the columella is an excellent model to study asymmetric cell division and cell differentiation. For the CSCs located just below the QC it has been shown that, after division, the daughter cells adjacent to the QC are maintained as initials, whereas the distal daughter cells undergo differentiation to columella cells (CCs). Subsequently, these CCs are characterized by starch granules and stop dividing, before as a last step, they enter terminal differentiation and are released as border-like cells. In the context of CSC maintenance the QC represents not only an organizing center, but is actively serving as a long term stem cell reservoir. The QC is dividing twice as slow as CSCs and from a QC division event the proximal daughter cells retain QC identity whereas the distal daughter cells acquire CSC identity (Cruz-Ramírez et al., 2013). In a longitudinal section of a wild type *Col-0* distal root meristem as shown in Figure 4, in average 1 layer of QC cells, 1 layer of CSCs, 3-4 layers of CCs and 1 layer of border-like cells can be seen.

1.6 Control of CSC maintenance

The control of CSC asymmetric division is mainly exerted by the homeodomain transcription factor WOX5 (Sarkar et al., 2007), which is expressed in the QC but moves to act non-cell autonomously, thereby building a protein gradient with high levels in the QC, intermediate levels in the CSCs and no detectable protein in CCs (Pi et al., 2015). Ectopic overexpression of *WOX5* leads to the production of additional files of stem cells, whereas in *wox5* mutants the CSCs are lost, resulting in an unorganized but functional root meristem with often enlarged QC cells which are dividing more often (Sarkar et al., 2007) (Figure 6 A, B and C). Thus, WOX5 functions in CSC maintenance in a fashion similar to the stem cell maintenance function of its closest homolog WUS in the SAM (see chapter 1.2) (Mayer et al., 1998). The enhanced QC division phenotype in *wox5* mutants is due to ectopic *CYCLIN D3;3* (*CYCD3;3*) expression in the QC and this phenotype is partly rescued in *wox5*/*cycd3;3* mutants (Forzani et al., 2014). Interestingly the accumulation of CSCs after overexpression of *WOX5* is not only a result of blocking differentiation of CSCs into CCs, but in part, also due to a dedifferentiation of already differentiated CCs (Bennett et al., 2014). This extreme phenotype might be due to ectopic expression of *WOX5*, as overexpression of *WOX5* in the QC and CSCs is not showing this phenotype (Pi et al., 2015). The function of WOX5 as a differentiation inhibitor is exerted by building a complex with the transcriptional co-repressors TOPLESS (TPL) and all TOPLESS-RELATED (TPR) family members to repress the expression of the transcription factor *CYCLIN DOF FACTOR 4* (*CDF4*) in the QC and CSCs (Pi et al., 2015). CDF4 functions as a differentiation factor, therefore antagonizing the role of WOX5 and allowing the distal daughter cells to enter CC fate. The initiation of CSC asymmetric division itself

is partly under control of the NAC-domain (*NO APICAL MERISTEM*; *ARABIDOPSIS TRANSCRIPTION ACTIVATION FACTOR 1/2*; *CUP-SHAPED COTYLEDON 2*) transcription factors FEZ and SOMBRERO (SMB). Just before an asymmetric division, *FEZ* is expressed in CSCs but after the division *FEZ* expression in the proximal daughter cells (CSCs) is lost until the next division event. In the distal daughter cells *FEZ* remains expressed but its function is counteracted by *SMB* which is upregulated by FEZ (Willemsen et al., 2008). While *SMB* is expressed in CCs and LRC cells, but not in CSCs, in *wox5* mutants *SMB* is expressed in CSCs indicating that WOX5 is repressing *SMB* in CSCs (Bennett et al., 2014). Besides repressing FEZ function in CCs, *SMB* plays also a prominent role in the terminal differentiation of CCs into border-like cells and in apoptosis of LRC cells at the end of the meristematic zone (Bennett et al., 2010; Yadav and Helariutta, 2014).

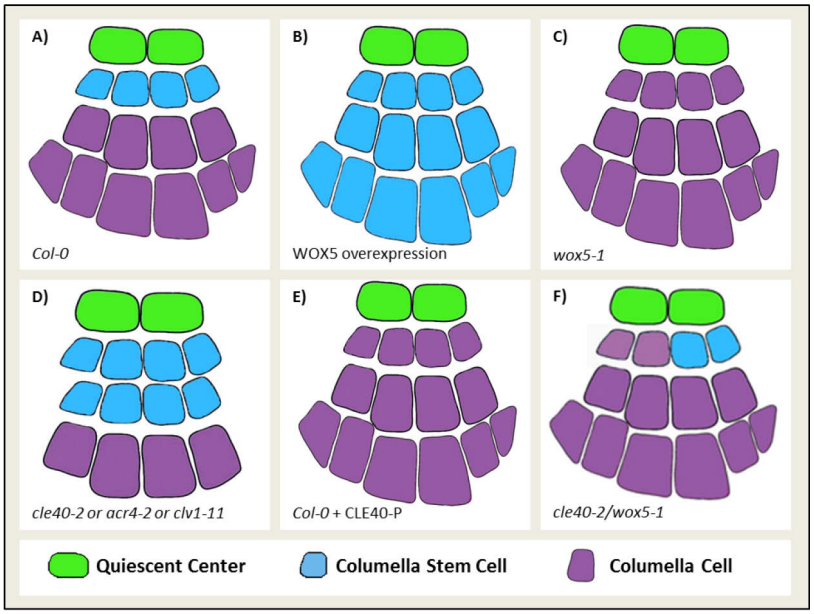

Figure 6 CSC phenotype of some important mutants

A) In *Col-0* wild type roots in average 1 layer of CSCs (cyan) can be seen, which are located distal to the QC (green) and proximal to differentiated CCs (violet).

B) After ectopic *WOX5* overexpression CCs dedifferentiate and layers of CSCs are accumulating.

C) In *wox5-1* mutants the former CSC layer is differentiated to CCs and the QC is dividing more often (not shown).

D) *cle40-2*, *acr4-2* or *clv1-11* mutants have in average 2 layers of CSCs instead of 1.

E) After treatment of *Col-0* wild type roots with synthetic CLE40 peptide CSCs are differentiating to CCs. This phenotype is CLE40 dosage dependent and a high dosage of CLE40 peptide leads to differentiation of the QC (not shown). *acr4-2* mutants are resistant to peptide treatment.

F) The *wox5-1* mutant phenotype (C) is partially rescued in *cle40-2*/*wox5-1* double mutants.

Schematic representative diagram. Just 3 layers of cells distal to the QC are shown.

1.7 Upstream regulators of *WOX5*

WOX5 functions as a master regulator of CSC homeostasis and therefore has to be controlled tightly on the transcriptional level. This control is exerted by multiple interconnected intercellular signaling processes, involving, among others, small peptides, phytohormones and transcription factors. In mature roots *WOX5*, expressed in the QC, and *SCARECROW* (*SCR*)

together with *PLETHORA* (*PLT*) 1/2 are acting in parallel to promote QC identity. Mutations in *PLT1*/*PLT2* or in *SCR* lead to loss of QC identity (Aida et al., 2004; Sabatini et al., 2003). While *WOX5* is still expressed in *plt1*/*plt2* double mutants, expression is lost in *scr* mutants indicating that WOX5 acts downstream of SCR but not of PLT1 and PLT2 (Sarkar et al., 2007). This also indicates that QC identity and *WOX5* expression is not necessarily connected, which is supported by the fact that *wox5* mutants possess a misshaped but partly functional QC (Sarkar et al., 2007). In the SAM the transcription factor BRCA1-ASSOCIATED RING DOMAIN 1 (BARD1) later renamed in REPRESSOR OF WUSCHEL 1 (ROW1) is restricting *WUS* expression to the organizing center and in *row1* mutants *WUS* is drastically overexpressed and has an enlarged expression domain (Han et al., 2008). Recently it was shown that also in the proximal RAM ROW1 represses *WOX5* by binding to histone H3 lysine 4 tri-methylations (H3K4me4). In *row1* mutants *WOX5* is accordingly ectopically expressed in the proximal RAM and this proximal expression of *WOX5* leads lo loss of *WOX5* expression in the QC, likely due to downregulation of *SCR* which expression in the QC is lost in *row1* mutants (Zhang et al., 2015). Thus ROW1 restricts the two closely related stem cell promoting factors WUS and WOX5 to their organizing centers in the SAM and the RAM, respectively. Auxin acts as a long range signaling molecule through AUXIN RESPONSE FACTOR 10 (ARF10) and AUXIN RESPONSE FACTOR 16 (ARF16) to negatively regulate *WOX5* expression in the QC but whether this is a direct regulation or indirect is not entirely clear (Bennett et al., 2014; Ding and Friml, 2010). The main regulatory mechanism controlling *WOX5* expression in the QC involve the small CLV3-related peptide CLAVATA3/ENDOSPERM SURROUNDING REGION-RELATED 40 (CLE40) which is acting in the CLE40-pathway (Stahl et al., 2009).

1.8 The CLE40-pathway

CLE40 has a very similar genomic structure as *CLV3* comprising 3 exons and 2 introns. It is coding for an 80aa long pre-pro-protein, which is supposed to be processed to a 13aa long signaling peptide, which acts non-cell autonomously. It is produced in and secreted from differentiated CCs and then acts through the interacting receptor-like kinases (RLK) CLV1 and ARABIDOPSIS CRINKLY 4 (ACR4) to repress *WOX5* expression in a dose-dependent manner (Stahl et al., 2013; Stahl et al., 2009). In roots *ACR4* and *CLV1* are expressed in the differentiated CCs, the undifferentiated CSCs, but also in the lateral root cap (LRC) and LRC/epidermis initial cells (Stahl et al., 2013). Interestingly, *ACR4* expression can additionally be detected in the QC and epidermis cells, whereas *CLV1* is also expressed in phloem companion cells (Araya et al., 2014; Gifford et al., 2003). Thus, their expression patterns overlap only partially, suggesting additional and independent functions of the two receptors (Figure 7 A). Mutations in either the *cle40* signaling peptide or its receptors *clv1* and *acr4* accumulate an additional file of CSCs, indicating unrestricted WOX5 activity (Stahl et al., 2013; Stahl et al., 2009) (Figure 6 D). Accordingly, in *cle40* mutants *WOX5* is partially de-repressed, leading to a lateral expansion of *WOX5* expression

(Stahl et al., 2009). In contrast, treatment of roots with synthetic CLE40 peptide leads to a proximal shift of *WOX5* expression from the QC into the vasculature and, interestingly, to an up regulation of *ACR4*, indicating a regulatory effect of the CLE40 ligand on the expression of its own receptor (Stahl et al., 2009). The question of whether this CLE40 peptide induced upregulation of *ACR4* expression is dependent on functional ACR4 and CLV1 receptor-kinases or if CLE40 is acting indirectly through other receptors to target *ACR4* so far is unanswered but will be addressed in this thesis.

Peptide treatment of the root furthermore leads to the differentiation of CSCs, reflected by starch accumulation in the former position of the CSCs (Figure 6 E), which is consistent with the role of WOX5 in maintaining CSC fate by inhibiting the differentiation factor CDF4 (Pi et al., 2015; Stahl et al., 2009). This effect is lost in *acr4* mutants, which seem to be insensitive to CLE40 peptide treatment (Stahl et al., 2009). Interestingly, CLE40 peptide is able to promote differentiation even in *wox5* mutants, suggesting a so far unknown parallel pathway for stem cell maintenance that is at least partially independent of WOX5 (Stahl et al., 2009). This is supported by the observation that the *wox5* mutant phenotype is partially rescued in *cle40*/*wox5* double mutants (Figure 6 F) and also a mathematical model is supporting this theory and predicts a factor X which acts redundantly to WOX5 (Richards et al., 2015). In this two-pathway model, the receptor ACR4 might function as the conjunction point for both pathways. Acting as a central player in root stem cell maintenance, ACR4 activity seems to be tightly regulated not only on expression but also on protein level, since after application of synthetic CLE40 peptide ACR4 protein is internalized and accumulates in vesicles (Stahl et al., 2013). This turnover of the ACR4 protein at the plasma membrane appears to be essential for ACR4 function, since mutated ACR4 versions which are stabilized at the plasma membrane are not able to complement the *acr4-2* mutant (Gifford et al., 2005). This internalization of the receptor could be a mechanism to downregulate signaling activity through sequestration of the receptors, however, the possibility that internalized receptors could also provide an intracellular signaling hub for the CLE40 peptide should not be excluded as well (Stahl and Simon, 2009). In either case it is apparent that the regulation of ACR4 protein concentration represents an additional mechanism to fine-tune CLE40/ACR4 signaling. As transcriptional control of gene expression is one part contributing to protein concentration, the composition of the ACR4 promoter and factors influencing transcription are of interest. Little is known about the potential regulatory sequences in the *ACR4* promoter, or potential binding sites for transcription factors regulating *ACR4* expression in the distal root meristem. One obvious candidate for *ACR4* regulation is WOX5, but so far there is no experimental evidence that WOX5 exhibits any influence on *ACR4* expression, which would create a feedback mechanism to stabilize the CLE40 pathway (Figure 7 B). However, some kind of feedback loop must be assumed to be in place as CLE40-ACR4 signaling would otherwise result in

more CCs due to CSC differentiation producing more CLE40, which would again increase CC number and so on, eventually leading to QC differentiation and meristem termination.

1.9 Current model of CSC maintenance

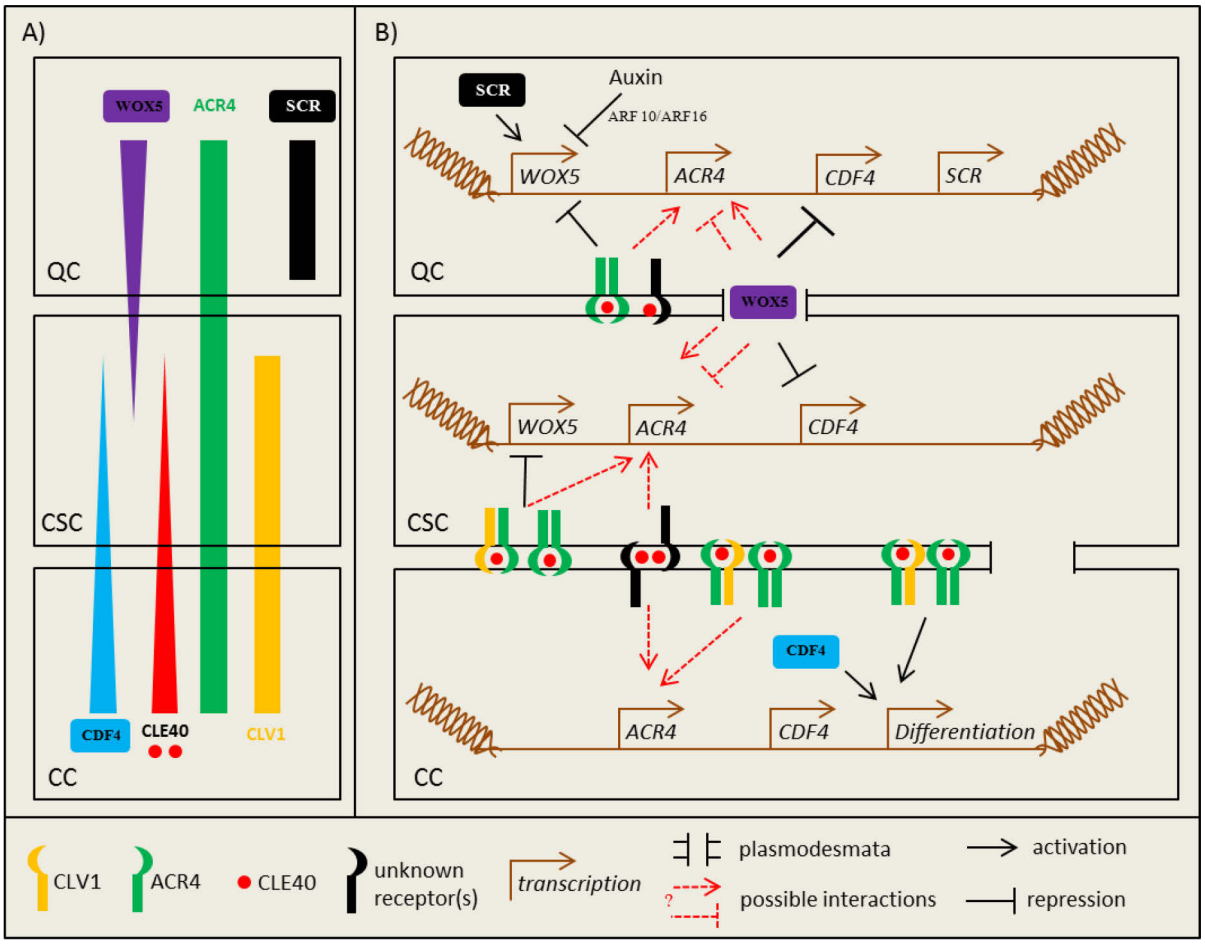

Figure 7 Current model for WOX5 dependent CSC maintenance and localization of proteins involved in CSC maintenance

A) Localizations of proteins involved in CSC maintenance: *WOX5* (violet) is expressed in the QC but WOX5 protein also is also found in CSCs in lower concentration. *CDF4* (blue) is expressed in CCs and to a lesser extend in CSCs but not in the QC. *ACR4* (green) expression and protein localization are overlapping in the QC, CSCs and CCs. *CLV1* (yellow) is expressed in and localized in CCs and CSCs. Expression of CLE40 (red) is restricted to CCs and then diffuses or is transported to CSCs. That the peptide reaches the QC cannot be excluded. SCR (black) is expressed in and localizes to the QC.

B) Current model for WOX5-dependent CSC maintenance: Top (QC cell): *WOX5* expression in the QC is modulated by auxin which acts through ARF10/16 to repress *WOX5*. SCR is expressed in the QC and is required for *WOX5* expression and QC identity.

Also, CLE40 (red dot below the QC cell) was shown to negatively regulate *WOX5* in the QC if applied as synthetic peptide by signaling via ACR4 (green receptors), which is expressed in the QC too. WOX5 protein accumulates in the QC, where it negatively represses *CDF4* transcription, thereby indirectly preventing differentiation. The WOX5 protein then moves to CSCs, most likely through plasmodesmata.

Middle (CSC): In the CSCs, WOX5 again represses *CDF4*. *WOX5* expression in CSCs is repressed by CLE40 (red dots below the CSC), coming from the underlying CCs and signaling through the receptors ACR4 and CLV1 (yellow receptor). If WOX5 is modulating *ACR4* expression in the QC and CSCs is unknown (doted arrows and repression bars). Bottom (CC): In CCs, no WOX5 is present and *CDF4* is therefore derepressed, leading to cell differentiation. In parallel to this, CLE40 is promoting cell differentiation independently of WOX5, again via ACR4 or ACR4/CLV1 complexes. Top (QC cell), Middle (CSC), Bottom (CC): CLE40 is upregulating the expression of *ACR4* but which receptors are involved in this upregulation is unknown.

1.10 Involvement of the receptor like kinase ACR4 in other developmental pathways

Besides its role in CSCs maintenance, ACR4 is also involved in specification of the epidermis and in the control of lateral root development. ACR4 is an ortholog of the *Zea mays* CRINKLY4 (CR4) protein and both are sharing the same domain organization (Tanaka et al., 2002). While *cr4* mutants are showing severe epidermal defects like graft-like fusions between organs and tumor-like cell proliferations of the epidermis, *acr4* mutants are showing more subtle phenotypes (Becraft et al., 1996; Jin et al., 2000; Tanaka et al., 2002). RNA *in-situ* hybridization experiments and promoter-reporter constructs of the upstream regulating sequence of *ACR4* are showing that *ACR4* is expressed from the octant stage of embryogenesis onwards to post embryonic development (Gifford et al., 2003; Tanaka et al., 2002). While in early embryogenesis *ACR4* is expressed in all tissues, after the dermatogen stage, expression is restricted to the L1 cell layer and to the developing columella of the radicula. In adult plants expression can be seen in the L1 of young developing organs and in the entire root cap. Mutants of *acr4* are aborting seeds and ovules with a rate of 40-85% and surviving seeds display an abnormal wizened morphology which is a consequence of malformed integuments (Gifford et al., 2003). The epidermis of homozygous mutants fail to deposit a smooth cuticula resulting in permeability of the epidermis to toluidine blue (Watanabe et al., 2004). Thus ACR4 is needed for proper differentiation of the L1 and was shown to act in the same pathway with ARABIDOPSIS THALIANA MERISTEM LAYER1 (AtML1) and PROTODERMAL FACTOR2 (PDF2), two transcription factors expressed in the L1 and needed for epidermis specification (San-Bento et al., 2014).

The sepal epidermis of the *A. thaliana* flower is characterized by cells showing a long range of different sizes ranging from very small cells to giant cells which are undergoing endoreduplication and are not dividing anymore (Roeder et al., 2010). Changes in the cell cycle are assumed to be responsible for giant cell development, and genes involved in epidermal identity like *AtML1* and *ACR4* were shown to positively influence this process (Roeder et al., 2012). Accordingly in *acr4* mutants less giant cells than in *Landsberg erecta* (*Ler*) wildtype can be observed (Roeder et al., 2012).

In the root *ACR4* is expressed in young lateral root primordia after the first divisions of the pericycle and was suggested to play a role in these formative divisions by lateral inhibition of proliferative cell divisions in nearby pericycle cells (De Smet et al., 2008; Gifford et al., 2003). *acr4* mutants initiate more lateral root primordia per centimeter (cm) but the overall rate of emerging lateral roots is reduced in comparison to wildtype plants (De Smet et al., 2008). This phenotype and also the CSCs phenotype of *acr4* mutants in the distal RAM are supposed to be enhanced when combined with mutations in other genes of the CRINKLY gene family (De Smet et al., 2008).

2 Aims of this thesis

The aim of this thesis is to perform a detailed analysis of the 5' upstream regulatory sequence of *ACR4* with regard to the contribution of specific sequence motifs within this region to overall *ACR4* expression. To this end, an *in silico* analysis of this putative promoter sequence will be combined with systematic sequence deletion experiments *in vivo*, and *in vivo* screening of transcription factor libraries for potential regulators binding to this genomic region. This will allow the identification of regions essential for general expression, and will reveal a potential modular organization of the promoter, which could explain the two distinct expression domains of *ACR4* in the epidermis and the distal root meristem (DRM). Moreover, the contribution of the ACR4-kinase domain on CLE40 signaling will be analyzed, and it will be tested if ACR4 is involved in an auto regulatory feedback-loop.

Following successful identification of a module necessary for expression in the DRM, it will be tested if the identified module is not only necessary, but also sufficient to confer meristematic expression. In this case, the DNA fragment will be used to identify transcription factors which specifically regulate *ACR4* expression in this domain, by binding to this fragment in a protoplast transactivation assay (PTA) and in a yeast-1-hybrid (Y1H) screen. Interaction of potential candidates with the *ACR4* promoter will be then confirmed with complementary methods and, if possible, the exact binding site of these transcription factors should be determined.

One potential candidate to regulate *ACR4* expression in the DRM is WOX5. WOX5 is acting non-cell autonomously and is a known transcriptional target of the ACR4-CLE40-pathway. Thus, it may act in a feedback loop to regulate *ACR4* expression. To analyze the influence of this transcription factor, *ACR4* expression will be quantified in a *wox5* mutant background and after *WOX5* overexpression. In this context, the influence of *CLE40* and *ACR4* itself on *ACR4* expression will also be tested.

Overall, these analyses will help to understand the transcriptional regulation of *ACR4* in the DRM in close detail and will introduce new players to the current model of the CLE40-ACR4/CLV1-WOX5 signaling module and its role in stem cell homeostasis in the *Arabidopsis* root.

3 Materials and Methods

3.1 Materials

3.1.1 Chemicals

All chemicals used in this thesis were ordered from the following companies: Biozym Scientific GmbH (http://www.biozym.com), Duchefa Biochemie bv (http://www.duchefa.com), Sigma-Aldrich (http://www.sigmaaldrich.com), Promega Corporation (http://www.promega.com) and Carl Roth GmbH + Co. KG (http://www.carlroth.com).

3.1.2 Enzymes

Enzymes for molecular procedures involving DNA or RNA manipulation like restriction, ligation, de-phosphorylation, reverse transcription of RNA and DNA amplification by Polymerase Chain Reaction (PCR) were purchase from Thermo Scientific (http://www.thermofisher.com) and its subsidiary companies (Fermentas, Invitrogen) and New England Biolabs (http://www.neb-online.de). All enzymes where used according to manufacturer's instructions.

3.1.3 Buffers and Media

Unless otherwise stated, buffers, solutions and growth media for bacteria and plants were prepared following the protocol collection "Current Protocols in Molecular Biology" (Ausubel et al., 1987). Frequently used media are listed in Table 1.

Table 1 Buffers and Media

Media	Organism	Composition
Solid Growth Media (GM)	*Arabidopsis* grown *in vitro*	2,2g/l Murashige and Skoog media; 0,5g/l MES; 1% (w/v) sucrose; pH adjusted with KOH to pH 5.7; 1,2% (w/v) plant agar
Double Yeast Tryptone (DYT) media	*Agrobacterium* grown in liquid culture	16g/l Tryptone; 10g/l Yeast Extract; 5g/l NaCl
Solid DYT media	*Agrobacterium* grown in petri dishes	DYT media; 12g/l agar
Lysogeny Broth (LB) media	*Escherischia coli* (*E.coli*) grown in liquid culture	10g/l Tryptone; 5g/l Yeast Extract; 5g/l NaCl
Solid LB media	*E.coli* grown in petri dishes	LB media; 12g/l agar

3.1.4 DNA size markers for electrophoresis

To estimate the sizes of linear DNA fragments, their relative positions were compared to DNA size markers purchased from Thermo Scientific. Following products were used: GeneRuler 1kb DNA Ladder and GeneRuler 50bp DNA Ladder.

3.1.5 Synthetic CLE40 peptide

Synthetic hydroxyprolinated CLE40 peptide was ordered from Thermo Scientific. The amino acid sequence is: R-Q-V-P(hydroxyproline)-T-G-S-D-P-L-H-H-K.

3.1.6 Oligonucleotides

Oligonucleotides were ordered from BioTeZ Berlin-Buch GmbH (http://www.biotez.de). Oligonucleotides with a length over 38 bp were purified by high performance liquid chromatography. Table 2 is showing oligonucleotides used for cloning, Table 3 oligonucleotides used for sequencing and Table 4 oligonucleotides used for genotyping. Listed are the names of the oligonucleotides and their corresponding sequences in 5’ -> 3’ orientation.

Table 2 Oligonucleotides used for cloning

Listed are the names of the oligonucleotides used for cloning and their corresponding sequences in 5’ -> 3’ orientation.

Oligonucleotides used for cloning	Sequence in 5' --> 3' orientation
pACR4_P1_F	CACCCTTGTTTGAAGGGTGAAGCATCC
pACR4_P2_F	CACCTGTGCTCTCTCTATAAATATACGATTG
pACR4_P3_F	CACCAAGTCAGTTTTTAGGTCAGTATGCAATTC
pACR4_P4_F	CACCATGTCGTTGATTAGAAGCAGTTTATC
pACR4_P5_F	CACCGAGTGGCCGGTTCTTATTCTTTGAAT
pACR4_P6_F	CACCGGTTCTTGTAATGAGACACAGAGAATAG
pACR4_P7_F	CACCAGAAACAGAGTTGAACTAAAAATATGTGC
pACR4_P8_F	CACCAAAAAAGGAAAAAGGAAGCTTTGAAGG
pACR4_P9_v2_F	CACCGTAAAAAAAAACGAGAAAGCAAGAAG
pACR4_P10_F	CACCATGACTCTCTCTTTGATAAGCTCCATG
pACR4_R	TCTTTTCAAAGTCAACACACACGC
pACR4-UTR_R	TTATACATTCAACAGTAGCTCATG
OVE_F	GTTCCCTACTCTCGCGTTAACGCTA
OVE_R	ATGGCTCATAACACCCCTTGTATTACTG
ACR4_P7_OVE9_R	GCTTTCTCGTTTTTTTTTACAATAATCTTTTTAATGGGTG
ACR4_P9_OVE7_F	CACCCATTAAAAAGATTATTGTAAAAAAAAACGAGAAAGC
ACR4_P6_OVE9_R	GCTTTCTCGTTTTTTTTTACCGAGACGCGAGACACAAACA
ACR4_P9_OVE6_F	TCGCGTCTCGGTAAAAAAAAACGAGAAAGC
ACR4_P5_OVE9_R	GCTTTCTCGTTTTTTTTTACAAAATTGAAAAACATAAGTT
ACR4_P9_OVE5_F	AACTTATGTTTTTCAATTTTGTAAAAAAAAACGAGAAAGC
ACR4_OVE_5-7_R	ATATTTTTAGTTCAACTCTGTTTCTAAAATTGAAAAACAT
ACR4_OVE_5-7_F	GAGTCAACTTATGTTTTTCAATTTTAGAAACAGAGTTGAA
ACR4_ASCI_F	TTTTTGGCGCGCCCTTGTTTGAAGGGTGAAGCA
ACR4_ASCI	AAAAAGGCGCGCCTCTTTTCAAAGTCAACACAC
ARE1-mut_R	CTCTGTTTCTCGAGACGCCTTGGTCAAACATCCTCTTTTGTC
ARE1-mut_F	GACAAAAGAGGATGTTTGACCAAGGCGTCTCGAGAAACAGAG
ARE2_mut_R	GTTTAACACAAGATTCAATCTTGGTTTAACTATTACTCATTCC
ARE2_mut_F	GGAATGAGTAATAGTTAAACCAAGATTGAATCTTGTGTTAAAC
WUS-Box-mut_R	CCTTTTTTAATAATCTTTTCTGGTCGTGTTTTACTTTCGCC
WUS-Box-mut_F	GGAATGAGTAATAGTTAAACCAAGATTGAATCTTGTGTTAAAC
ARE1-mut_R	CTCTGTTTCTCGAGACGCCTTGGTCAAACATCCTCTTTTGTC
ARE1-mut_F	GACAAAAGAGGATGTTTGACCAAGGCGTCTCGAGAAACAGAG
ARE2_mut_R	GTTTAACACAAGATTCAATCTTGGTTTAACTATTACTCATTCC
ARE2_mut_F	GGAATGAGTAATAGTTAAACCAAGATTGAATCTTGTGTTAAAC

ARE2_mut_R	GTTTAACACAAGATTCAATCTTGGTTTAACTATTACTCATTCC
ARE2_mut_F	GGAATGAGTAATAGTTAAACCAAGATTGAATCTTGTGTTAAAC
pACR4ΔS1_R	ACATATTTTTAGTTCAACTCTGTTTACAAACATCCTCTTT
pACR4ΔS1_F	AAAGAAGACAAAAGAGGATGTTTGTAAACAGAGTTGAACT
pACR4ΔS2_R	TGTGAGGTTTCATGCACATATTTTTCTCGAGACGCGAGAC
pACR4ΔS2_F	GGATGTTTGTGTCTCGCGTCTCGAGAAAAATATGTGCATG
pACR4ΔS3_R	TAATAGTAAATGGCTTGTGAGGTTTAGTTCAACTCTGTTT
pACR4ΔS3_F	GCGTCTCGAGAAACAGAGTTGAACTAAACCTCACAAGCCA
pACR4ΔS4_R	CAATCTCTTAACTTATAATAGTAAACATGCACATATTTTT
pACR4ΔS4_F	GAGTTGAACTAAAAATATGTGCATGTTTACTATTATAAGT
pACR4ΔS5_R	CAAAACATTTTAGATCAATCTCTTATGGCTTGTGAGGTTT
pACR4ΔS5_F	TATGTGCATGAAACCTCACAAGCCATAAGAGATTGATCTA
pACR4ΔS6_R	TGGTTTCGAGCAATCCAAAACATTTACTTATAATAGTAAA
pACR4ΔS6_F	TCACAAGCCATTTACTATTATAAGTAAATGTTTTGGATTG
pACR4ΔS7_R	GTTGCCGTCGGTGTTTGGTTTCGAGTAGATCAATCTCTTA
pACR4ΔS7_F	TATTATAAGTTAAGAGATTGATCTACTCGAAACCAAACAC
pACR4ΔS8_R	TGTTTTACTTTCGCCGTTGCCGTCGCAATCCAAAACATTT
pACR4ΔS8_F	GATTGATCTAAAATGTTTTGGATTGCGACGGCAACGGCGA
pACR4ΔS9_R	TAATCTTTTTAATGGGTGTTTTACTTGTGTTTGGTTTCGA
pACR4ΔS9_F	TTTTGGATTGCTCGAAACCAAACACAAGTAAAACACCCAT
pACR4ΔS10_R	TTTTCCTTTTTTAATAATCTTTTTATCGCCGTTGCCGTCG
pACR4ΔS10_F	AACCAAACACCGACGGCAACGGCGATAAAAAGATTATTAA
pACR4ΔS11_R	CCTTCAAAGCTTCCTTTTTCCTTTTATGGGTGTTTTACTT
pACR4ΔS11_F	GCAACGGCGAAAGTAAAACACCCATAAAAGGAAAAAGGAA
pACR4ΔB1_R	TTCATGCACATATTTTTAGTTCAACAGAAATGTTTTGTCC
pACR4ΔB1_F	AGTCTAAAGAGGACAAAACATTTCTGTTGAACTAAAAATA
pACR4ΔB2_R	TTTAATAATCTTTTTAATGGGTGTTCATTTTAGATCAATC
pACR4ΔB2_F	TAAGTTAAGAGATTGATCTAAAATGAACACCCATTAAAAA
pACR4ΔB3_R	TTAATAATCTTTTTAATGGGTGTTTAGAAATGTTTTGTCC
pACR4ΔB3_F	AGTCTAAAGAGGACAAAACATTTCTAAACACCCATTAAAA
pACR4ΔB4_R	TAATAATCTTTTTAATGGGTGTTTTTTTAGTTCAACTCTG
pACR4ΔB4_F	TCTCGAGAAACAGAGTTGAACTAAAAAAACACCCATTAAA
pACR4ΔB5_R	ATCTCTTAACTTATAATAGTAAATGCATCCTCTTTTGTCT
pACR4ΔB5_F	AGGAGAAAGAAGACAAAAGAGGATGCATTTACTATTATAA
pACR4ΔB6_R	ATCTCTTAACTTATAATAGTAAATGAACTAACAGACCTCT
pACR4ΔB6_F	AGAGAGGGAGAGAGGTCTGTTAGTTCATTTACTATTATAA
pACR4ΔA/B_R	GCCGTCGGTGTTTGGTTTCGAGCAATTTTTAGTTCAACTC
pACR4ΔA/B_F	TCGAGAAACAGAGTTGAACTAAAAATTGCTCGAAACCAAA
pACR4ΔB/C_R	TTAATAATCTTTTTAATGGGTGTTTTGAGGTTTCATGCAC
pACR4ΔB/C_F	CTAAAAATATGTGCATGAAACCTCAAAACACCCATTAAAA
pACR4ΔB_R	GCCGTCGGTGTTTGGTTTCGAGCAATGAGGTTTCATGCACATATT
pACR4ΔB_F	CTAAAAATATGTGCATGAAACCTCATTGCTCGAAACCAAACACCG
E7_60mini35S_ad1_R	GGTCTTGCGAAGGATAGTGGGAAATAATCTTTTTAATGGG
E8_60mini_35S_ad1_R	GGTCTTGCGAAGGATAGTGGGAAATAATCTTTTTAATGGG

E8_60mini_35S_ad1_R	GTCTTGCGAAGGATAGTGGGAGAATTTTTCCCCATTCTTC
-60mini_35S_ad2_R	ACTTCCTTATATAGAGGAAGGGTCTTGCGAAGGATAGTGG
35S_ad3_R	GTCCTCTCCAAATGAAATGAACTTCCTTATATAGAGGAA
E8-48mini35S_ad1_R	CTTCCTTATATAGAGGAAGGGTCTTGCGAATTTTTCCCCATTCTTCC
attB1-60minimal_F	GGGGACAAGTTTGTACAAAAAAGCAGGCTTATCCCACTATCCTTCGCA
attB2-60minimal_RA	GGGGACCACTTTGTACAAGAAAGCTGGGTAGTCCTCTCCAAATGAAAT
PTA-K1-60S_EcoRI_F	GGGGGGAATTCGGACAAAACATTTCTTTTGTTG
PTA-K1-add1_60S_R	AAGGGTCTTGCGAAGGATAGTGGGACATTGGAGTTTAACACAAGATTCA
PTA-K1-add2_60S_R	TGAAATGAACTTCCTTATATAGAGGAAGGGTCTTGCGAAGGATAGTG
PTA-K1-add2_60S_NcoI_R	CCCCCCCATGGGTCCTCTCCAAATGAAATGAACTTCCTTATATAG
PTA3_EcoRI_F	GGGGGAATTCCTTGTTTGAAGGGTGAAGCA
PTA3_NCOI_R	CCCCCCCATGGTCTTTTCAAAGTCAACACAC
Berta_Topo_F	CACCATGGCGACTTCGTCACCG
Berta_R	TCACAACATTCCAACTTTGTCA
Berta_without_Stop_R	TTTCAACATTCCAACTTTGTCAA
Berta_del_zinc_R	TAGAAAGTTGCCGGATTGACGAAACATTGAGACCACGGAG
Berta_del_zinc_F	TCCCAAAACTCTCCGTGGTCTCAATGTTTCGTCAATCCGG
TMO6_Topo_F	CACCATGGATCATTTGTTACAACACCAGGATGTTTTTGGGA
TMO6_R	CATTAAAGCACCAGAATTAATGTAGTTC
pACR4_P1_KpnI_F	GGGGGGGTACCCTTGTTTGAAGGGTGAAG
pACR4_P1_BAMHI_R	CCCCCGGATCCTCTTTTCAAAGTCAACAC
pACR4_P4_KpnI_F	GGGGGGGTACCATGTCGTTGATTAGAAGCAGTTTATC
pACR4_P7_KpnI_F	GGGGGGGTACCAGAAACAGAGTTGAACTAAAAATATGTGC
pACR4_P8_KpnI_F	GGGGGGGTACCAAAAAAGGAAAAAGGAAGCTTTGAAGG
pACR4-UTR_BAMHI_R	CCCCCGGATCCTTATACATTCAACAGTAGCTCATG
pBERTA_geno_F	CGTCCAAATCAAAGCTTCGAGTTACAA
pBERTA_R	TGATAAAAAGTAACGGTTTAAATTAAA
H2B_PacI_F	TTAATTAAATGGCGAAGGCAGATAAGAAACC
H2B_PacI_R	TTAATTAAAGAACTCGTAAACTTCGTAACCG
CRR1_F	CACCGTTTTTTTTAGCGCTTTGGTT
CRR1_R	TGGAGGTGAAGTTCATGAACTG
CRR3_F	CACCATTTATCAGTACATGCATG
CRR3_R	CTACAGAGGTTGAAGTTGACTGG
pACR4_Y1H_attB4_F	GGGGACAACTTTGTATAGAAAAGTTGGAAAAAGAGGATGTTTGTGTCTC
pACR4_Y1H_attB1R_R	GGGGACTGCTTTTTTGTACAAACTTGTCATTGGAGTTTAACACAAGA

Table 3 Oligonucleotide used for sequencing

Listed are the names of the oligonucleotides used for sequencing and their corresponding sequences in 5’ -> 3’ orientation.

Oligonucleotide used for sequencing	**Sequence in 5' --> 3' orientation**
pACR4_Seq3	GGTAATTTGCAAATGTAGAGTCTCC
pACR4_Seq4	AATATGTGCATGAAACCTCACAAGC
pACR4_Seq5	GTGTTAAACTCCAATGTGCATAGAG
pACR4_Seq6	CTTAGCTTCAAAGGGTCTTTGGAGGA
pBERTA_Seq3	CGGTCACCACTAAATCTTTCATAAT

pBERTA_Seq4	TTGGAATCTACTTGATCTCT
pBERTA_Seq5	ACTAGATCCACAAAAGATCC
pBERTA_Seq6	CCGAAATAGACATACGACAAATCTT
pBERTA_Seq7	GCGAATGATTGCAATTTACAAG
pBERTA_Seq8_v2	TCGTCGTGTGGACTCTTGAC
pBERTA_Seq9	TGATGTTCTATTGTTCATATGA
pCRR3_seq1	TCATTTCCTCTCTCACTTTT
pCRR3_seq2	TTTGGAGACATCTATAGCTAGCG
M13_F	TGTAAAACGACGGCCAG
M13_R	CAGGAAACAGCTATGAC
ACR4seq1F	GGGAGATGAGAATAGTAGTCA
ACR4seq2F	TGTGTTTACAACTGCTCCAG
ACR4seq3F	TGCACAACCATCTTCATGGA

Table 4 Oligonucleotides used for genotyping

Listed are the names of the oligonucleotides used for genotyping and their corresponding sequences in 5’ -> 3’ orientation.

Oligonucleotides used for genotyping	**Sequence in 5' --> 3' orientation**
LBB1V2	AAACCAGCGTGGACCGCTTGCTGCAACTCT
WOX5F	AAACAGTTGAGGACTTTACATCTGA
WOX5Rv3	AGTTGATGGTTGATGATG
YS_ACR4-LP	TTGTGAACTTCGTGTGACTCG
YS_ACR4-RP	GTGAGAACTCCGCAAGTGAAG
YS_LB3-(SAIL)	TAGCATCTGAATTTCATAACCAATCTCGATACA
RM_AL2	GGAGAAACACAAGATACGAAAGCCATG
CLE40R3´gen	ATTGTGATTTGATACCAACTTAAAA

3.1.7 Plasmids

Plasmids, which were constructed in this thesis were cloned by Gateway cloning, overlap extension PCR or by restriction and ligation. They were tagged with “pAH” (plasmid Adrian Hülsewede) followed by a unique sequential number. In Table 5 a list of all plasmids used in this thesis can be found. Plasmid maps can be found in the appendix (see chapter 10).

Table 5 Plasmids used in this thesis

Listed are the numbers, the names and the types of the plasmids used in this thesis. All vectors except *pBT10* and *pGreenII-0800Luc* are gateway compatible.

No.	**Description**	**Type**
pAH06	*ACR4 without stop codon Entry*	Entry vector (Hülsewede, 2010)
pAH21	*GW:H2B-tdTomato*	Destination vector
pAH22	*pACR4_P1 Entry*	Entry vector
pAH23	*pACR4_P2 Entry*	Entry vector
pAH24	*pACR4_P3 Entry*	Entry vector
pAH25	*pACR4_4 Entry*	Entry vector

pAH26	*pACR4_P5 Entry*	Entry vector
pAH27	*pACR4_P6 Entry*	Entry vector
pAH28	*pACR4_P7 Entry*	Entry vector
pAH29	*pACR4_P8 Entry*	Entry vector
pAH30	*pACR4_P9 Entry*	Entry vector
pAH31	*pACR4_P10 Entry*	Entry vector
pAH32	*pACR4-UTR Entry*	Entry vector
pAH33	*pACR4_P1 :Venus-H2B*	Expression vector
pAH34	*pACR4_P2 :Venus-H2B*	Expression vector
pAH35	*pACR4_P3 :Venus-H2B*	Expression vector
pAH36	*pACR4_4 :Venus-H2B*	Expression vector
pAH37	*pACR4_P5 :Venus-H2B*	Expression vector
pAH38	*pACR4_P6 :Venus-H2B*	Expression vector
pAH39	*pACR4_P7 :Venus-H2B*	Expression vector
pAH40	*pACR4_P8 :Venus-H2B*	Expression vector
pAH41	*pACR4_P9 :Venus-H2B*	Expression vector
pAH42	*pACR4_P10 :Venus-H2B*	Expression vector
pAH43	*pACR4-UTR :Venus-H2B*	Expression vector
pAH44	*pACR4ΔE8:Venus-H2B*	Expression vector
pAH45	*pACR4ΔE7+E8:Venus-H2B*	Expression vector
pAH46	*pACR4ΔE6+E7+E8:Venus-H2B*	Expression vector
pAH47	*pACR4ΔE6+E8:Venus-H2B*	Expression vector
pAH48	*X:ACR4-Venus*	Expression vector with restriction site
pAH50	*pACR4_P1 :ACR4-Venus*	Expression vector
pAH51	*pACR4ΔE8:ACR4-Venus*	Expression vector
pAH52	*pACR4ΔE6+E7+E8:ACR4-Venus*	Expression vector
pAH53	*pACR4_AREI_mut:Venus-H2B*	Expression vector
pAH54	*pACR4_AREII_mut:Venus-H2B*	Expression vector
pAH55	*pACR4_WUS_mut:Venus-H2B*	Expression vector
pAH56	*pACR4_AREI+WUS_mut:Venus-H2B*	Expression vector
pAH57	*pACR4_WUS+AREII_mut:Venus-H2B*	Expression vector
pAH58	*pACR4_AREI+WUS+AREII_mut:Venus-H2B*	Expression vector
pAH59	*pACR4_WUS_mut Entry*	Entry vector
pAH60	*pACR4_AREI+WUS_mut Entry*	Entry vector
pAH61	*pACR4ΔS1:Venus-H2B*	Expression vector
pAH62	*pACR4ΔS2:Venus-H2B*	Expression vector
pAH63	*pACR4ΔS3:Venus-H2B*	Expression vector
pAH64	*pACR4ΔS4:Venus-H2B*	Expression vector
pAH65	*pACR4ΔS5:Venus-H2B*	Expression vector
pAH66	*pACR4ΔS6:Venus-H2B*	Expression vector
pAH67	*pACR4ΔS7:Venus-H2B*	Expression vector
pAH68	*pACR4ΔS8:Venus-H2B*	Expression vector
pAH69	*pACR4ΔS9:Venus-H2B*	Expression vector
pAH70	*pACR4ΔS10:Venus-H2B*	Expression vector

pAH71	*pACR4ΔS11:Venus-H2B*	Expression vector
pAH72	*pACR4ΔB1:Venus-H2B*	Expression vector
pAH73	*pACR4ΔB2:Venus-H2B*	Expression vector
pAH74	*pACR4ΔB3:Venus-H2B*	Expression vector
pAH75	*pACR4ΔB4:Venus-H2B*	Expression vector
pAH76	*pACR4ΔB5:Venus-H2B*	Expression vector
pAH77	*pACR4ΔB6:Venus-H2B*	Expression vector
pAH78	*pACR4ΔA/B:Venus-H2B*	Expression vector
pAH79	*pACR4ΔB/C:Venus-H2B*	Expression vector
pAH80	*pACR4ΔB:Venus-H2B*	Expression vector
pAH81	*pACR4ΔA/C1 Entry*	Entry vector
pAH82	*pACR4ΔA/C2 Entry*	Entry vector
pAH83	*pACR4ΔA/C1:Venus-H2B*	Expression vector
pAH84	*pACR4ΔA/C2:Venus-H2B*	Expression vector
pAH85	*E7-48CaMV Entry*	Entry vector
pAH86	*E7-60CaMV Entry*	Entry vector
pAH87	*E7+E8-48CaMV Entry*	Entry vector
pAH88	*E7+E8-60CaMV Entry*	Entry vector
pAH89	*-60CaMV Entry*	Entry vector
pAH90	*E7-48CaMV:Venus-H2B*	Expression vector
pAH91	*E7-60CaMV:Venus-H2B*	Expression vector
pAH92	*E7+E8-48CaMV:Venus-H2B*	Expression vector
pAH93	*E7+E8-60CaMV:Venus-H2B*	Expression vector
pAH94	*-60CaMV:Venus-H2B*	Expression vector
pAH95	*pPTA-Mini (1/2E6+E7+1/2E8-60CaMV:Luc)*	Expression vector
pAH96	*pPTA-pACR4_P1*	Expression vector
pAH97	*BTA stop Entry*	Entry vector
pAH98	*BTA Entry*	Entry vector
pAH99	*Ind::BTA-Cerulean*	Expression vector
pAH100	*Ind::BTA*	Expression vector
pAH101	*Ind::BTAΔZincF-Cerulean*	Expression vector
pAH102	*TMO7 Entry*	Expression vector
pAH103	*Ind::TMO7-Cerulean*	Expression vector
pAH104	*pACR4_P1:Fluc*	Expression vector
pAH105	*pACR4_P4:Fluc*	Expression vector
pAH106	*pACR4_P7:Fluc*	Expression vector
pAH107	*pACR4_P8:Fluc*	Expression vector
pAH108	*pACR4-UTR:Fluc*	Expression vector
pAH109	*pACR4ΔE6+E7+E8:Fluc*	Expression vector
pAH110	*pBTA Entry*	Entry vector
pAH111	*pBTA:Venus-H2B*	Expression vector
pAH112	*pACR4_P1:H2B-tdTomato*	Expression vector
pAH113	*pCRR1 Entry*	Entry vector
pAH114	*pCRR1:Venus-H2B*	Expression vector

pAH115	*pCRR3 Entry*	Entry vector
pAH116	*pCRR3:Venus-H2B*	Expression vector
pAH117	*pACR4_Y1H-Min P4P1R Entry*	Entry vector
pAH118	*pACR4_Y1H-Min MW2*	Expression vector
pAH119	*pACR4_Y1H-Min MW3*	Expression vector
pAB146	*GW:Venus-H2B*	Destination vector
pAB130	*GW:Venus*	Destination vector (Bleckmann, 2010)
pAB131	*GW:Cerulean*	Destination vector (Bleckmann, 2010)
-	*pMW2*	Destination vector (multi gateway) (Deplancke et al., 2006)
-	*pMW3*	Destination vector (multi gateway) (Deplancke et al., 2006)
-	*pBT10*	Expression vector (pUC) with cloning site (provided by W. Dröge-Laser)
-	*pGreenII_0800Luc*	Expression vector (pGreen) with cloning site (Hellens et al., 2005)
-	*pMASNF2*	Destination vector (provided by Marc Somssich)
-	*Ind::WOX5-mCherry*	Expression vector (provided by Frédéric Boyer)
-	pENTR	Donor vector (Thermo scientific)
-	*pDONR_P4P1r*	Donor vector (Thermo scientific)
-	*pDONR_201*	Donor vector (Thermo scientific)

3.1.8 Microorganisms

For clonal propagation of plasmids chemically competent *Escherichia coli* cells "One Shot® TOP10" (Thermo Scientific®) or chemically competent *Escherichia coli* cells "One Shot® ccdB Survival™ 2 T1R" (Thermo Scientific®) were used. Transformation was done according to manufacturer's instructions. For transient transformation of *Nicotiana benthamiana* or for stable transformation of *Arabidopsis thaliana*, *Agrobacterium tumefaciens* GV3101 (pMP90) was used (Koncz and Schell, 1986). Genotypes of used microorganisms can be seen in Table 6.

Table 6 Microorganisms

Listed are the microorganisms used and their corresponding genotypes.

Microorganism	**Genotype**
Escherichia coli One Shot® TOP10 (Thermo scientific)	F- mcrA Δ(mrr-hsdRMS-mcrBC) Φ80lacZΔM15 Δ lacX74 recA1 araD139 Δ(araleu)7697 galU galK rpsL (StrR) endA1 nupG
Escherichia coli One Shot® ccdB Survival™ 2 T1R (Thermo scientific)	F-mcrA Δ(mrr-hsdRMS-mcrBC) Φ80lacZΔM15 ΔlacX74 recA1 araΔ139 Δ(ara-leu)7697 galU galK rpsL (StrR) endA1 nupG fhuA::IS2
Agrobacterium tumefaciens GV3101 (pMP90) (Koncz and Schell, 1986)	C58C1 (Rif r), pMK90 (Gm r)

3.1.9 Plants

Arabidopsis thaliana ecotype Columbia-*0* (Col-*0*) was used as wildtype plant in this thesis. Mutants of *Col-0* are listed in Table 7. For transient expression of proteins *Nicotiana benthamiana* was used.

Table 7 Mutants of *Col-0*

Listed are the mutants used in thesis. *acr4-2* and *cle40-2* are transgenic T-DNA insertion lines. The mutant *cle40-2* carries a point mutation leading to a stop codon in exon 3.

Mutants of *Col-0*	Type of mutation	Reference
acr4-2	T-DNA insertion	Gifford et al., 2003
cle40-2	Point mutation	Stahl et al., 2009
wox5-1	T-DNA insertion	SALK_038262

3.2 Methods

3.2.1 Software

Images were analyzed and processed with ImageJ (Image processing and analysis in Java) and Carl Zeiss ZEN 2011. Digital analysis of DNA and protein sequences was done with VectorNTI (Invitrogen). For large scale processing of protein sequences protein-protein Blast and for parsing of data scripts written in phyton were used. Experimental data was organized with Microsoft Excel 2010 and Microsoft PowerPoint 2010. Literature cited was organized and formatted with EndNoteX7 from Thomson Reuters and the thesis was written with Microsoft Word 2010.

3.2.2 Web resources

Phytozome (http://phytozome.jgi.doe.gov) was used to download the genomes and proteomes of plant species. To access the genome and proteome of *Arabidopsis thaliana* the web interface of TAIR http://www.arabidopsis.org) was used. To analyze protein sequences the “sequence manipulation suite” (http://www.bioinformatics.org/sms2/) was used (Stothard, 2000). To predict cis-acting elements inside the 5’ upstream regulating sequence of *A. thaliana* the “Arabidopsis cis-regulatory element database” on the Arabidopsis Gene Regulatory Information Server (http://arabidopsis.med.ohio-state.edu) was used. Multiple Em for Motif Elicitation (http://meme-suite.org/) was employed to search for conserved motifs in the 5’ upstream regulating sequence of *ACR4* orthologs. The subcellular localization of At1g32730 was predicted with the *Arabidopsis* Subcellular Localization Prediction Server (http://bioinfo3.noble.org/AtSubP) and the nuclear localization signal in the protein sequence of At1g32730 was predicted with Sequential Pattern Mining Algorithm for Nuclear Localization Signals (http://mleg.cse.sc.edu/seqNLS). To access gene expression data the Arabidopsis eFP Browser (http://bar.utoronto.ca/efp/cgi-bin/efpWeb.cgi) was used. To identify conserved domains inside proteins the Protein Families Database B (http://pfam.xfam.org/) and the Plant Transcription Factor Database v3.0 (http://planttfdb.cbi.pku.edu.cn/) were employed.

3.2.3 Plant growth conditions

Arabidopsis plants were grown in climate chambers under continuous light at 21 °C either in pots filled with soil or in square petri dishes containing GM. Petri dishes were placed vertical into the climate chambers with the surface of the media perpendicular to the gravitation axis. *Nicotiana* plants were grown in the greenhouse under controlled conditions.

3.2.4 Sterilization and stratification of seeds

Seeds were sterilized in 1.5 ml microcentrifuge tubes with the vapor-phase sterilization method as described in Clough and Bent, 2000 (Clough and Bent, 2000). After sterilization seeds were embedded with 0.1 % (m/v) agarose solution and stored at 4°C for 2 days in the dark. After stratification, seeds were plated on sterile GM in square petri dishes for *in vitro* culture.

3.2.5 Analysis of reporter expression in roots with a confocal laser scanning microscope

5 days after germination (dag) roots of transgenic *Arabidopsis* seedlings were chopped off with a razor blade and analyzed with a confocal laser-scanning microscope (CLSM). Roots of plants expressing yellow fluorescent protein (YFP) or the fluorophore Venus were stained with 10µM propidium iodide for visualization of the cell walls. Emission of propidium iodide and the fluorescent reporters was detected using the CLSM system "LSM780" (Zeiss) with appropriate settings. For emission quantification of the fluorophore tandem-Tomato, all images were taken with the same settings. The mean grey values of the images were then analyzed with the software imageJ.

3.2.6 Crossbreeding of *Arabidopsis thaliana*

To cross breed two different plants, flowers of the acceptor-plant were emasculated prior to fertility to prevent self-fertilization. Then pollen of the donor-plant was transferred to the stigma of the acceptor-plant. After 1 day the procedure was repeated.

3.2.7 Transformation of *Arabidopsis thaliana*

Agrobacterium-mediated transformation of *A. thaliana* was carried out using the floral dip method as described in Clough and Bent, 1998 (Clough and Bent, 1998).

3.2.8 Selection of transgenic *A. thaliana* seedlings

Seeds of transformed *A. thaliana* plants were sown on sterile GM containing 20µg/ml Hygromycin. After 8-14 days, resistant plants were transferred to soil.

3.2.9 Transient transformation of *Nicotiana benthamiana*

Transient transformation of *N. benthamiana* was carried out as described in Bleckman et al. 2010 (Bleckmann, 2010).

3.2.10 Transformation of *E. coli* and *A. tumefaciens*

Transformation of *E. coli* (One Shot® TOP10 and One Shot® ccdB Survival™ 2 T1R) was carried out according to manufacturer's instructions and transformation of *A. tumefaciens* was done with the thawing-freezing method as previously described (Höfgen and Willmitzer, 1988).

3.2.11 Basic molecular methods

Unless otherwise stated, basic molecular methods like DNA precipitation and amplification of DNA by PCR were carried out according to protocols from Sambrook et al., 1989 (Sambrook et al., 1989).

3.2.11.1 Isolation of genomic DNA from plants

Isolation of genomic DNA (gDNA) from plants was carried out according to the protocol from Dellaporta, 1983 (Dellaporta et al., 1983).

3.2.11.2 Isolation of plasmid DNA from *E. coli*

Isolation of plasmids from *E*. *coli* was carried out using the peqGOLD Plasmid Miniprep Kit I (peqlab; http://www.peqlab.de) according to manufacturer's instructions.

3.2.11.3 Isolation of RNA from *E. coli*

Isolation of total ribonucleic acid (RNA) from *E*. *coli* was carried out using the RNeasy Plant Mini Kit (Qiagen, https://www.qiagen.com) according to manufacturer's instructions.

3.2.11.4 Synthesis of complementary DNA

For complementary DNA (cDNA) synthesis via reverse transcription SuperScriptII (Thermo Scientific) was used according to manufacturer's instructions.

3.2.11.5 Purification of DNA from agarose gels

Purification of DNA from agarose gels was carried out using the peqGOLD Gel Extraction Kit (peqlab) according to manufacturer's instructions.

3.2.11.6 Purification of DNA from PCR reactions

Purification of DNA from PCR reactions were carried out using the peqGOLD MicroSpin Cycle-Pure Kit (peqlab) according to manufacturer's instructions.

3.2.11.7 Measurement of DNA and RNA concentrations

Measurement of DNA and RNA concentrations was carried out by absorption measurements with the spectrophotometer NanoDrop 2000c (Thermo Scientific) using default built-in profiles.

3.2.12 Cloning

Cloning was done either by restriction and ligation, overlap extension PCR, gateway cloning, or by combination of these methods. All plasmids were sequenced by a third-party service (Sequence Laboratories Göttingen GmbH, http://www.seqlab.de)

3.2.12.1 Gateway cloning

Gateway cloning (Thermo Scientific) was done according to manufacturers' instructions. Entry vectors were cloned by BP recombinations, by using the pENTR™/SD/D-TOPO® Cloning Kit (Thermo Scientific) or the MultiSite Gateway® Pro 3.0 Kit (Thermo Scientific).

3.2.12.2 Cloning by restriction and ligation

If not otherwise stated cloning by restriction and ligation was done with a standard protocol. Therefore the target plasmid and its DNA insert were incubated with the same (combination of) restriction enzyme(s) according to the manufacturer's instructions. After gel purification, the plasmid and its insert were mixed in a 1:3 molar ratio and incubated with T4 DNA Ligase (New England Biolabs) according to manufacturer's instructions. After transformation into competent *Escherichia coli* (One Shot® TOP10) cells, the bacteria were selected for bacteria colonies harboring the correct plasmid.

3.2.12.3 Overlap extension PCR

To delete or mutate specific regions in a DNA sequence of interest overlap extension PCR was employed as described in Atanassov et al. 2009 (Atanassov et al. 2009). As template, Entry clones were used with attL-gateway-sites flanking the target sequence. As forward primer binding upstream (5') of the attL1 site, oligonucleotide OVE_F was used and as reverse primer, binding downstream (3') of the attL2 site, OVE_R was used. In a first step two overlapping fragments (fragment A and fragment B) were amplified, carrying the deletion or mutation. For fragment A, OVE_F and a target specific revers primer was used and for fragment B, OVE_R and a target specific forward primer. After gel purification of the fragments a second PCR was done with equimolar amounts of fragment A and B. In this PCR no additional oligonucleotides were added and each fragment type served as a primer for the other fragment type. After this second PCR the PCR products were purified and the entire eluate was used in a gateway LR recombination reaction with a destination vector of choice. After recombination the reaction volume was transformed into *E. coli* One Shot® TOP10 cells.

3.2.12.4 Cloning of Entry vectors *pACR4_P1 (pAH22), pACR4_P2 (pAH23), pACR4_P3 (pAH24), pACR4_P4 (pAH25), pACR4_P5 (pAH26), pACR4_P6 (pAH27), pACR4_P7 (pAH28), pACR4_P8 (pAH29), pACR4_P9 (pAH30), pACR4_P10 (pAH31)* and *pACR4-UTR (pAH32)*

The 5' upstream regulating sequence of *ACR4* was amplified from genomic DNA of *A. thaliana* with oligonucleotides pACR4_P1_F and pACR4_R. The PCR product was then used in a TOPO cloning reaction to generate the entry vector *pACR4_P1* (pAH22). This plasmid served as a template in further PCRs to amplify promoter versions of ACR4 with different length. The used oligonucleotide combinations for each PCR are shown in Table 8. The different promoters were then used in TOPO cloning reactions to build the Entry vectors *pACR4_P2* (*pAH23*), *pACR4_P3* (*pAH24*), *pACR4_P4* (*pAH25*), *pACR4_P5* (*pAH26*), *pACR4_P6* (*pAH27*), *pACR4_P7* (*pAH28*), *pACR4_P8* (*pAH29*), *pACR4_P9* (*pAH30*), *pACR4_P10* (*pAH31*) and pACR4-UTR (*pAH32*).

Table 8 Oligonucleotides used for cloning of pAH22 - pAH32

Name of vector	Oligonucleotide used as forward primer	Oligonucleotide used as reverse primer
pACR4_P1 (pAH22)	pACR4_P1_F	pACR4_R
pACR4_P2 (pAH23)	pACR4_P2_F	pACR4_R
pACR4_P3 (pAH24)	pACR4_P3_F	pACR4_R
pACR4_P4 (pAH25)	pACR4_P4_F	pACR4_R
pACR4_P5 (pAH26)	pACR4_P5_F	pACR4_R
pACR4_P6 (pAH27)	pACR4_P6_F	pACR4_R
pACR4_P7 (pAH28)	pACR4_P7_F	pACR4_R
pACR4_P8 (pAH29)	pACR4_P8_F	pACR4_R
pACR4_P9 (pAH30)	pACR4_P9_F	pACR4_R
pACR4_P10 (pAH31)	pACR4_P10_F	pACR4_R
pACR4-UTR (pAH32)	pACR4_P1_F	pACR4-UTR_R

3.2.12.5 Cloning of Expression vectors *pACR4_P1:Venus-H2B (pAH33), pACR4_P2:Venus-H2B (pAH34), pACR4_P3:Venus-H2B (pAH35), pACR4_P4:Venus-H2B (pAH36), pACR4_P5: Venus-H2B (pAH37), pACR4_P6:Venus-H2B (pAH38), pACR4_P7:Venus-H2B (pAH39), pACR4_P8:Venus-H2B (pAH40), pACR4_P9:Venus-H2B (pAH41), pACR4_P10:Venus-H2B (pAH42)* and *pACR4-UTR:Venus-H2B (pAH43)*

The expression vectors were cloned by a LR recombination of the destination vector *GW:Venus-H2B* (*pAB146*) with the Entry vectors listed in Table 8.

3.2.12.6 Cloning of Expression vectors *pACR4ΔE8:Venus-H2B (pAH44), pACR4ΔE7+E8:Venus-H2B (pAH45), pACR4ΔE6+E7+E8:Venus-H2B (pAH46), pACR4ΔE6+E8:Venus-H2B (pAH47)* and *pACR4ΔE8 Entry (pAH48)*

Plasmids *pAH44*, *pAH45* and *pAH46* were cloned through overlap extension PCR using *pACR4_P1* (*pAH22*) as a template. For each constructs two overlapping fragments (fragment A and fragment B) were amplified with oligonucleotides listed in Table 9. These fragments were then used as templates for overlap extension PCR without additional oligonucleotides. After purification, the final PCR reaction was used in a LR recombination together with *GW:Venus-H2B* (*pAB146*). For *pACR4ΔE8 Entry* (*pAH48*) the expression vector *pACR4ΔE8:Venus-H2B* (*pAH44*) was used in a BP reaction together with the donor vector *pDONR201*. Plasmid *pACR4ΔE6+E8:Venus-H2B* (*pAH47*) was cloned by overlap extension PCR using *pACR4ΔE8 Entry* (*pAH48*) as template with oligonucleotides listed in Table 9, followed by LR recombination with *pAB146*.

Table 9 Oligonucleotides used for cloning of *pAH44 – pAH47*

Name of vector	Used template	Oligonucleotide used as forward primer	Oligonucleotide used as reverse primer	Fragment type
pACR4ΔE8:Venus-H2B (*pAH44*)	*pAH22*	OVE_F	ACR4_P7_OVE9_R	A
pACR4ΔE8:Venus-H2B (*pAH44*)	*pAH22*	ACR4_P9_OVE7_F	OVE_R	B
pACR4ΔE7+E8:Venus-H2B (*pAH45*)	*pAH22*	OVE_F	ACR4_P6_OVE9_R	A
pACR4ΔE7+E8:Venus-H2B (*pAH45*)	*pAH22*	ACR4_P9_OVE6_F	OVE_R	B
pACR4ΔE6+E7+E8:Venus-H2B (*pAH46*)	*pAH22*	OVE_F	ACR4_P5_OVE9_R	A
pACR4ΔE6+E7+E8:Venus-H2B (*pAH46*)	*pAH22*	ACR4_P9_OVE5_F	OVE_R	B

pACR4ΔE6+E8:Venus-H2B (*pAH47*)	*pAH48*	OVE_F	ACR4_OVE_5-7_R	A
pACR4ΔE6+E8:Venus-H2B (*pAH47*)	*pAH48*	ACR4_OVE_5-7_F	OVE_R	B

3.2.12.7 Construction of *ASCI:ACR4-Venus (pAH48), pACR4_P1 :ACR4-Venus (pAH50), pACR4ΔE8:ACR4-Venus (pAH51)* and *pACR4ΔE6+E7+E8:ACR4-Venus (pAH52)*

For *ASCI:ACR4-Venus* (*pAH48*), the destination vector *GW:Venus* (*pAB130*) was LR recombined with *ACR4 Entry* (*pAH06*) (Hülsewede 2010). The resulting plasmid and its corresponding inserts were cut with the restriction enzyme ASCI and ligated. Inserts were amplified with oligonucleotides ACR4_ASCI_F and ACR4_ASCI_R. As templates *pAH22* (for *pAH50*), *pAH44* (for *pAH51*) and *pAH22* (for *pAH52*) were used.

3.2.12.8 Cloning of *pACR4_AREI_mut:Venus-H2B (pAH53), pACR4_AREII_mut:Venus-H2B (pAH54), pACR4_WUS_mut:Venus-H2B (pAH55), pACR4_AREI+WUS_mut:Venus-H2B (pAH56), pACR4_WUS+AREII_mut:Venus-H2B (pAH57), pACR4_AREI+WUS+AREII_mut: Venus-H2B (pAH58), pACR4_WUS_mut Entry (pAH59)* and *pACR4_AREI+WUS_mut Entry (pAH60)*

All expression vectors were cloned by overlap extension PCR with oligonucleotides listed in Table 10, followed by LR reactions with *pAB146*. Plasmids *pACR4_WUS_mut Entry* (*pAH59*) and *pACR4_AREI+WUS_mut Entry* (*pAH60*) were constructed by a BP recombination reactions of *pAH55* and *pAH56* with pDONR 201, respectively.

Table 10 Oligonucleotides used for cloning of *pAH53 – pAH58*

Name of vector	Used template	Oligonucleotide used as forward primer	Oligonucleotide used as reverse primer	Fragment type
pACR4_AREI_mut:Venus-H2B (*pAH53*)	*pAH22*	OVE_F	ARE1-mut_R	A
pACR4_AREI_mut:Venus-H2B (*pAH53*	*pAH22*	ARE1-mut_F	OVE_R	B
pACR4_AREII_mut:Venus-H2B (*pAH54*)	*pAH22*	OVE_F	ARE2_mut_R	A
pACR4_AREII_mut:Venus-H2B (*pAH54*)	*pAH22*	ARE2_mut_F	OVE_R	B
pACR4_WUS_mut:Venus-H2B (*pAH55*)	*pAH22*	OVE_F	WUS-Box-mut_R	A
pACR4_WUS_mut:Venus-H2B (*pAH55*)	*pAH22*	WUS-Box-mut_F	OVE_R	B
pACR4_AREI+WUS_mut:Venus-H2B (*pAH56*)	*pAH59*	OVE_F	ARE1-mut_R	A
pACR4_AREI+WUS_mut:Venus-H2B (*pAH56*)	*pAH59*	ARE1-mut_F	OVE_R	B
pACR4_WUS+AREII_mut:Venus-H2B (*pAH57*)	*pAH59*	OVE_F	ARE2_mut_R	A
pACR4_WUS+AREII_mut:Venus-H2B (*pAH57*)	*pAH59*	ARE2_mut_F	OVE_R	B
pACR4_AREI+WUS+AREII_mut:Venus-H2B (*pAH58*)	*pAH60*	OVE_F	ARE2_mut_R	A
pACR4_AREI+WUS+AREII_mut:Venus-H2B (*pAH58*)	*pAH60*	ARE2_mut_F	OVE_R	B

3.2.12.9 Cloning of *pACR4ΔS1:Venus-H2B (pAH61)*, *pACR4ΔS2:Venus-H2B (pAH62)*, *pACR4ΔS3:Venus-H2B (pAH63)*, *pACR4ΔS4:Venus-H2B (pAH64)*, *pACR4ΔS5:Venus-H2B (pAH65)*, *pACR4ΔS6:Venus-H2B (pAH66)*, *pACR4ΔS7:Venus-H2B (pAH67)*, *pACR4ΔS8:Venus-H2B (pAH68)*, *pACR4ΔS9:Venus-H2B (pAH69)*, *pACR4ΔS10:Venus-H2B (pAH70)* and *pACR4ΔS11:Venus-H2B (pAH71)*

All expression vectors were cloned by overlap extension PCR with oligonucleotides listed in table Table 11 followed by LR reactions with *pAB146*. Plasmid *pAH22* was used as a template.

Table 11 Oligonucleotides used for cloning of *pAH61* – *pAH71*

Name of vector	Oligonucleotide used as forward primer	Oligonucleotide used as reverse primer	Fragment type
pACR4ΔS1:Venus-H2B (*pAH61*)	OVE_F	pACR4ΔS1_R	A
pACR4ΔS1:Venus-H2B (*pAH61*)	pACR4ΔS1_F	OVE_R	B
pACR4ΔS2:Venus-H2B (*pAH62*)	OVE_F	pACR4ΔS2_R	A
pACR4ΔS2:Venus-H2B (*pAH62*)	pACR4ΔS2_F	OVE_R	B
pACR4ΔS3:Venus-H2B (*pAH63*)	OVE_F	pACR4ΔS3_R	A
pACR4ΔS3:Venus-H2B (*pAH63*)	pACR4ΔS3_F	OVE_R	B
pACR4ΔS4:Venus-H2B (*pAH64*)	OVE_F	pACR4ΔS4_R	A
pACR4ΔS4:Venus-H2B (*pAH64*)	pACR4ΔS4_F	OVE_R	B
pACR4ΔS5:Venus-H2B (*pAH65*)	OVE_F	pACR4ΔS5_R	A
pACR4ΔS5:Venus-H2B (*pAH65*)	pACR4ΔS5_F	OVE_R	B
pACR4ΔS6:Venus-H2B (*pAH66*)	OVE_F	pACR4ΔS6_R	A
pACR4ΔS6:Venus-H2B (*pAH66*)	pACR4ΔS6_F	OVE_R	B
pACR4ΔS7:Venus-H2B (*pAH67*)	OVE_F	pACR4ΔS7_R	A
pACR4ΔS7:Venus-H2B (*pAH67*)	pACR4ΔS7_F	OVE_R	B
pACR4ΔS8:Venus-H2B (*pAH68*)	OVE_F	pACR4ΔS8_R	A
pACR4ΔS8:Venus-H2B (*pAH68*)	pACR4ΔS8_F	OVE_R	B
pACR4ΔS9:Venus-H2B (*pAH69*)	OVE_F	pACR4ΔS9_R	A
pACR4ΔS9:Venus-H2B (*pAH69*)	pACR4ΔS9_F	OVE_R	B
pACR4ΔS10:Venus-H2B (*pAH70*)	OVE_F	pACR4ΔS10_R	A
pACR4ΔS10:Venus-H2B (*pAH70*)	pACR4ΔS10_F	OVE_R	B
pACR4ΔS11:Venus-H2B (*pAH71*)	OVE_F	pACR4ΔS11_R	A
pACR4ΔS11:Venus-H2B (*pAH71*)	pACR4ΔS11_F	OVE_R	B

3.2.12.10 Cloning of *pACR4ΔB1:Venus-H2B (pAH72)*, *pACR4ΔB2:Venus-H2B (pAH73)*, *pACR4ΔB3:Venus-H2B (pAH74)*, *pACR4ΔB4:Venus-H2B (pAH75)*, *pACR4ΔB5:Venus-H2B (pAH76)* and *pACR4ΔB6:Venus-H2B (pAH77)*

All expression vectors were cloned by overlap extension PCR with oligonucleotides listed in table Table 12 and LR reaction with *pAB146*. Plasmid *pAH22* was used as a template.

Table 12 Oligonucleotides used for cloning of *pAH72 – pAH77*

Name of vector	Oligonucleotide used as forward primer	Oligonucleotide used as reverse primer	Fragment type
pACR4ΔB1:Venus-H2B (*pAH72*)	OVE_F	pACR4ΔB1_R	A
pACR4ΔB1:Venus-H2B (*pAH72*)	pACR4ΔB1_F	OVE_R	B
pACR4ΔB2:Venus-H2B (*pAH73*)	OVE_F	pACR4ΔB2_R	A
pACR4ΔB2:Venus-H2B (*pAH73*)	pACR4ΔB2_F	OVE_R	B
pACR4ΔB3:Venus-H2B (*pAH74*)	OVE_F	pACR4ΔB3_R	A
pACR4ΔB3:Venus-H2B (*pAH74*)	pACR4ΔB3_F	OVE_R	B
pACR4ΔB4:Venus-H2B (*pAH75*)	OVE_F	pACR4ΔB4_R	A
pACR4ΔB4:Venus-H2B (*pAH75*)	pACR4ΔB4_F	OVE_R	B
pACR4ΔB5:Venus-H2B (*pAH76*)	OVE_F	pACR4ΔB5_R	A
pACR4ΔB5:Venus-H2B (*pAH76*)	pACR4ΔB5_F	OVE_R	B
pACR4ΔB6:Venus-H2B (*pAH77*)	OVE_F	pACR4ΔB6_R	A
pACR4ΔB6:Venus-H2B (*pAH77*)	pACR4ΔB6_F	OVE_R	B

3.2.12.11 Cloning of *pACR4ΔA/B:Venus-H2B (pAH78), pACR4ΔB/C:Venus-H2B (pAH79)* and *pACR4ΔB:Venus-H2B (pAH80)*

All expression vectors were cloned by overlap extension PCR with oligonucleotides listed in table Table 13 and LR reaction with *pAB146*. Plasmid *pAH22* was used as a template.

Table 13 Oligonucleotides used for cloning of *pAH78 – pAH80*

Name of vector	Oligonucleotide used as forward primer	Oligonucleotide used as reverse primer	Fragment type
pACR4ΔA/B:Venus-H2B (*pAH78*)	OVE_F	pACR4ΔA/B_R	A
pACR4ΔA/B:Venus-H2B (*pAH78*)	pACR4ΔA/B_F	OVE_R	B
pACR4ΔB/C:Venus-H2B (*pAH79*)	OVE_F	pACR4ΔB/C_R	A
pACR4ΔB/C:Venus-H2B (*pAH79*)	pACR4ΔB/C_F	OVE_R	B
pACR4ΔB:Venus-H2B (*pAH80*)	OVE_F	pACR4ΔB_R	A
pACR4ΔB:Venus-H2B (*pAH80*)	pACR4ΔB_F	OVE_R	B

3.2.12.12 Construction of *pACR4ΔA/C1 Entry (pAH81), pACR4ΔA/C2 Entry (pAH82), pACR4ΔA/C1:Venus-H2B (pAH83)* and *pACR4ΔA/C2:Venus-H2B(pAH84)*

For *pAH81* and *pAH82* synthesized DNA fragments of *pACR4* were ordered (Thermo Scientific®) in which Domain A/C1 and Domain A/C2 were deleted, respectively. These fragments and the entry vector *pAH22* were cut with restriction endonucleases XhoI and BglII. The linearized entry vector was separated from its wild type DNA insert through electrophoresis and ligated with the synthesized DNA pieces. The plasmids *pAH81* and *pAH82* were then LR recombined with *pAB146* giving rise to *pACR4ΔA/C1:Venus-H2B* (*pAH83*) and *pACR4ΔA/C2:Venus-H2B*(*pAH84*).

3.2.12.13 Construction of *E7-48CaMV Entry (pAH85), E7-60CaMV Entry (pAH86), E7+E8-48CaMV Entry (pAH87), E7+E8-60CaMV Entry (pAH88)* and *-60CaMV Entry (pAH89)*

The plasmids *pAH85*, *pAH86*, *pAH87* and *pAH88* were cloned by adding the last 48bp or 60bp of the *35S CaMV* promoter 3' to the corresponding DNA elements (*E7* or *E7+E8* of *pACR4*) by PCR. The minimal promoters *E7-60CaMV and E7+E8-60CaMV* were cloned in 3 consecutive PCR reactions using *pAH22* as template and oligonuctides pACR4_P7_F as a forward primer and E7_60mini35S_ad1_R or E8_60mini_35S_ad1_R as reverse primer, respectively. After purification of the PCR products, they were used as templates for the second PCR with pACR4_P7_F and -60mini_35S_ad2_R . In a last PCR step the products of the second PCR were used as templates with oligonucleotides pACR4_P7_F and 35S_ad3_R. The Minimal promoters *E7-48CaMV* and *E7+E8-48CaMV* were cloned in 2 consecutive PCR steps, using *pAH22* as template and oligonuctides pACR4_P7_F and E7-48_mini35S_ad1_R or E8-48mini35S_ad1_R as reverse primer, respectively. The PCR products of the first reaction were used after purification in a second PCR with pACR4_P7_F and 35S_ad3_R. All 4 promoter versions were then integrated into a donor vector by TOPO cloning. Plasmid *-60CaMV Entry* (*pAH89*) was cloned by amplifying the last 60bp of the *35S CaMV* promoter with attB1 and attB2 sequences by PCR, followed by a BP cloning reaction with pDONR201. As oligonucleotides attB1 -60 minimal_F and attB2 -60 minimal_R were used and *pAH86* served as template.

3.2.12.14 Cloning of *E7-48CaMV:Venus-H2B (pAH90), E7-60CaMV:Venus-H2B (pAH91), E7+E8-48CaMV:Venus-H2B (pAH92), E7+E8-60CaMV:Venus-H2B (pAH93)* and *-60CaMV:Venus-H2B (pAH94)*

The expression vectors *pAH90, pAH91, pAH92, pAH93 and pAH94* were cloned by LR recombination using entry vectors *pAH85, pAH86, pAH87, pAH88* and *pAH89* together with *pAB146*, respectively.

3.2.12.15 Cloning of *pPTA-Mini:Luc (pAH95)*

The plasmid *pAH95* was cloned by adding the last 60bp of the *35S CaMV* promoter 3' to element (*1/2E6_+E7+_1/2E8* of *pACR4*) by PCR. Therefore 3 consecutive PCR reactions were performed. In the first PCR, oligonucleotides PTA-K1-60S_EcoRI_F and PTA-K1-add1_60S_R were used, while *pAH22* served as a template. The purified PCR product of the first PCR was used as a template in the second PCR with oligonucleotides PTA-K1-60S_EcoRI_F and AH_PTA-K1-add2_60S_R. In the final PCR, oligonucleotides PTA-K1-60S_EcoRI_F and PTA-K1-add2_60S_NcoI_R were used. After restriction of *pBT10* and the DNA insert with restriction endonucleases EcoRI and NcoI, insert and vector were ligated.

3.2.12.16 Construction of *pPTA-pACR4_P1:Luc (pAH96)*

pAH96 was cloned by insertion of a restricted DNA insert into *pBT10* (linearized with NCOI and EcoRI) followed by ligation. For amplification of the insert oligonucleotides PTA3_EcoRI_F and PTA3_NCOI_R were used and *pAH22* served as template.

3.2.12.17 Construction of *BTA stop Entry (pAH97), BTA Entry (pAH98), ind::BTA-Cerulean (pAH99), ind::BTA (pAH100)*

pAH97 was cloned by amplification of *BTA* from genomic DNA with stop codon using oligonucleotides Berta_Topo_F and Berta_R. *pAH98* was cloned by amplification of the CDS of *BTA* without stop codon from cDNA. For this PCR oligonucleotides Berta_Topo_F and Berta_without_Stop_R were used. The PCR products of both reactions were purified and integrated into a donor vector through TOPO cloning. Expression vector *pAH99* was cloned by LR recombination of *pAH98* with *pAB131* (*ind::GW-Cerulean*). Expression vector *pAH100* was cloned by LR recombination of *pAH97* with *pAB111* (*ind::GW*).

3.2.12.18 Cloning of *ind::BTAΔZincF-Cerulean (pAH101)*

pAH101 was cloned by overlap extension PCR with oligonucleotides OVE_F and Berta_del_zinc_R for construction of fragment A and Berta_del_zinc_F + OVE_R for fragment B. After overlap extension the final product was LR recombined with *pAB131*.

3.2.12.19 Cloning of *TMO6 Entry (pAH102)* and *ind::TMO6-Cerulean (pAH103)*

pAH102 was cloned by amplification of the CDS of *TMO6* without stop codon from cDNA using oligonucleotides TMO6_Topo_F and TMO6_R.

3.2.12.20 Cloning of *pACR4_P1:Fluc (pAH104), pACR4_P4:Fluc (pAH105), pACR4_P7:Fluc (pAH106), pACR4_P8:Fluc (pAH107), pACR4-UTR:Fluc (pAH108)* and *pACR4ΔE6+E7+E8:Fluc (pAH109)*

To clone *pAH104, pAH105*, *pAH106, pAH107*, *pAH108* and *pAH109*, the plasmid *pGreenII_0800Luc* was cut with restriction enzymes KpnI and BAMHI. After de-phosphorylation and purification, the linearized plasmid was ligated with corresponding DNA inserts, which were cut with the same restriction enzymes. The inserts were amplified from *pAH22* (except for *pAH109*) through PCR with primer listed in Table 14. For *pAH109* the plasmid *pAH46* was used as template.

Table 14 Oligonucleotides used for cloning of *pAH104 – pAH109*

Name of vector	Oligonucleotide used as forward primer	Oligonucleotide used as reverse primer
pACR4_P1:Fluc (*pAH104*)	pACR4_P1_KpnI_F	pACR4_P1_BAMHI_R
pACR4_P4:Fluc (*pAH105*)	pACR4_P4_KpnI_F	pACR4_P1_BAMHI_R
pACR4_P7:Fluc (*pAH106*)	pACR4_P7_KpnI_F	pACR4_P1_BAMHI_R
pACR4_P8:Fluc (*pAH107*)	pACR4_P8_KpnI_F	pACR4_P1_BAMHI_R
pACR4-UTR:Fluc (*pAH108*)	pACR4_P1_KpnI_F	pACR4-UTR_BAMHI_R
pACR4ΔE6+E7+E8:Fluc (*pAH109*)	pACR4_P1_KpnI_F	pACR4_P1_BAMHI_R

3.2.12.21 Cloning of *pBTA Entry (pAH110)* and *pBTA:Venus-H2B (pAH111)*

A DNA fragment 2500bp upstream of the start codon of At1g32730 was amplified with oligonucleotides pBERTA_geno_F and pBERTA_R by PCR, using genomic DNA of *A. thaliana* as template. This fragment was used in a TOPO cloning reaction to construct *pAH110*. For *pAH111* the entry vector *pAH110* was LR recombined with *pAB146*.

3.2.12.22 Cloning of *GW:H2B-tdTomato (pAH21)* and *pACR4_P1:H2B-tdTomato (pAH112)*

The destination *pAH21* (*GW:H2B-tdTomato*) was cloned by restriction of *pMASNF2* (*GW:tdTomato*, unpublished) and its PCR amplified insert with PacI. After de-phosphorylation and purification of the plasmid, the linearized vector and its insert were ligated. The insert was amplified from *pAH33* using H2B_PacI_F and H2B_PacI_R. For *pAH112* the entry vector pAH22 was LR recombined with destination vector pAH21.

3.2.12.23 Cloning of *pCRR1 (pAH113), pCRR1:Venus-H2B (pAH114), pCRR3 (pAH115)* and *pCRR3:Venus-H2B (pAH116)*

The entry vectors *pAH113* and *pAH115* were cloned through TOPO cloning by amplification of a 948 bp and 2005 bp fragment by PCR from genomic DNA, respectively. For *pAH113* the oligonucleotides pCRR1_F and pCRR1_R were used. For *pAH115* the oligonucleotides pCRR3_F and pCRR3_R were used. The entry vectors were than recombined with *pAB146* resulting in *pCRR1:Venus-H2B* (*pAH114*) and *pCRR3:Venus-H2B* (*pAH116*).

3.2.12.24 Cloning of *pACR4_Y1H-Min P4P1R Entry (pAH117), pACR4_Y1H-Min MW2 (pAH118)* and *pACR4_Y1H-Min MW3 (pAH119)*

The entry vector *pAH117* was clone by amplification of a 300 bp DNA fragment from *pAH95* using the oligonucleotides pACR4_Y1H_attB4_F and pACR4_Y1H_attB1R_R. After gel-purification the fragment

was recombined with the plasmids MW2 and MW3 through a BP recombinase reaction resulting in the plasmids *pAH118* and *pAH119*.

3.2.13 Yeast-one-hybrid (Y1H) screen

The Y1H screen was performed in collaboration according to the protocol described in Gaudinier et al.2011 (Gaudinier et al.2011). Cloning of the DNA baits was done by Adrian Hülsewede, yeast transformation and Y1H screen was performed by Allison Gaudinier and Mallorie Taylor-Teeples.

3.2.14 Protoplast transactivation assay (PTA)

The PTA was performed as a third-party service according to the protocol described in Wehner et al. 2011 (Wehner et al., 2011). Cloning of plasmids was done by Adrian Hülsewede. The transformation of Arabidopsis mesophyll protoplasts and the assay was performed by a service provider.

3.2.15 Luciferase assay in *Nicotina benthamiana*

For this assay *N*. *benthamiana* leafs were transiently transformed with a *pACR4* version of choice conferring firefly luciferase expression (*pAH104*, *pAH105*, *pAH106*, *pAH107*, *pAH108*, pAH109), together with an estradiol inducible transcription factor (*pAH99*, *pAH100*, *pAH101*, *pAH103*, *ind::WOX5-mCherry*). Following transient transformation, gene expression was only induced in one half of the leaf blade (right half induced, left half not induced), thereby each leaf contained its own control. After 13 – 15 hours of induction (overnight) luciferase activity was measured with the NightOwl system (Berthold). As substrate for the luciferase reaction, a 5 mM D-Luciferin potassium salt solution (in H_2O) was used.

4 Results

4.1 Contribution of the ACR4-Kinase domain on CLE40 signaling

Following CLE40 peptide treatment, *ACR4* was shown to be upregulated on the transcriptional level and, furthermore, enhanced protein internalization was observed (Stahl et al., 2013; Stahl and Simon, 2009). Since ACR4 is the proposed receptor for CLE40, this suggests that ACR4 could be involved in an auto regulatory feedback-loop. Alternatively, other receptors could perceive CLE40, leading to an upregulation of *ACR4*. To distinguish between these two possibilities it was tested if upregulation of *ACR4* is dependent on a functional ACR4 protein (see chapter 1.9 and Figure 8 A).

To this end, the same 5' upstream regulating sequence of *ACR4* as used in Stahl et al. 2009 was cloned 5' to the coding region of a nuclear localized version of the tandem-Tomato (tdTomato) fluorophore (*pACR4_P1:H2B-tdTomato*) and transformed into *Arabidopsis thaliana* Col-*0* plants. This reporter line was then crossed into an *acr4-2* mutant background. Additionally, a signaling-inactive version of ACR4 lacking the kinase domain, expressed from its native promoter and tagged with a GFP, was used (*pACR4:ACR4ΔK-GFP*). This translational reporter was shown to be unable to rescue the epidermal seed phenotype of *acr4-2* mutants and also showed reduced internalization by endocytosis in epidermal cells of *Arabidopsis* roots, thereby confirming that it is signaling inactive (Gifford et al. 2005). Both strains were analyzed 5 days after germination (dag) with or without exogenous CLE40 peptide treatment. In the *acr4-2* background, the transcriptional reporter *pACR4_P1:H2B-tdTomato* showed no differences in expression strength between the plants grown on growth media (GM) or on GM supplemented with 200nM synthetic CLE40 peptide (Figure 8 B). This indicates that *ACR4* upregulation depends on a functional ACR4 protein. However, with the non-functional translational reporter *pACR4:ACR4ΔK-GFP* significant upregulation of GFP signal intensity could be observed following CLE40-treatment. While this finding was unexpected, an explanation for this result is that the ACR4ΔK version of ACR4 is still able to build complexes with its co-receptor CLV1 and that these receptor complexes are still signaling active via the CLV1 kinase and can compensate for the missing ACR4 kinase in our growth conditions (Stahl et al., 2013).

4.2 Influence of *ACR4*, *WOX5* and *CLE40* on *ACR4* expression

To further analyze how *ACR4* expression is controlled in the context of CLE40-signaling, the *pACR4_P1:H2B-tdTomato* reporter was subsequently crossed into *wox5* and *cle40* mutant backgrounds. In *acr4-2*, *wox5-1* and *cle40-2* mutants no change in *ACR4* expression could be observed compared to the *Col-0* wild type control (Figure 8 C It was then tested if overexpression of *WOX5* influences *ACR4* expression. Therefore an inducible version of *WOX5*

(*WOX5-GR*) was crossed into the *pACR4:H2B-tdTomato* line. *WOX5* expression was then induced for 24 hours, leading to a significant upregulation of the *ACR4* reporter by 21 % (Figure 8 D). Therefore, it appears, that basal expression of *ACR4* is independent of ACR4, WOX5 and CLE40, since mutations in any of these gene had no impact on *ACR4* reporter expression. However, ectopic overexpression of *WOX5*, as well as treatment with exogenous CLE40-peptide resulted in upregulation of *ACR4* expression, indicating that CLE40-WOX5 pathway activity does at least indirectly affect *ACR4* expression.

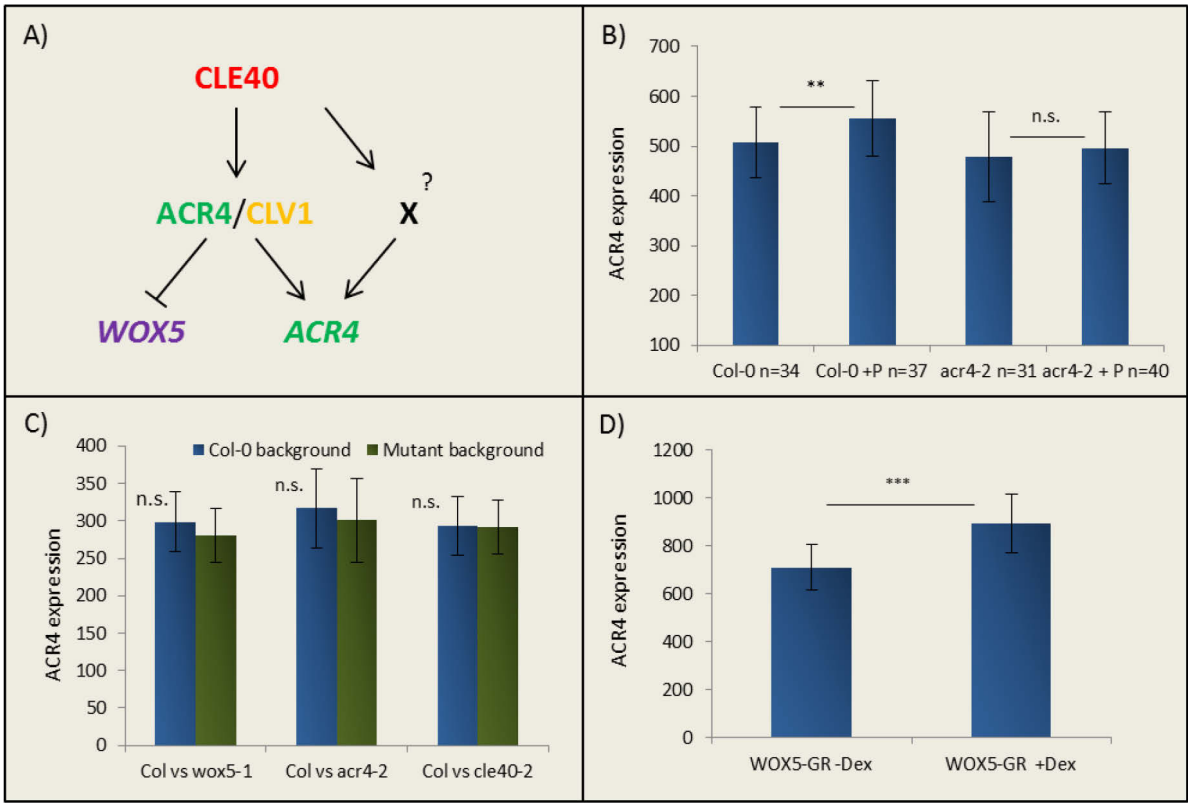

Figure 8 ACR4 is involved in a CLE40-dependent auto regulatory feedback-loop, but basal ACR4 expression is independent of ACR4, WOX5

A) Model of *ACR4* upregulation after CLE40 peptide treatment: Upregulation of *ACR4* could be ACR4-dependent, whereas *WOX5* repression was previously shown to be ACR4 dependent.

B) *ACR4* expression (mean gray value of *pACR4:H2B-tdTomato*) in Col-*0* and *acr4-2* mutants with (+P) or without CLE40 petide treatment. In Col-*0* peptide treatment leads to upregulation of the reporter. In *acr4-2* mutants this upregulation is lost.

C) Comparrison of *ACR4* expression in Col-*0*, *acr4-2* and *wox5-1*: In all mutant backgrounds no significant change (n.s.) in expression could be observed in comparrison to the corresponding wild type control.

D) *ACR4* expression before (-Dex) and after induction (+Dex) of *WOX5*: 24 h after induction of *WOX5 ACR4* expression was upregulated by 21%.

Seedlings grown on GM with 200nM synthetic CLE40 peptide are marked with "+P" and induction of WOX5 was done by treatment with dexamethasone for 24 hours "+Dex" or without treatment "-Dex". Quantification of *ACR4* expression was done by comparing mean grey values. Error bars represent standard diviation and significance was calculated via student's t test. p = 0,01 ≙ **; p= 0,001 ≙ ***; n.s. ≙ not sicnificant

4.3 Promoter analysis of *ACR4*

To identify cis-acting elements within the 5' upstream regulating sequence of ACR4 a detailed promoter analysis was performed. The full-length promoter was defined as the 1925 bp intergenic region between the stop codon of the 5' located gene AT3G59430 and the start codon of ACR4, and will be referred to as *pACR4_P1*. This promoter was shown to drive expression of a H2B-YFP reporter in a pattern overlapping with RNA *in situ* data (Gifford et al., 2003; Tanaka et al., 2002). Furthermore, *pACR4_P1:ACR4*, or *pACR4_P1:ACR4-GFP* constructs complement *acr4-2* mutants regarding their epidermal seed phenotype (Gifford et al., 2005). Based on these results it can be assumed that this promoter version harbors all cis-acting elements necessary for wild type expression

4.3.1 Promoter composition and predicted cis-acting elements

The 1925bp long promoter of *ACR4* can be divided into a 1442bp long region upstream of the transcriptional start site and a 483bp long 5' untranslated region (UTR) (The Arabidopsis Information Resource; TAIR) (Figure 9 A). The 5' UTR contains 4 upstream open reading frames (uORFs) of variable sizes. The uORF1 beginning -380bp from the translational start site, consist of a start codon immediately followed by a stop codon, uORF2 (-375bp) is the longest coding region comprising 30 codons, uORF3 (-150bp) consists of 10 codons and uORF4 (-55bp) has 14 codons. In a first step to identify potential binding sites for transcription factors (TF), an *in silico* analysis of the *pACR4_P1* promoter sequence with the Arabidopsis cis-regulatory element database (AtcisBD) on the Arabidopsis Gene Regulatory Information Server (AGRIS) (Sun et al. 2003; Ylmaz et al. 2011) was performed. This analysis revealed several predicted cis-elements (Figure 9 A). Among those, the L1-box, auxin response elements (AREs) and the WUS-binding sites were considered as specifically interesting for the following reasons. The L1-box was previously shown to be essential for epidermal expression of *ACR4* in a PROTODERMAL FACTOR 2 (PDF2) and ARABIDOPSIS THALIANA MERISTEM LAYER 1 (AtML1) dependent manner (San-Bento et al., 2014). The AREs could provide a link to the previously described auxin-dependent regulation of ACR4 and the WUS-binding site could function as a cis-acting element for WOX5 (Wink, 2013).

4.3.2 Functionality of the predicted WUS binding site and its adjacent AREs

The predicted AREs and WUS-binding sites were tested for their ability to manipulate *ACR4*-expression *in vivo*. For this, the two AREs located at -1039 bp and -832 bp upstream of the start codon of *ACR4* and the WUS-binding site at -892 bp were mutated by introducing point mutations. The original ARE sequence of "TGTCTC" was mutated to "ACCAAG" and the WUS-binding site, with the sequence of "CCATTA", was mutated to "GACCAG".

The WUS-binding-site is situated between the two AREs (AREI and AREII) and offers a possibility of cross-regulation between auxin- and WOX5-signaling, as WOX5 and potential auxin response factors (ARFs) would have to compete for binding to this site (Figure 9 B). It was also shown that some AREs are needed but not sufficient for auxin responsiveness in combination with a core promoter (Ulmasov et al., 1995). These composite AREs need an adjacent constitutive cis-acting element for their function. At low auxin concentrations the ARE represses the function of the constitutive cis-acting element, whereas at high auxin concentrations the repression is released [reviewed in (Guilfoyle et al., 1998)]. As the predicted WUS-binding site could be a component of such a composite ARE, besides the constructs harboring a single mutated motif (*AREI_mut*, *WUS_mut* and *AREII_mut*), promoter versions were cloned with different combinations of these mutated motifs, to test if they possess combinatorial effects or if they are acting redundantly (Figure 9 B).

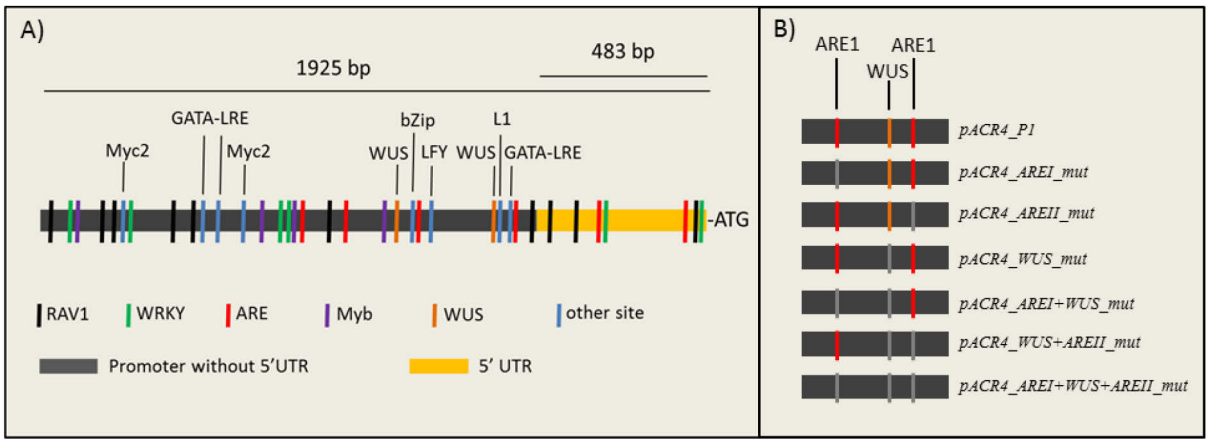

Figure 9 Structure of the 5' upstream regulating sequence of ACR4 and predicted cis-acting elements; mutated promoter versions cloned to test if WOX5 is influencing ACR4 expression

A) The promoter of *ACR4* consists of a1442bp long region upstream of the transcriptional start site and a 483bp long 5' UTR (1925bp in total). Several predicted cis-acting elements were found by the AtcisBD (http://arabidopsis.med.ohio-state.edu/AtcisDB).

B) Overview of mutated promoter versions of *ACR4*. To test if the WUS-binding site is part of a composite ARE the binding site and its adjacent AREs were mutated to a random sequence and additionally multiple combinations of these mutated motifs were combined into a single promoter. The original ARE sequence of TGTCTC was mutated to ACCAAG and the WUS-binding site with the sequence of CCATTA was mutated to GACCAG.

The two AREs are separated by 201 bp and it was shown before that ARFs can homodimerize to cooperatively bind two AREs, with the distance between them being determinant for the efficiency of binding (Boer et al., 2014). Although the distance between the two AREs is too long to serve as a spacer for an ARF homodimer, the DNA at this region might form a loop to bring these elements together. Such a loop formation was shown for the promoter of the gene *VERDANDI* (*VDD*), which is regulated by the MADS (MCM1, AGAMOUS, DEFICIENS, SRF) domain transcription factors SEEDSTICK (STK) and SEPALLATA3 (SEP3) (Mendes et al., 2013). After cloning of the different promoter versions to nuclear localized Venus-Histone2B (*Venus-H2B*),

the constructs were transformed into *A. thaliana* and the *Venus* expression pattern in the roots of transgenic plants was analyzed.

In roots, no differences in expression pattern between the wild type promoter driving expression of a nuclear localized yellow fluorescent protein (*pACR4_P1:H2B-YFP*) or the mutated promoters could be observed (Figure S 1) Sometimes expression in the QC was lost in all constructs including the wild type promoter *pACR4_P1*. This phenomenon was described previously, and no obvious change in frequency between the wild type and mutant lines could be observed (Stahl et al., 2009).

4.4 A 542bp long promoter fragment is necessary to control *ACR4* expression

Since the potential regulatory motifs from the *in silico* analysis did not appear to be of relevance for *ACR4* expression in the root meristem, a systematic promoter deletion series was generated to identify regions with regulatory activity. For this, the putative promoter region of 1442 bp upstream of the 5' UTR was subdivided into ten 150 bp elements (E1-E10). These 10 elements were sequentially removed one by one from the 5'-end (Figure 10 A). Therefore, promoter version *pACR4_P1* represents the full-length promoter with 1442bp + 483 bp 5' UTR (1925bp in total), while *pACR4_P10* is the shortest promoter with only 91 bp + 483 bp 5' UTR (574 bp in total) (fig. 3 A). Additionally a promoter version without the 5 ' UTR was cloned, which was named *pACR4-UTR* (Figure 10 A). The different generated constructs were tested for their ability to control expression of a *Venus-H2B* reporter in wild type Col-*0* root meristems. Representative pictures of root tips for all constructs are displayed in Figure 11 (Figure 11). The expression pattern for the constructs *pACR4_P1* to *pACR4_P6* was identical to the previously described *ACR4* expression pattern, showing expression in the CSCs, CCs, QC, lateral root cap (LRC), LRC/epidermis initials and epidermis in all lines analyzed. For the constructs *pACR4_P7*, *pACR4_P8* and *pACR4_P9* expression in the root tip was lost (29%, 100% and 92 % of analyzed individual transformants, respectively), while the epidermal expression was retained. This is in compliance with previous results, showing that the L1-box located at the end of element 9 is needed for epidermal expression of *ACR4* during the heart stage of embryogenesis (San-Bento et al., 2014). In the case of the *pACR4_P10* variant, in which only 91 bp upstream of the 5' UTR remained, no expression was detected anymore. The construct containing the full promoter, but lacking the 5' UTR (*pACR4_P1 –UTR*) displayed the wild type expression pattern, interestingly though the expression strength appeared to be generally higher in these plants. A direct quantification of expression strength turned out to be difficult, since the expression strength between independent transformants was variable in all generated transgenic plants and seemed to be dependent on the site of t-DNA insertion into the genome.

From these results it can be concluded that the region between P1 and P6, covering the first 750 bp of the 1925 bp potential promoter region and the last 483 bp (5' UTR), are not necessary to confer *ACR4* expression in the distal root meristem. On the other hand, the 542bp long region consisting of element E6 to element E10, located between -1025 bp and -483 bp from the start codon is essential for distal root meristem expression.

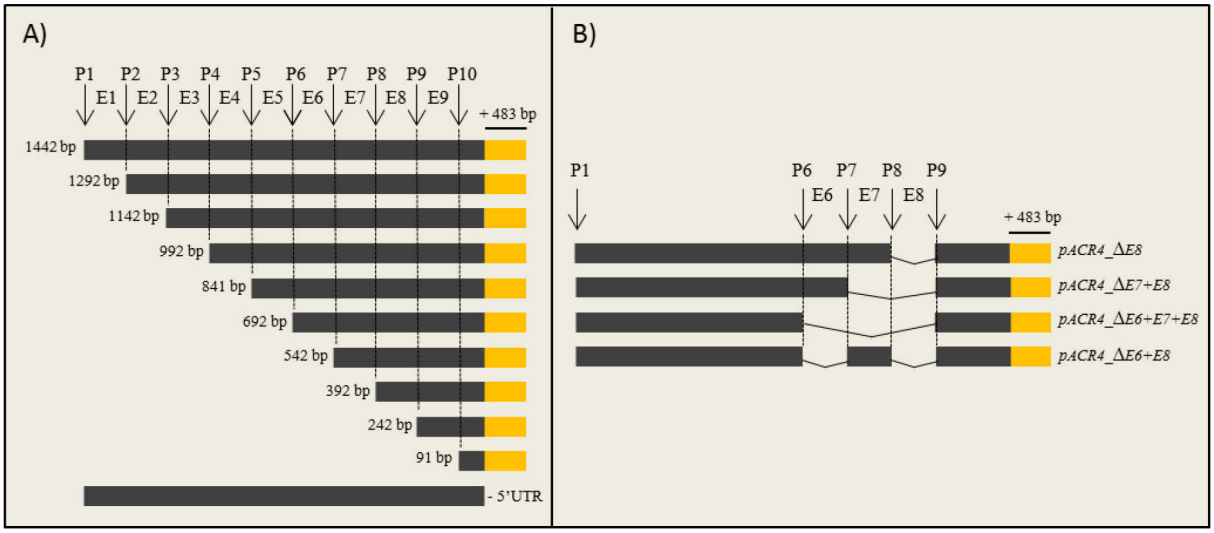

Figure 10 Overview of the first round of generated promoter deletions of *pACR4*

A) Promoter versions *pACR4_P1* to *pACR4_P10* and *pACR4_P1-UTR*: *pACR4_P1* represents the full-length promoter with 1442 bp DNA sequence upstream of the transcriptional initiation site and 483 bp of 5' UTR (1925bp in total). Each promoter version is 150 bp shorter than the previous one. Additionally, a promoter version without the 5 ' UTR was cloned which was named *pACR4_P1-UTR*. All constructs were cloned 5' to Venus-H2B.

B) *ACR4* promoter versions with deletions of 150bp: In one construct the element between P8 and P9 (*pACR4 _ΔE8*) was deleted, in another version the two elements between P7 and P9 (*pACR4_ΔE7+E8*) were deleted and in a last construct the elements between P6 and P9 (*pACR4_ΔE6+E7+E8*) were deleted. Additionally a combinatorial deletion of element E6 and element E8 was done, while element E7 was retained (*pACR4_ΔE6+E8*). All constructs were cloned 5' to Venus-H2B.

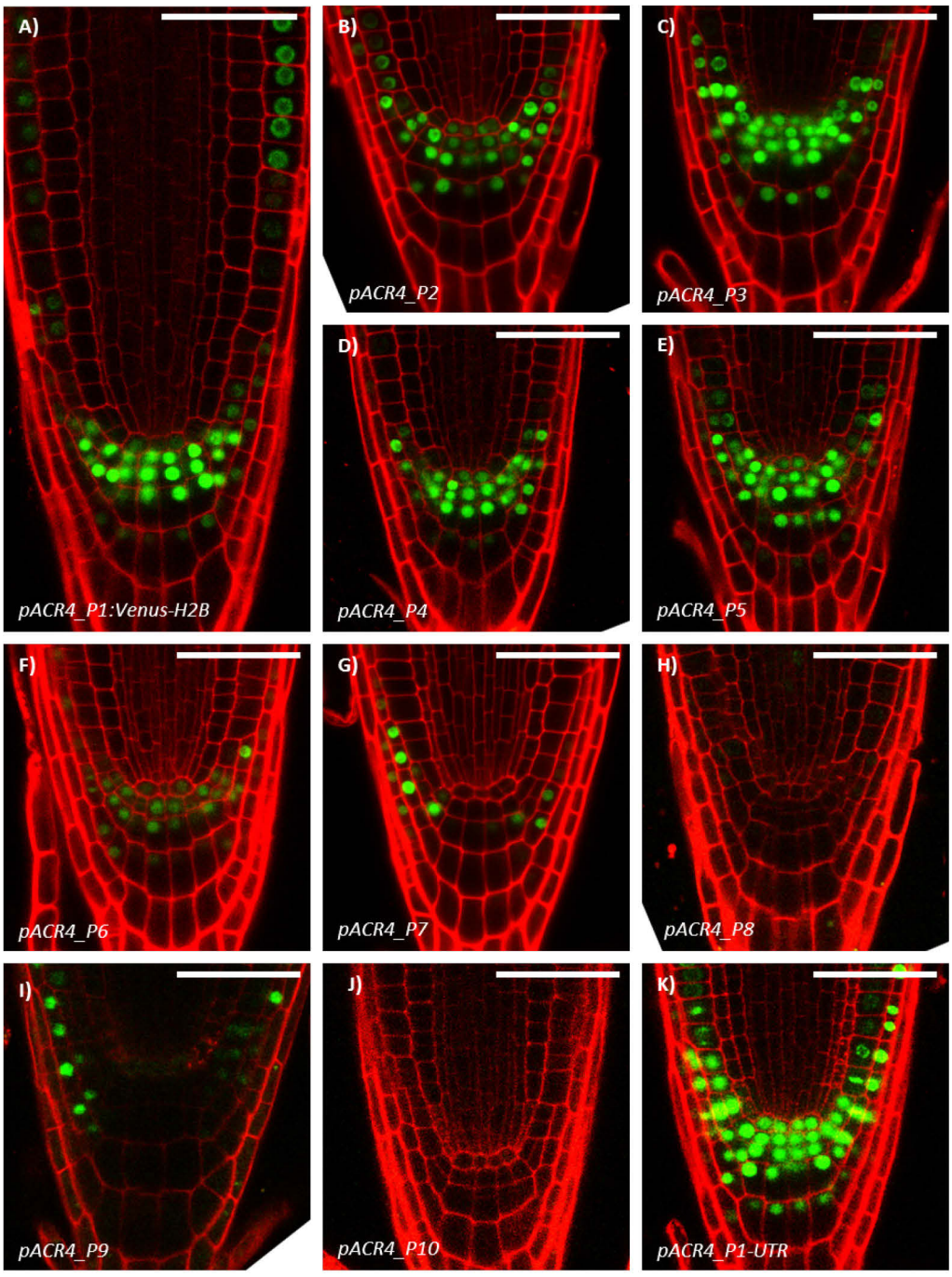

Figure 11 The 542bp long region located between -1025 bp and -483 bp from the start codon is necessary to control ACR4 expression in the distal root meristem

A) - F): The expression pattern of *pACR4_P1:Venus-H2B* to *pACR4_P6:Venus-H2B* was identical with the described *ACR4* expression pattern of *pACR4_P1*, showing expression in the columella initials, columella cells, QC, lateral root cap and epidermis. G) - I): For constructs *pACR4_P7:Venus-H2B* , *pACR4_P8:Venus-H2B* and *pACR4_P9:Venus-H2B* expression in the root tip was often lost, while the epidermal expression was retained. *pACR4_P10:Venus-H2B* showed no expression. K): expression of *pACR4_P1 –UTR:Venus-H2B* was generally higher than with *pACR4_P1:Venus-H2B*. Scale bar: 50 µM.

4.5 Element E7 of the p*ACR4* is required for expression of *ACR4* in the DRM

As the distal expression of *Venus-H2B* was lost in 29% of the strains harboring *pACR4_P7*, element E6 of the *ACR4* promoter (located between P6 and P7) seems to contribute to the expression in this region. However plants expressing *pACR4_P8:Venus-H2B* showed an additive effect (100% of strains showed no distal expression), indicating that element E7 is important as well. No additive effect was observed with *pACR4_P9:Venus-H2B*, but it cannot be excluded that element E8 also has impact on expression. This impact could be masked because element E6 and element E7 are missing in *pACR4_P9* too. Subsequently, the region between P6 to P9 (elements E6, E7 and E8) was further analyzed for their role in *ACR4* transcriptional regulation. Therefore, a fine-mapping was performed by first deleting only the element E8, then elements E7 and E8 or the full region E6 – E8 (Figure 10 B). The promoter version *pACR4_ΔE8* was able to drive the expression of the reporter in a wild type pattern, whereas *pACR4_ΔE7+E8* and *pACR4_ΔE6+E7+E8* showed no expression in the root tip, but retained expression in the epidermis, therefore resembling the constructs *pACR4_ΔP7*, *pACR4_ΔP8* and *pACR4_ΔP9* (Figure 12 A-C). From this result, it can be assumed that element 7, or a combination of element 7 and element 8 is required for expression of *ACR4* in the distal root meristem. To distinguish between these two possibilities, a promoter version was cloned in which element 6 and element 8 were deleted (*pACR4_ΔE6+E8*). This version showed expression in the wild type expression pattern of *ACR4* showing that element 7 is required for expression of *ACR4* In the distal root meristem (Figure 12 D). Additionally to the transcriptional reporters, the promoter versions *pACR4_ΔE8* and *pACR4_ΔE6+E7+E8* were used to establish translational reporters of *ACR4*, by cloning them 5' to the coding region of *ACR4* without the stop codon and in frame with a *Venus* reporter. The promoter *pACR4_ΔE6+E7+E8* was used as a version lacking distal expression and *pACR4_ΔE8* was used as a promoter showing the wild type expression pattern. The expression pattern of these constructs in *Arabidopsis* was similar and confirmed the results obtained with the transcriptional reporters (Figure 12 E+F). Expression strength was much lower with the translational reporters, which can be explained by the fact that the reporter is not concentrated to the nucleus as with a H2B reporter but is attached to the receptor kinase. As the ACR4 protein has a high turnover rate and is also subject of degradation the reporter signal does not accumulate and the expression domain was more restricted. Apparently not all cells showing a Venus-H2B signal are expressing *ACR4*, because a part of the Venus-H2B protein may persist in nuclei after expression has terminated. This phenomenon was reported for transcriptional nuclear localized reporters of *ACR4* before (Gifford et al. 2003). To enhance the signal of the translational reporters, the transgenic plants were incubated 24 h hours in the dark before imaging. This incubation leads to an increase in vacuolar pH and enables visualization of pH sensitive fluorophores like Venus (Tamura et al., 2003). Consequently, the reporter was not only visible at the plasma membrane but also in vacuoles, which are most likely lytic vacuoles.

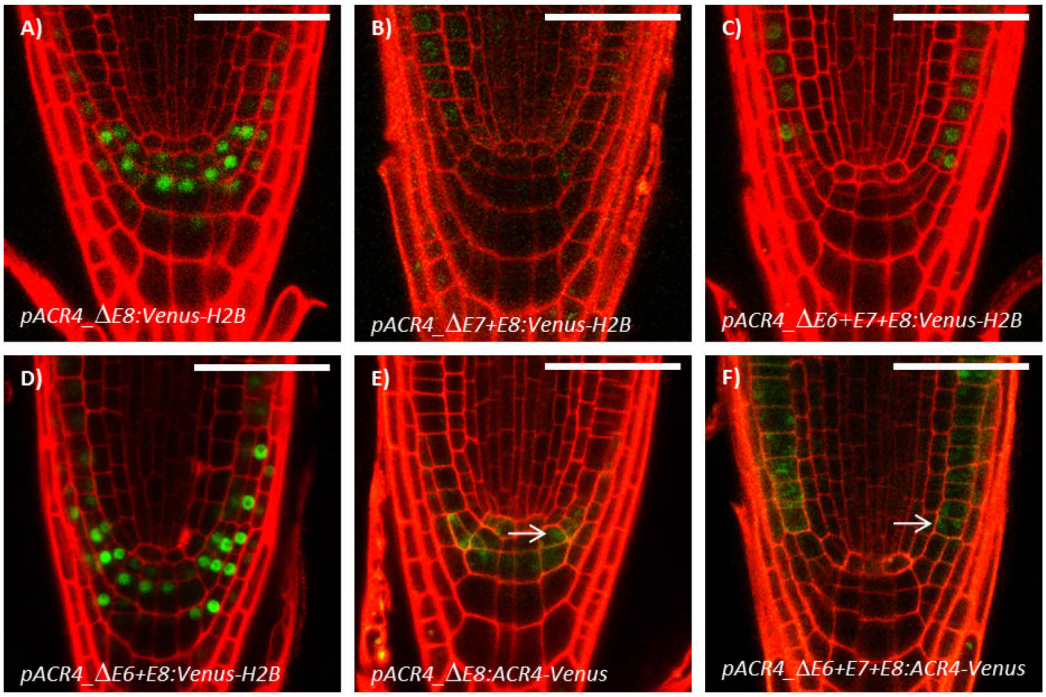

Figure 12 Element 7 of the ACR4 promoter is required for expression in the distal root meristem

A)-D): Transcriptional reporters consisting of *ACR4* promoter versions cloned 5' to *Venus-H2B*. E)-F): Translational reporters consisting of *ACR4* promoter versions cloned 5' to *ACR4-Venus*.

A): Deletion of element E8 had no influence on the expression, wereas deletion of elements E7 +E8, or elements E6+E7+E8 [B) and C)] led to a loss of distal expression. D): Deletion of E6+E8 resembles wild type expression. E) – F): Translational reporters *pACR4_ΔE8:ACR4* -Venus and pACR4_*ΔE6+E7+E8:ACR4* -Venus. Arrows are pointing towards vacuolar loclization of the reporters. Scale bar: 50 µM.

4.6 Element E7 of *pACR4* is sufficient for expression of *ACR4* in the DRM

Having identified two motifs in promoter element 7 that are needed synergistically to drive *ACR4* expression in the distal root meristem it was tested if this element is also not only necessary but also sufficient to confer this expression pattern. As element E7 lacks a core promoter with ribosomal binding sites it was combined with a -*60bp core 35S CaMV* promoter. This core promoter of the cauliflower mosaic virus was shown to not be active without additional enhancer elements (Benfey et al., 1989). Additionally, a longer fragment of *pACR4* consisting of element 7 and element 8 was used as a control and a *-60bp 35S CaMV* core promoter without any cis-acting elements served as negative control (Figure 13 A). Plants expressing *Venus-H2B* under control of these minimal promoter versions showed distal expression in the RAM very similar to the wild type expression pattern of *ACR4* (50% and 92% of analyzed individual transformants for *E7-60CaMV* and *E7+E8-60CaMV*, respectively), except for the negative control (Figure 13 B-E). In many plants carrying these minimal promoters, expression of the reporter in CSCs was lost or reduced. In the epidermis expression was seen occasionally and the percentage

was varying between and also within single transformants. The negative control showed only very weak scattered background expression that could clearly be distinguished from all other promoter versions. To confirm that element E7 is sufficient to effectuate the distal expression pattern of ACR4, translational reporters were cloned. For this, the *ACR4* minimal promoter consisting of *E7-60CaMV* was cloned 5' to the coding region of *ACR4* without stop codon in frame with a Venus reporter (*E7-60CaMV:ACR4-Venus*) and the expression in *Arabidopsis* was compared to plants harboring a translational reporter for ACR4 under the control of its full length promoter (*pACR4_P1:ACR4-Venus*). The translational reporter with the full length promoter of ACR4 showed almost the identical expression pattern as the transcriptional full length reporter (*pACR4-P1:Venus-H2B*), although fluorescence intensity appeared weaker and the expression pattern was more restricted. The translational minimal reporter *E7-60CaMV:ACR4-Venus* exhibited the same expression pattern as the transcriptional minimal reporter *E7-60CaMV:Venus-H2B*. In accordance with the transcriptional minimal promoters also the expression of the translational reporter was sometimes reduced or lost in CSCs (Figure 13 F + G). This experiment shows that element 7 of the ACR4 promoter is not only needed but also sufficient to drive expression of *ACR4* in the distal root meristem of *A. thaliana*, but DNA elements that are contributing to robust expression in CSCs might be missing.

4.7 Fine-mapping of element E7

Since the region of the putative *ACR4* promotor that might contain functional cis-acting elements could be narrowed down to the 150 bp element E7, a fine-mapping of this element was performed next. From other studies it is expected that transcription factors bind to very short stretches of DNA, such as the "TGTCTC" DNA sequence, which is known as the typical auxin responsive element and is bound by AUXIN RESPONSE FACTOR 1 (ARF1) (Ulmasov et al., 1997b). If the loss of transcription factor binding sites is the cause for the failure of *pACR4_ΔE7+E8* to confer expression in the distal root meristem, it should be possible to further confine the region necessary for expression within element E7. Therefore, a fine-mapping with a resolution of 15 bp was conducted.

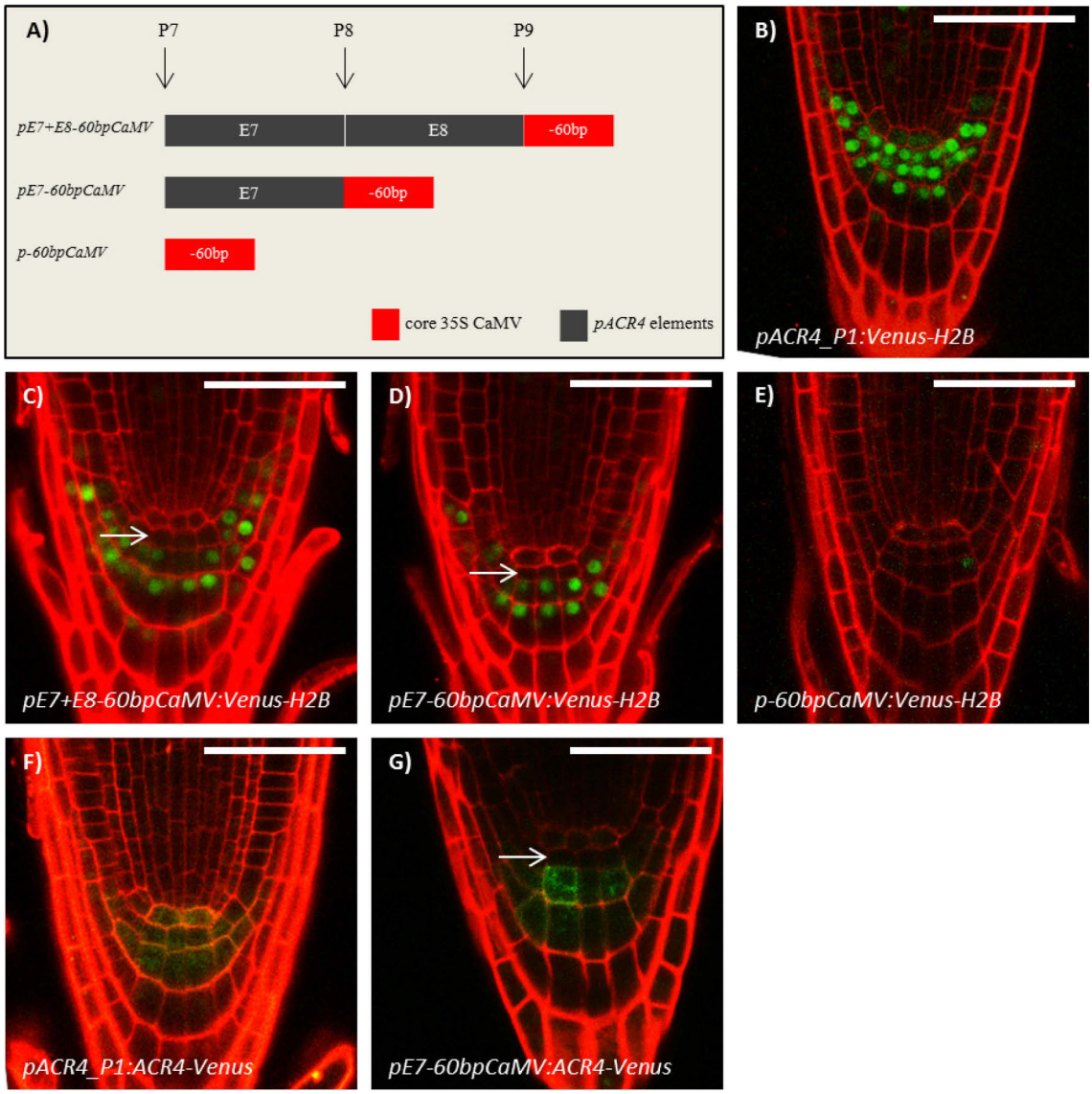

Figure 13 Minimal promoter versions of ACR4 and their expression pattern in *Arabidopsis thaliana*

A) Two versions of minimal *ACR4* promoters were cloned: One version consists of element E7 and one version of element E7 + element E8 of p*ACR4*. These fragments were cloned 5' to a core *-60bp 35S* promoter from the cauliflower mosaic virus. As negative controle a core *-60bp 35S CaMV* without any enhancer or cis-acing elements was used.

B) Full length promoter *pACR4_P1* driving expression of *Venus-H2B*.

C) Expression of *pE7+E8-60bpCaMV:Venus-H2B*

D) Expression of *pE7-60bpCaMV:Venus-H2B*

Expression of the two minimal promoters (C+D) was similar to the wildtype expression pattern. Often the expression in the CSC was lost or reduced (arrows).

E) Expression of *p-60bpCaMV:Venus-H2B*: The negative control showed some scattered background expression that could clearly be distinguished from all other promoter versions.

F) Expression of the translational reporter *pACR4_P1:ACR4-Venus*: Expression was seen in the QC, CSC, CC and to a lesser extent in the lateral root cap as with the transcriptional reporter (B)

G) Expression of the translational minimal *ACR4* reporter *pE7-60bpCaMV:ACR4-Venus*: In contrast to the full length promoter, but in line with the transcriptional reporter in C and D, expression in CSCs was often lost or very weak (arrow).

Scale bar: 50µM

Deletions of 15 bp length were introduced in a systematic way covering the entire element E7 (Figure 14). Expression analysis was again performed using the Venus-H2B reporter. From these constructs, all showed the normal *ACR4* expression pattern (Figure S 2), and no single region could be identified as being singularly responsible of controlling *ACR4* expression. It is therefore likely that a combination of several cis-elements is needed to control the expression, or that the regions deleted were too small to fully abolish functionality of any potential cis-acting elements.

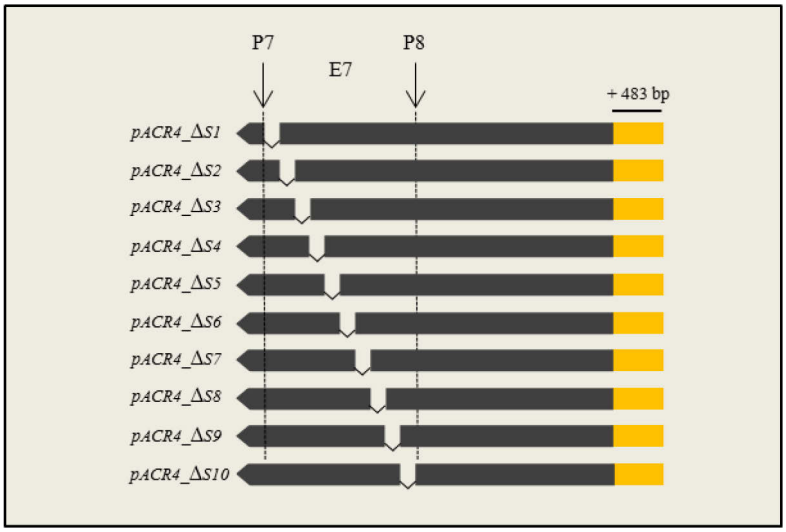

Figure 14 *ACR4* promoter versions cloned for fine-mapping of element E7

For fine-mapping deletions of 15bp length were introduced in a systematic way covering the entire element E7 of the *ACR4* promoter. These promoter versions were named *pACR4ΔS1* to *pACR4ΔS10* and all constructs were cloned 5' to Venus-H2B.

4.8 Identification of conserved motifs in the promoter of *ACR4*

Since the introduction of small deletions of 15 bp in element E7 did not result in the identification of a single motif responsible to control the *ACR4* expression pattern, a more sophisticated approach was chosen to identify potential motifs in element E7. Given that the expression of *ACR4* in the epidermis and the distal root meristem is evolutionary conserved across species and is underlying a similar transcriptional control, the cis-acting elements needed for this expression patterns should, at least to some extent also be conserved within species. In a bioinformatics approach, orthologs of *ACR4* in other species were identified, based on the protein sequence of ACR4 in *Arabidopsis thaliana*. Species were chosen to cover a broad range of phylogenetic relationships. As very distant related plants the aquatic species *Clamydomonas reinhardtii* and *Volvox cateri* from the group *Chlorophyta* were chosen. As a member from the *Charophyta*, *Klebsormidium flaccidum* was used. Although all three species are often referred to as "green algae" (or the paraphyletic taxon *Chlorobionta*) it is to note, that the *Charophyta* together with the *Embryophyta* (land plants) form one taxon and are in evolutionary terms closely related. As a basal land plant the bryophyte *Physcomitrella patens* (*Funariales*) was used and *Zea mays*, *Sorghum bicolor*, *Brachypodium distachyon* (*Poales*) are representing monocot

grass species. *Vitis vinifera* (*Vitales*) was used as a basal rosid species and *Populus trichocarpa* (*Malpighiales*), *Glycine max* + *Medicago truncatula* (*Fabales*), *Cucumis sativus* (*Cucurbitales*) were employed as representatives of the fabids. *Eucalyptus grandis* (*Myrtales*) form together with *Brassica rapa*, *Capsella rubella*, *Arabidopsis lyrata* and *Arabidopsis thaliana* (*Brassicales*) the malvid group (Figure 15).

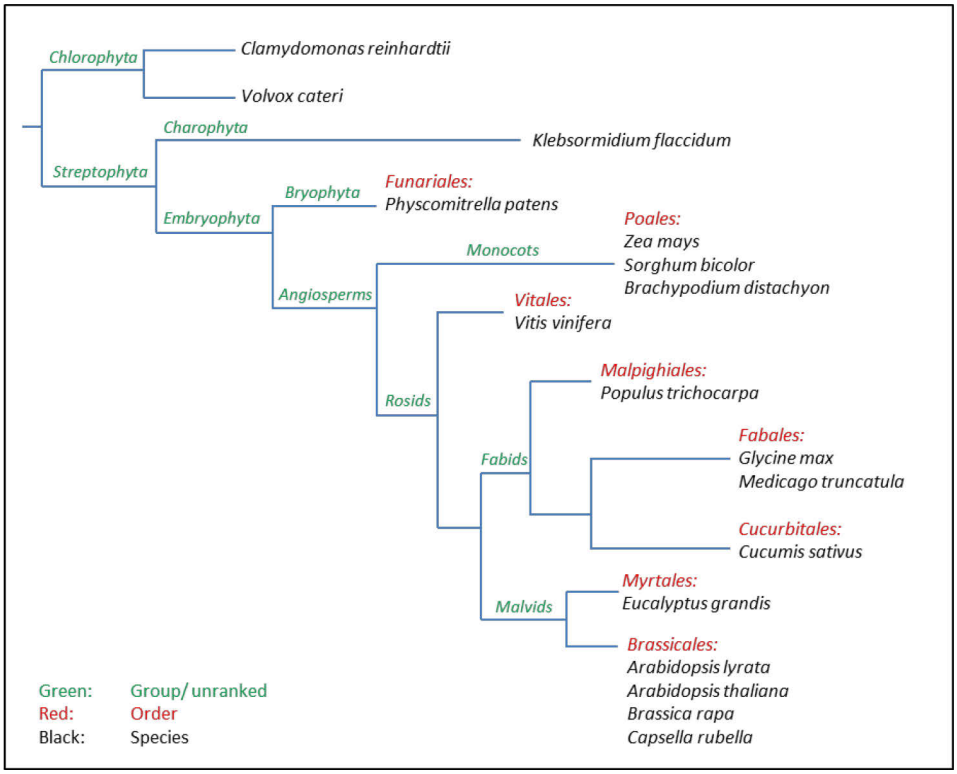

Figure 15 Species used for identification of *ACR4* orthologs and their relationship towards each other

The phylogenetic tree was created with data from Quentin et al. 2001 (Quentin et al. 2001) and based on the classification of the "Angiosperm Phylogeny Group III system" (APG III, 2009). Groups and unranked taxons are written with green colored letters. Orders are written with red colored letters and species are written with black colored letters. The most closely related species investigated here of *Arabidopsis thaliana* is *Arabidopsis lyrata* and the two most distant related species are *Clamydomonas reinhardtii* and *Volvox cateri*.

In all 14 species of the *Embryophyta*, except the *Chlorophyta* and *Charophyta* species, orthologs of *ACR4* could be identified (Figure 16 A). Interestingly, even the moss *Physcomitrella patens,* which as a *Bryophyte* does not have roots but rhizoids, has an *ACR4* ortholog in its genome (Kenrick and Strullu-Derrien, 2014). This indicates that the *Physcomitrella patens* version of CR4 (PtCR4) is involved in other pathways than CSC maintenance, most likely in the specification of epidermal identity as in *Arabidopsis thaliana*. In *Populus trichocarpa* two orthologs were found which share sequence identity of 89.91 % and sequence similarity of 93.06 %. It is likely that both genes belong to the 8000 pairs of duplicated genes which survived from a recent whole genome duplication event (Tuskan et al., 2006).

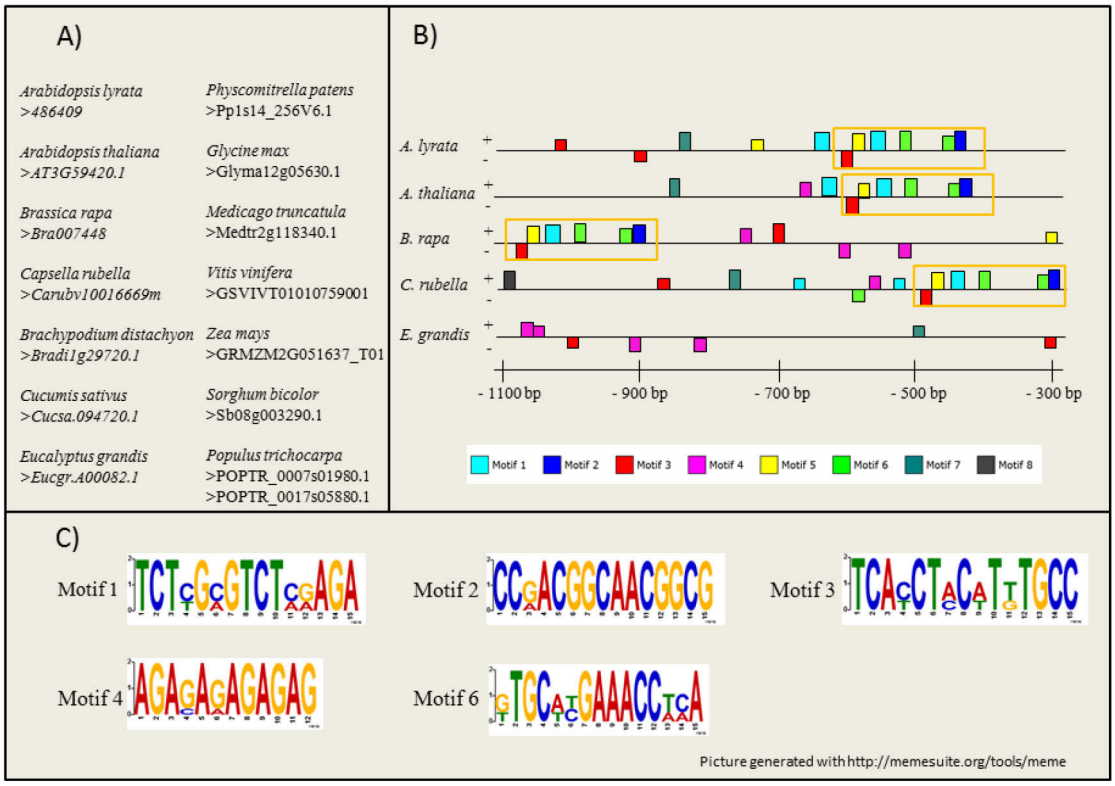

Figure 16 Orthologs of ACR4 in other plant species and conserved elements located in their promoter regions

A) Orthologs of ACR4 in other plant species: For *Populus trichocarpa* two orthologs were found which are likely originating from a recent whole genome duplication event. In the *Chlorophyta* and *Charophyta* species no orthologs could be found.

B) Analysis of the promoters sequences of ACR4 orthologs in 4 *Brassicacea* species with the MEME algorithm: In all promoters a stretch of 5 conserved motifs was found (highlighted with an orange box), in which the motifs were arranged in the same order and almost the same distances relative to each other. In all other species with an ACR4 ortholog this pattern was absent (not shown). As an example for a species without this pattern *Eucalyptus grandis* (*E. grandis*) is shown here. On the X-axis the distance from the transcriptional start site is plotted. + : 5' strand; - : 3' strand.

C) Graphical representation of position weight matrixes from motifs found in the stretch of conserved elements.

To identify conserved elements in the 5' upstream regulating sequences from those genes, their promoter sequences were analyzed with the MEME (Multiple Expectation Maximization for Motif Elicitation) algorithm on the MEME web server (http://meme-suite.org). This algorithm is able to identify de novo motifs in a set of related DNA or protein sequences (Bailey et al., 2006). For the analysis, 1500bp of DNA sequence upstream of the transcriptional start point were chosen, as the 5' UTR of *ACR4* was shown not to be needed for *ACR4* expression. Inside the *Brassicacea* family, a 180 bp stretch of 5 conserved motifs was found in which the motifs were arranged in the same order and almost the same distance to each other (Figure 16 B and C). Although some of these elements were also found in promoters of non- brassicacean species, their distribution on the promoter was random. Intriguingly, this conserved pattern of elements is located exactly in elements E6 and E7, which were shown to be essential for *ACR4* expression in *Arabidopsis thaliana*. Therefore, the effects of these elements were evaluated by deleting them in multiple combinations (Figure 17 A). In construct *pACR4_ΔX1* the motifs M3, M5 and M1 were deleted, whereas in *pACR4_ΔX2* the motifs M6-2 and M2 were deleted. The promoter

pACR4_ΔX3 carries a bigger deletion spanning all motifs except the first M1 motif and in *pACR4_ΔX4* the motifs M6-1, M6-2 and M2 were deleted. In construct *pACR4_ΔX5* motifs M1 + M6-1 are missing and in *pACR4_ΔX6* all motifs except M6-1 and M2 are missing. Out of the created deletion variants, plants carrying constructs *pACR4_ΔX1*, *pACR4_ΔX2*, *pACR4_ΔX5* and *pACR4_ΔX6* expressed a *Venus-H2B* reporter in its wild type pattern, while constructs *pACR4*_ΔX3 and *pACR4*_ΔX4 exhibited an expression pattern without expression in the distal root meristem (expression was lost in 71% and 42%, respectively), thus resembling the expression patterns of the *pACR4_P8*, *pACR4_P9*, pACR4_ΔE7+E8 and pACR4_ΔE6+E7+E8 variants (Figure 18). This experiment again suggests that DNA sequences in element 7 are responsible for driving expression of *ACR4* in the root tip and is supporting previous findings. As the sequence deleted in *pACR4*_ΔX4 (zone X4) is smaller than element E7, the region necessary for distal expression of ACR4 was further narrowed down to 106bp.

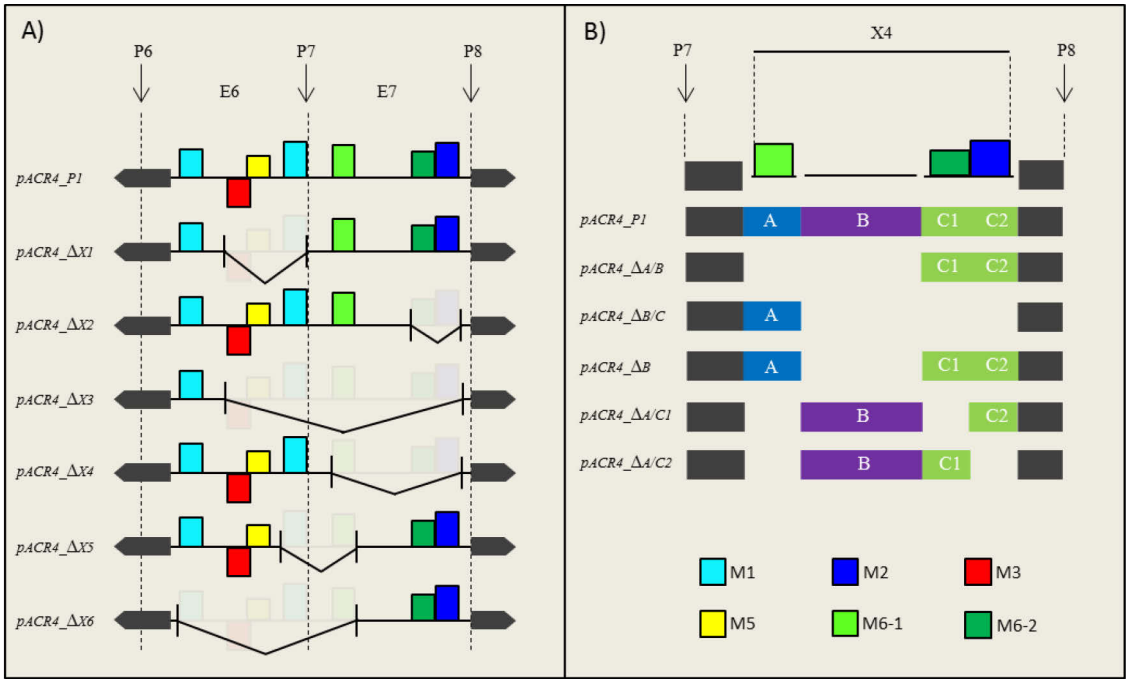

Figure 17 Deletion of conserved motifs found in the promoter of *ACR4*

A) Deletion series X: The 180bp stretch of conserved motifs found in several orthologs of ACR4 is located in element 6 and element 7 in *Arabidopsis thaliana*. These motifs were deleted in 6 different combinations named *pACR4_ΔX1* to *pACR4_ΔX6.* Thes promoter versions were then cloned 5' to *Venus-H2B*.

B) Deletion series ABC of region X4: Region X4 consists of 3 domains. "Domain A" harboring motif M6-1, "domain B" which separates domain A from "domain C" and domain C consisting of motifs M6-2 and M2. Domain C can be further divided into subdomain C1 (M6-2) and subdomain C2 (M2). These domains were deleted in 5 different combinations and the resulting promoter versions were cloned 5' to *Venus-H2B*.

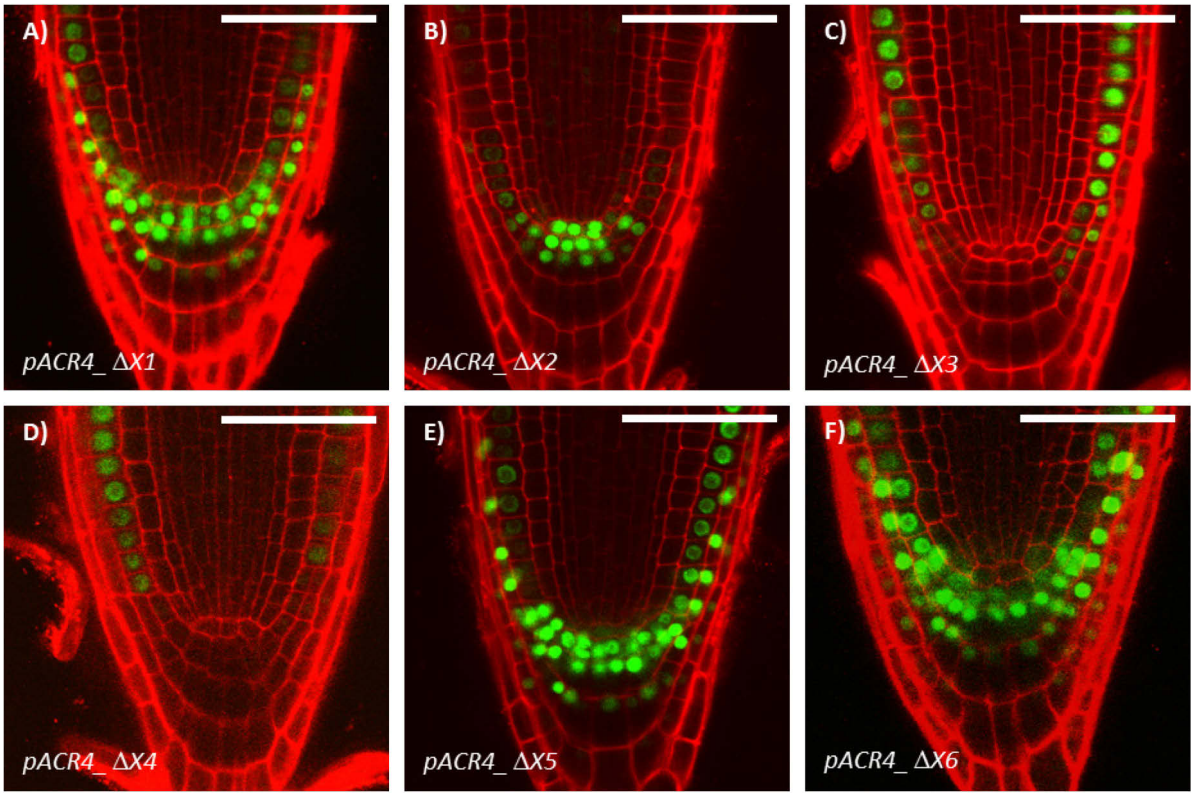

Figure 18 Expressions patterns of deletions series X

A)+B) and E)+F): The constructs *pACR4_ΔX1:Venus-H2B*, *pACR4_ΔX2:Venus-H2B* and constructs *pACR4_ΔX5:Venus-H2B* + *pACR4_ΔX6:Venus-H2B* are expressing in the distal root meristem and in the epidermis.

C)+D): Expression of *pACR4_ΔX3: Venus-H2B* and *pACR4_ΔX4:Venus-H2B* is lost in the distal root meristem, whereas the expression in the epidermis is preserved.

Scale bar: 50µM

4.9 Combinatorial deletions of the *ACR4* promoter

The smallest deletion disrupting distal *ACR4* expression is located in deletion construct *pACR4_ΔX4* and is 106 bp in size (region X4) and contains three conserved motifs (Figure 17 B). To test if these three motifs synergistically promote *ACR4* expression in the root tip, this region was subdivided into 3 domains: Domain A, domain B, and domain C. Domain A is 18 bp long and contains motif M6-1 (15 bp in size) + 3 additional bp 5' to M6-1. This domain was previously deleted as a part of a bigger deletion in construct *pACR4_ΔX5* (Figure 17 A). As *pACR4_ΔX5:Venus-H2B* is showing wildtype expression it can be concluded that deletion of domain A (M6-1) alone is not sufficient to disrupt distal expression (Figure 18 E). Domain B is 49 bp long and separates domain A from domain C. Although this domain has no conserved or predicted cis-acting elements, all constructs, which showed distal expression contained this domain. Therefore it cannot be excluded that it is necessary for, or is promoting distal expression. Domain C is 39 bp long and consists of motif M6-2 (15bp) and motif M2 (15bp), which are separated by 2 nucleotides. Additionally it contains 7 bp 3' to motif M2. This domain

was previously deleted as part of a larger region deleted in construct *pACR4_ΔX2:Venus-H2B* (the deletion in *pACR4_ΔX2* consists of domain C and the last 7 nucleotides of domain B) (Figure 17 A) and this deletion did not alter wildtype expression (Figure 18 B). This domain was further subdivided into domains C1 and C2, containing either only motif M6-2 (C1) or M2 (C2). To further analyze the contributions of the different motifs to *ACR4* expression, several different combinatorial deletion variants were created (Figure 17 B) and the promoter versions were cloned 5' to *Venus-H2B*. All of those constructs, with the exception of *pACR4_ΔA/C2:Venus-H2B* (carrying deletions of motifs M6-1 + M2 and showing loss of distal expression in 34 % of all individual independent transgenic lines), retained expression in the distal meristem (Figure 19). Accordingly, it can be concluded that domain A, containing motif M6-1, together with domain C2, containing motif M2 are acting synergistically and are together important for distal meristematic expression of *ACR4*.

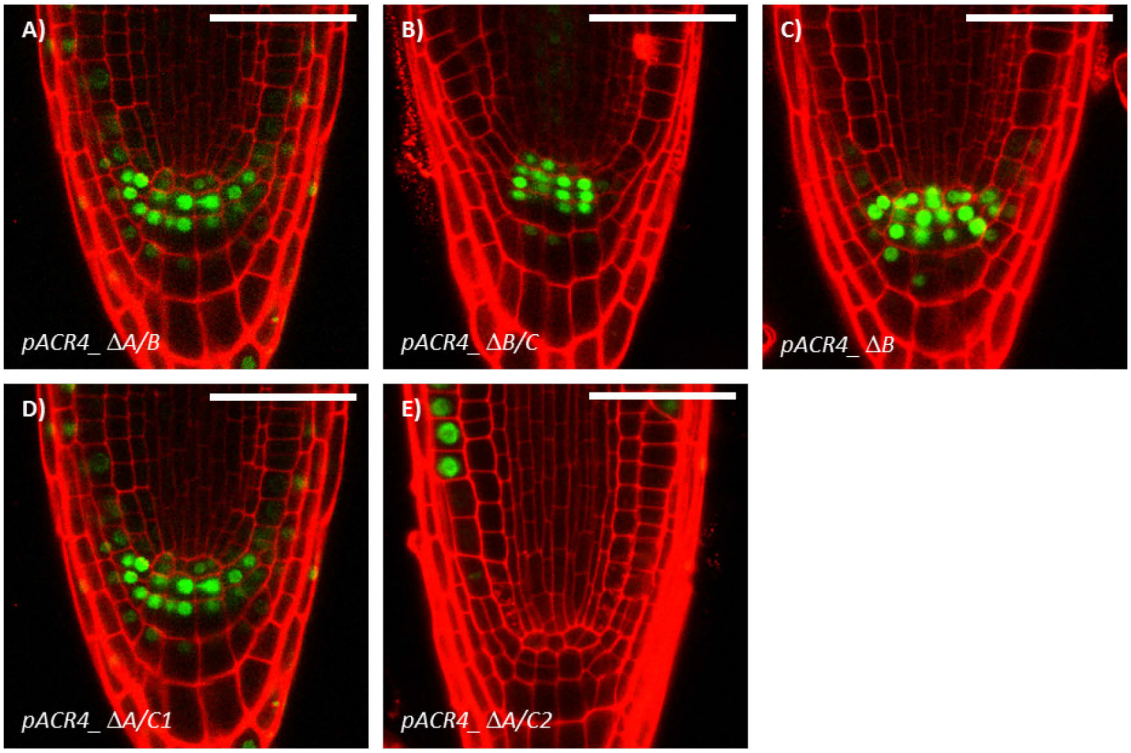

Figure 19 Expressions patterns of deletions series ABC

A)-D): Almost all constructs showed the wildtype expression pattern of *ACR4*.

E): Expression of *pACR4_ΔA/C2:Venus-H2B* was lost in the distal root meristem but showed expression in the epidermis.

Scalebar: 50µM

4.10 Identification of proteins influencing *ACR4* expression (Protoplast transactivation system)

To identify proteins which are able to bind to the promoter of *ACR4* a protoplast transactivation system was employed as described in Wehner et al. 2001 (Wehner et al., 2011). In this assay, a DNA element (called the "bait"), containing possible transcription factor binding sites, is cloned

upstream of a firefly luciferase reporter gene. The transcription factor of interest, which is to be tested for binding to the DNA fragment, is expressed from a *35S CaMV* promoter. These two constructs are then transiently transformed into *Arabidopsis* mesophyll protoplast cells. In order to identify regulators of *ACR4* expression in the distal root meristem, *ACR4* promoter element E7 with adjacent sequences from elements E6 and E8 and a minimal *-60bp 35S CaMV* promoter were used as bait (*pPTA-Mini*). Additionally, the full-length promoter *pACR4_P1* was tested (Figure 20 A). The final assay was performed by a service provider (see chapter 3.2.14). From all transcription factors tested in this screen, 4 proteins were found to bind to *pPTA-Mini* and 3 proteins bound to *pACR4_P1* (Figure 20 B + C). There was no overlap between the proteins found in those two screens.

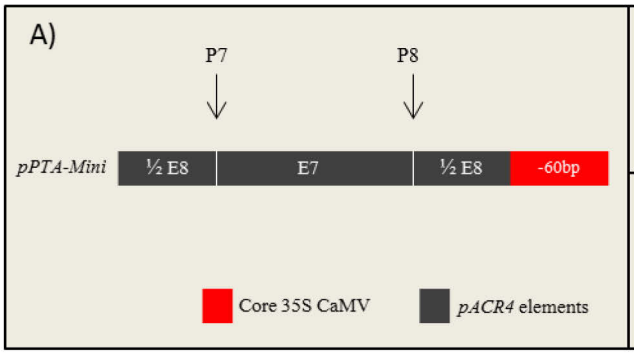

B)

pACR4_P1	fold change	Name
At4g25560	3,9	Myb18
At1g12890	4,3	AtERF
At1g32730	5,6	Unknown protein

C)

pPTA-Mini	fold change	Name
At5g49450	3,1	AtbZIP01
At2g18160	4,9	AtbZIP02
At5g44080	4,0	AtbZIP13
At2g16770	10,7	AtbZIP23

Figure 20 Proteins binding to *pPTA-Mini* and *pACR4_P1*

A) The minimal *ACR4* promoter *pPTA-Mini* was used in a protoplast transactivation system (PTA) to search for transcription factors binding to it. Additionally to this construct, *pACR4_P1* was used in the PTA screen.

B) Proteins binding to *pPTA-Mini* and *pACR4_P1*. Cut-off threefold induction. 4 bZIP transcription factors were found to bind to *pPTA-Mini* and 3 proteins bound to *pACR4_P1*. Out of those 3 proteins, At1g32730 is an unknown protein which is expressed in the root of *A. thaliana* and showed the strongest upregulation of the reporter used in this screen.

Interestingly, all proteins found to bind to *pPTA-Mini* belong to the basic-leucine zipper domain (bZIP) family of transcription factors and indeed element E8 contains the cis-acting element "ACTCAT" which was shown to be a target of AtbZIP02, AtbZIP11, AtbZIP44 and AtbZIP53 in the promoter of *PROLINE DEHYDROGENASE 1* (*PDH1*) (Satoh et al., 2004). From the identified proteins we focused on At1g32730 because it is co-expressed with *ACR4* in the distal RAM of *Arabidopsis thaliana*, according to available microarray data (Brady et al., 2007) (data accessed through eFP browser). Other than that, nothing is known about the protein or its function. *At1g32730*, henceforth referred to as *BINDING TO PROMOTER OF ACR4* (*BTA*), comprises 5 exons and 4 introns and is in total 1880 bp long (exon 1: 122bp, exon 2: 62bp, exon 3: 88bp, exon 4: 103bp, intron 1: 293bp, intron 2: 283 bp, intron 3: 218 bp, intron 4: 102 bp). It is framed by a 167 bp long 5 ' UTR and by a 301bp long 3' UTR and is coding for a 327 amino acid protein (Figure 21). The sequence of the gene can be seen in supplemental Figure S 3 (Figure S 3). According to the "*Arabidopsis* Subcellular Localization Prediction Server" (AtSupP) this protein is supposed to be nuclear localized and the "Sequential Pattern Mining Algorithm for Nuclear Localization Signals"

(seqNLS) predicts a small nuclear localization signal in its C-terminal region (Kaundal et al., 2010; Lin and Hu, 2013) (Figure S 4). A comparison of the protein sequence with the "Protein Families Database" (Pfam B) revealed that it has a domain with similarities to the "domain of unknown function 702" (DUF702) (Figure S 5). DUF702 is only found in the SHORT INTERNODES (SHI)/ STYLISH (STY) family of transcription factors. However, the DUF702 domain of BTA is far less conserved than it is between the other members of the SHI family. The DUF702 domain in the SHI/STY family is characterized by a zinc RING finger-like motif with the consensus sequence C-X2-C-X7-C-X-H-X2-C-X2-C-X7-C-X2-H, which was named C3HC3H RING, and differs from the classical C3HC4 zinc RING finger motif in the spacing of the cysteines and by a replacement of the last cysteine with a histidine (Fridborg et al., 2001). In three members of this group named SHI RELATED SEQUENCE 3 (SRS3), SHI RELATED SEQUENCE 6 (SRS6) and LATERAL ROOT PROMODRIUM 1 (LRP1) the first histidine is not conserved, which is also the case for BTA (Figure 21). These 4 proteins share the consensus sequence C-X2-C-X7-C-X4-C-X2-C-X7-C-X2-H. It is therefore likely that BTA either is a very distant member of this protein family, or that DUF702 domain function evolved in BTA through convergent evolution.

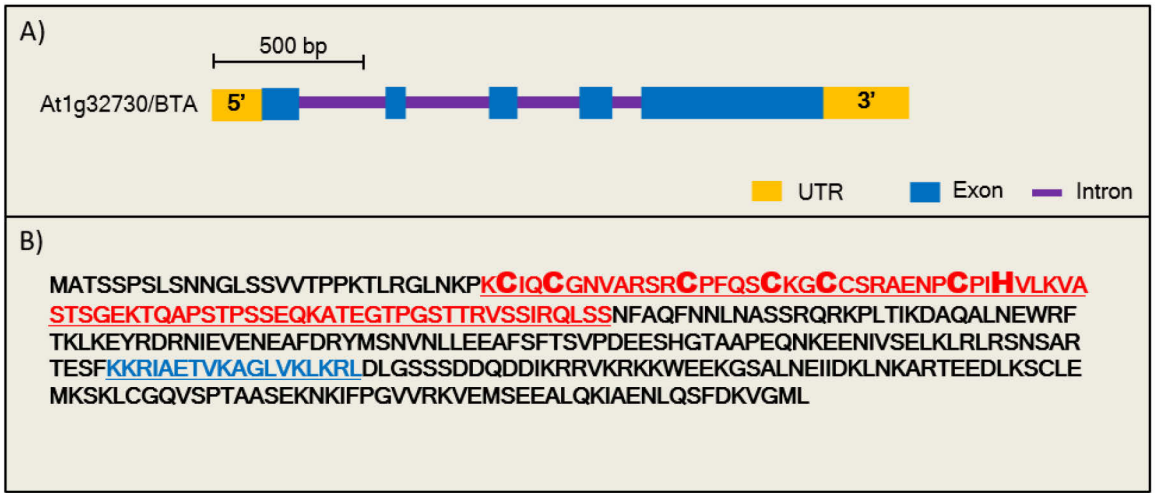

Figure 21 Gene structure and protein sequence of BTA

A) Gene structure of *At1g32730*: *BTA* comprises 5 exons (blue) and 4 introns (violett) and is in total 1880 bp long. It is framed by a 167 bp long 5 ' UTR (yellow) and by a 301bp long 3' UTR. Scale bar 500bp.

B) Protein sequence of BTA: The 327 aa protein contains a domain with similarities to the domain of unknown function (DUF) 702 (red underlined letters). Inside this domain a RING finger-like zinc finger motif is located and its conserved aa are displayed in bold letters. The predicted nuclear localization signal (NLS) is shown in blue. Amino acids are shown in the one-letter aa code.

To evaluate if the zinc RING finger-like motif within the DUF702 domain is important for BTA protein function and/or subcellular localization, a mutant variant lacking the 68 aa DUF702 domain was created (*BTA_ΔZincF)*. If this domain is a functional zinc finger, this mutation will abolish the proteins ability to either directly bind to DNA or form complexes with other proteins. To test this, a β-estradiol inducible reporter version of this mutant BTA variant, using the XVE

system and a cerulean fluorophore, was cloned (*ind::BTA_ΔZincF-Cerulean*) (Zuo et al., 2000). This variant was then tested for its intracellular localization. As a control the wild type coding sequence was used to clone *ind::BTA-Cerulean*. Both constructs were transiently transformed into *Nicotiana benthamiana* leafs and, after induction of gene expression with β-estradiol, the subcellular localization was analyzed *in vivo* with a confocal laser scanning microscope (Figure 22).

Both versions of BTA localized in the nucleus, as it is expected from a transcription factor that is supposed to bind DNA. While *ind::BTA-Cerulean* showed a cloudy distribution in the nucleus, *ind::BTA_ΔZincF-Cerulean* was mainly localized in nuclear bodies of different sizes. This particular localization of the mutated variant could be due to failure of binding to DNA, but also a disruption of protein-protein interactions. Furthermore, this experiment also shows that the ability of nuclear import is not affected with the mutated protein variant. Interestingly, fluorescence was also detected coming from chloroplasts, which did not occur with the wild type protein.

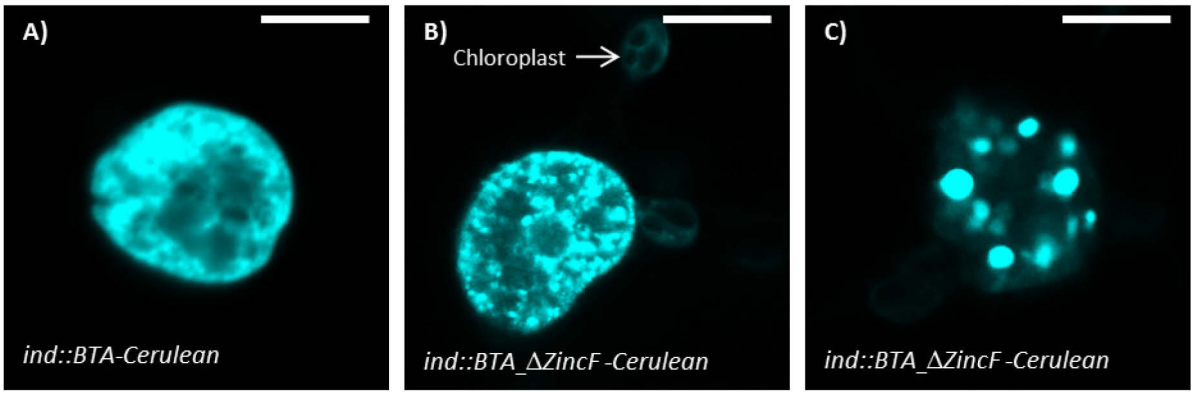

Figure 22 Subcellular localization of BTA-Cerulean and BTA_ΔZincF-Cerulean in *N. benthamiana* epidermal cells

A) *ind::BTA-Cerulean*: The wild type protein localized to the nucleus as it is expected from a transcription factor and showed a cloudy distribution.

B) *ind::BTA ΔZincF-Cerulean*: The muted protein lacking the DUF702 domain still localized to the nucleus but also to chloroplasts (arrow). In contrast to the wildtype protein it was showing a speckled distribution in nuclear bodies.

C) *ind::BTA ΔZincF-Cerulean:* Often the nuclear bodies seemed to fuse after longer overexpression and increased in size.

Scalebar: 10µM

4.11 Confirmation of *pACR4* BTA interaction in *Nicotiana benthamiana*

To confirm that BTA is regulating *ACR4* promoter activity, *Nicotiana benthamiana* leaves were transiently transformed with *ind::BTA-Cerulean* together with *pACR4*_P1 controlling the expression of a firefly-luciferase reporter (*pACR4_P1:Fluc*). As controls an inducible version of *WOX5* (*ind::WOX5-mCherry*) and *TMO6* (*ind::TMO6-Cerulean*) were used, as WOX5 has an overlapping expression pattern with ACR4 and both proteins are known to function as

transcription factors. Additionally to these two controls, *ind::BTA_ΔZincF-Cerulean* as a non-functional protein were used.

Following transient transformation of leaves, gene expression of *BTA*, *WOX5*, *TMO6* and *BTA_ΔZincF* was only induced in one half of the leaf blade (right half induced, left half not induced), thereby each leaf contained its own control. As *pACR4* is constantly active at a basal level in *N. benthamiana* epidermal cells, any change in firefly expression on the right half of the leaf should be due to the action of the induced transcription factor. In contrast to TMO6, WOX5 and BTAΔZincF, expression of BTA led to a downregulation of the firefly reporter on the induced half of the leaf, whereas the not induced half still showed basal expression of the reporter (Figure 23 A-D). Although this result is in conflict with the idea that BTA is a transcriptional activator (BTA overexpression leads to upregulation of *pACR4* activity in the PTA), it indicates that BTA is able to regulate *ACR4* promoter activity, possibly by binding to it. Leaves transformed with *ind::WOX5-mCherry*, *ind::TMO6-Cerulean* and *ind::BTA_ΔZincF-Cerulean* showed no differences between the induced and not induced half of the leaf blade, showing that repression of *pACR4* activity by BTA is specific and requires the DUF702 domain of BTA.

4.12 Binding site of BTA on the *ACR4* promoter

To find potential binding sites of BTA inside the promoter of *ACR4* some previously generated promoter deletions of *ACR4* that still showed epidermal expression were used (*pACR4_P4*, *pACR4_P7*, *pACR4_P8*, *pACR4_P1-UTR* and *pACR4_ΔE6+E7+E8*) (Figure 10 A+B) to repeat the luciferase experiment. All of these promoter variants exhibited basal luciferase expression in the uninduced half of the leaf, whereas in the induced half expression was down regulated, just as it was with the full-length promoter *pACR4_P1* (Figure 23 E-I). *ind::BTA_ΔZincF-Cerulean* with *pACR4_P4* was used as negative control. In this combination the mutated protein was not able to downregulate *pACR4_P4* activity, again confirming that BTA_ΔZincF is a nonfunctional protein variant (Figure 23 J). To exclude that the induction of protein expression with β-estradiol or the luciferase substrate itself has an influence on luminescence pattern two additional controls were used. First, untransformed wild type leaves were induced with β-estradiol (right half of the leaf blade) and treated with D-luciferin (Figure 23 K) Secondly, transformed leaves with *pACR4_P1* + *ind::BTA-Cerulean* were induced and measured without the luciferin substrate (Figure 23 L). In both cases no luminescence could be detected. From these experiments it appears that BTA could act as a general repressor of *ACR4* gene expression. However, the exact binding site within the *ACR4* promoter could not be determined.

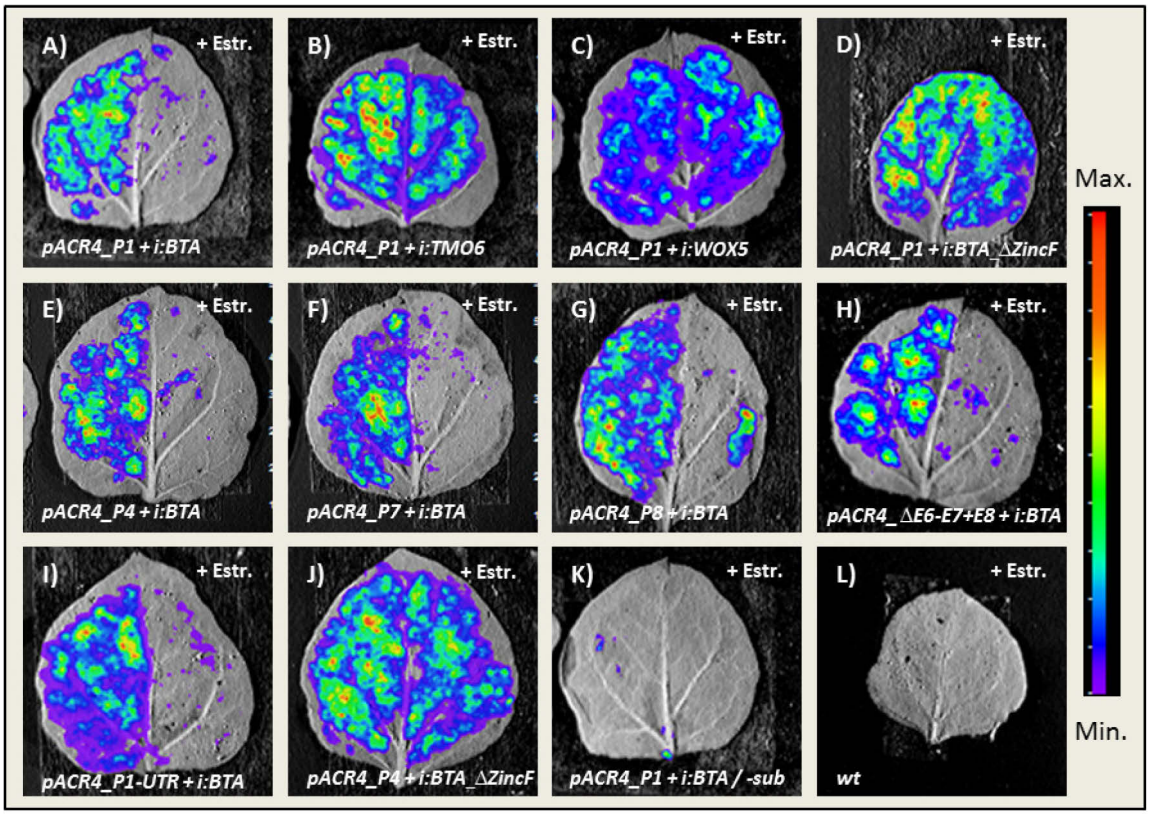

Figure 23 Leaves transiently transformed with pACR4 variants and inducible transcription factors

Left half of the leaf was not induced and the right half (+ Estr.) was treated with β-estradiol to induce transcription factor expression. Expression of BTA-Cerulean led to a downregulation of luciferase with all promoter versions tested: *pACR4_P1* (A); *pACR4_P4* (E); *pACR4_P7* (F); *pACR4_P8* (G); *pACR4_ΔE6+E7+E8* (H) and *pACR4_P1-UTR* (I). Expression of luciferase driven by *pACR4_P1* was not altered after induction of TMO6-Cerulean (B) and WOX5-mCherry (C). BTA_ΔZincF-Cerulean was unable to repress the activity of *pACR4_P1* (D) and *pACR4_P4* (J). No luminescence could be detected without the substrate D-Luciferin (K) and with wild type leafs (L).

Color code indicate relative signal intensities (red: high; violet: low) in counts per second for each individual leaf separately.

4.13 Expression pattern of *BTA* in *A. thaliana*

To analyze the expression pattern of *BTA* in the root meristem, a 2.5 kb DNA sequence upstream of the ATG codon was used as putative promoter (*pBTA*) controlling the expression of a nuclear localized fluorescent reporter (*pBTA:Venus-H2B*). In the distal RAM of plants expressing this reporter, fluorescence was observed in CSCs, young CCs adjacent to the CSCs, the LRC and in the LRC/epidermis initials. No expression was observed in the QC, the last one or two layers of CCs most distal to the QC and in border-like cells. In the proximal RAM expression was seen in the endodermis/cortex initials, the initials of the stele, in the stele (vasculature and pericycle), the epidermis and in young dividing cells of the endodermis and cortex (Figure 24 A+D). While strongest fluorescence was observed in the stele, LRC, CSCs, CCs, the signal intensity was generally weaker in the epidermis, cortex and endodermis. In more proximal regions of the meristematic zone and in the elongation zone expression in the cortex and endodermis was very weak or completely absent (Figure 24 B+C). In this region of the root, expression of BTA was

strongest in the vasculature and the pericycle, whereas the expression in the epidermis was in comparison lower.

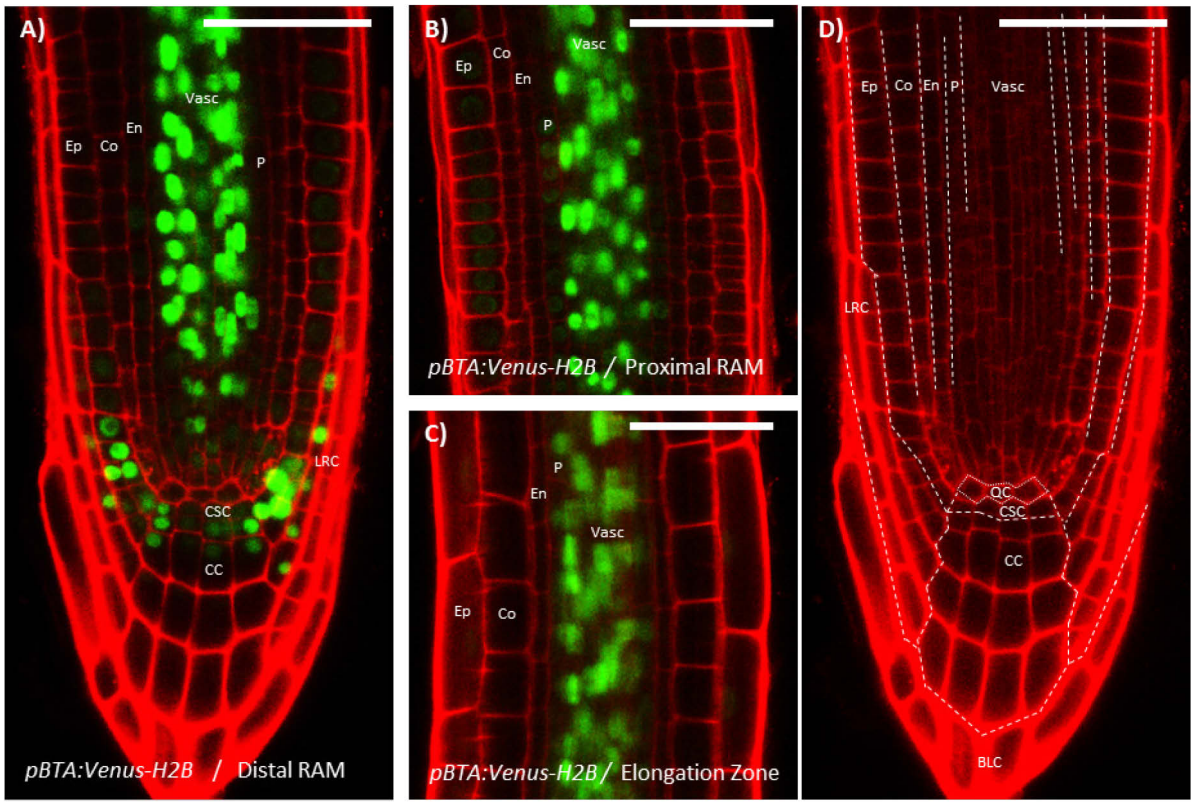

Figure 24 Expression pattern of *BTA* in the root apical meristem of *A. thaliana*

A) Expression of *pBTA:Venus-H2B* in the root tip (distal RAM): Expression was seen in almost all tissues, except the QC, the CCs most distal to the QC and in border-like cells.

B) Expression of *pBTA:Venus-H2B* in the proximal RAM: Strong expression was seen in the stele and low expression was seen in the epidermis. Expression in cortex and endodermis cells was very low or absent.

C) Expression of *pBTA:Venus-H2B* in the elongation zone of the RAM

D) Visualization of the different tissue types of the RAM. Same picture as in (A) but the red channel is shown only. Dotted lines separate the borders of the different tissues.

Ep: Epidermis; Co: Cortex; En: Endodermis; P: Pericycle; Vasc: Vasculature; LRC: lateral root cap; QC: Quiescent center; CSC: Columella stem cells; CC: Columella cells; BLC: Border-like cells; Scalebar: 50µM

The expression pattern of *BTA* is therefore partially overlapping with the expression pattern of *ACR4*. Both are expressed in cells of the distal root meristem, more precisely in CSCs, CCs and the lateral root cap but also in the epidermis. *BTA* is furthermore expressed in the vasculature, while *ACR4* is also expressed in the QC. In summary, the overlapping expression domains of *ACR4* and *BTA*, together with the exhibited modulation of *ACR4* promoter activity by BTA in both, *Arabidopsis thaliana* mesophyll protoplasts and *Nicotiana benthamiana* epidermal cells, potentially position BTA as regulator of *ACR4* in root meristem maintenance.

4.14 Yeast-one-hybrid-screen

As complementary assay to the protoplast transactivation assay (PTA), an enhanced yeast-one-hybrid-screen (Y1H) was performed in parallel to identify regulators of *ACR4* expression. The Y1H assay provides a method to detect protein DNA interactions. To minimize the chances of detecting false positives, an automated experimental setup, in combination with a protein library consisting exclusively of transcription factors was used. These transcription factors cover approximately 92% of transcription factors expressed in the root stele and 74.5% of overall expressed transcription factors in the root (Gaudinier et al., 2011), therefore making the system suitable to identify root-specific transcription factors regulating *ACR4* expression. The same minimal *ACR4* promoter version, which was used in the PTA, consisting of *ACR4* promoter element E7 with adjacent sequences from elements E6 and E8 was used, just without the -60bp 35S CaMV core promoter (*pACR4_Y1H-Min*) (Figure 20 A). As a second bait in this experiment regulatory sequences of *WOX5* were used, since WOX5 too plays a central role in CSC maintenance. For this the 2000 bp of DNA upstream from the *WOX5* start codon was used (*pWOX5-Y1H*). These two promoters were cloned in 5' orientation to the reporter genes *LacZ* and *His3* and the final assay was performed in collaboration (see chapter 3.2.13). The screen with *pACR4_Y1H*-Min, yielded 21 transcription factors that activated reporter gene expression and are therefore supposed to bind to the promoter (Figure S 6). These obtained results were then compared to the results of the PTA, but there was no overlap between the 7 proteins found in the PTA and the 21 transcription factors found in the Y1H. It is to note however that the libraries used in the two screens are vastly different in size (1412 transcription factors for the PTA and 653 transcription factors for the Y1H), and 6 out of the 7 proteins found in the PTA are not included in the yeast-one-hybrid library, among them BTA.

For the WOX5 promotor bait, 37 transcription factors were identified (Figure S 6) that led to transcriptional activation of the reporters. Three of the proteins appeared in both, the *ACR4* and *WOX5* screen (Figure 25). These three transcription factors (AT4G36930: SPATULA (SPT), AT5G25160: ZINC FINGER PROTEIN 3 (ZFP3), AT1G24625: ZINC FINGER PROTEIN 7 (ZFP7)) could provide a link between the transcriptional regulation of both genes, but this would have to be determined by additional experiments and characterization of these transcription factors, since there is no published data available regarding a potential role of ZFP3 and ZFP7 transcription factors in root meristem maintenance. For SPT however a role in regulating root meristem length and in regulating the amount and size of QC cells is reported (Makkena and Lamb, 2013). In *spt* mutants the size of the root meristem is longer and the QC cells are enlarged. Additionally there are up to 10 cells in QC position (in wild type 4 cells) and the QC often consists of 2 layer of cell files (Makkena and Lamb, 2013). In a published screen for direct targets of WOX5 using mRNA profiling of root tips after inducible *WOX5* overexpression and treatment with cycloheximide to prevent protein synthesis, 18 genes were identified with altered gene

expression compared to not-induced plants (Pi et al., 2015). From these 18 genes, 17 were downregulated and 1 was upregulated, confirming that WOX5 acts mainly as a transcriptional repressor similar to the function of WUS in the SAM (Ikeda et al., 2009; Pi et al., 2015). A comparison of these direct targets with the two sets of transcription factors found with the yeast-one-hybrid-screen revealed one common member: ZFP3 (Figure 25). Thus, WOX5 is repressing *ZFP3*, while ZFP3 is binding to the promoters of *WOX5* and *ACR4*.

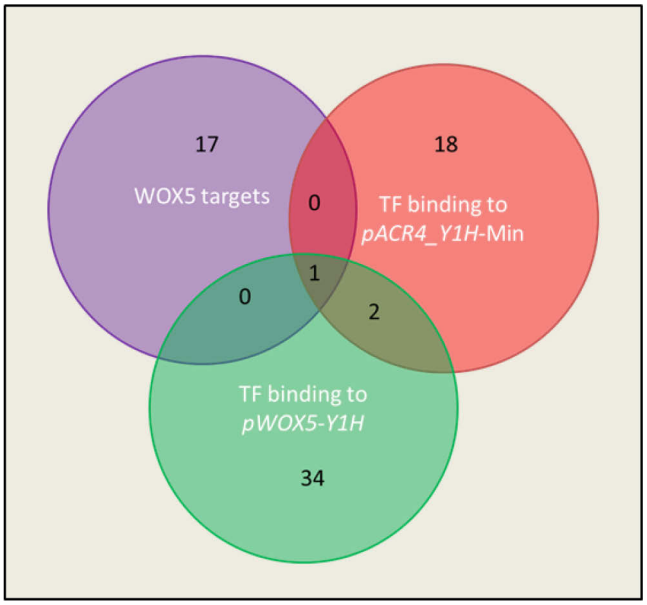

Figure 25 Venn diagram comparing obtained Y1H results with direct targets of WOX5

The Y1H screen with *pACR4_Y1H-Min* as a bait, yielded 21 transcription factors and the screen with *pWOX5_Y1H* yielded 37 transcription factors. Three transcription factors were found with both screens: AT4G36930: SPATULA (SPT), AT5G25160: ZINC FINGER PROTEIN 3 (ZFP3), AT1G24625: ZINC FINGER PROTEIN 7 (ZFP7). The two datasets were then compared with direct targets of WOX5. All datasets have one common member: ZFP3.

4.15 Expression patterns of *CRR1* and *CRR3*

ACR4 is a member of the *CRINKLY* gene family comprising 5 members. All members of this family share an uncommon extracellular domain consisting of seven ‘‘crinkly repeats’’, which are predicted to fold into a β-propeller (Cao et al., 2005; Gifford et al., 2005). The most closely related proteins of ACR4 are CRINKLY4 RELATED 1 (CRR1) and CRINKLY4 RELATED 2 (CRR2), which are supposed to be kinase inactive, while the proteins CRINKLY4 RELATED 3 (CRR3) and CRINKLY4 RELATED 4 (CRR4) are more distantly related (Cao et al., 2005). It has been speculated that these proteins may act in the same pathways, and that they interact with each other to form complexes (De Smet et al., 2008; Gifford et al., 2003; Meyer et al., 2015; Watanabe et al., 2004). Although it has been shown that all 5 genes are expressed in *Arabidopsis* roots (Cao et al., 2005), no expression pattern on cellular level is known for either of these proteins, aside from ACR4. To analyze the expression of *CRR1* and *CRR3* the 5’ upstream regulating sequence of these genes (consisting 949 bp (*CRR1*) or 2005 (*CRR3*) bp upstream of the start codon) were cloned 5’ to a *Venus-H2B* reporter and transformed into *A. thaliana* Col-*0* plants. Roots of these plants

were then analyzed. Interestingly, both *pCRR1* and *pCRR2* conferred expression of the Venus-H2B reporter in roots, but in a pattern clearly different from the *ACR4* expression pattern. Neither gene is expressed in the QC, CSCs or CCs, which is the expression domain of *ACR4* needed for ACR4 function in the distal root meristem. Expression of *pCRR1:Venus-H2B* was observed in the epidermis and the cortex but was absent from all other tissues (Figure 26 A + B). Expression of *pCRR3:Venus-H2B*, interestingly, was very weak and restricted to the LRC (Figure 26 C). Thus *ACR4* and *CRR1* expression are overlapping in the epidermis and *ACR4* and *CRR3* expression are overlapping in the LRC, but otherwise these three genes have perfectly complementary expression domains. From these results it appears that *CRR1* and *CRR3* are likely not involved in the CLE40 pathway controlling columella stem cell maintenance. However *CRR1* may act in concert with *ACR4* in the epidermis, possibly in proximal root meristem pathways or in the maintenance of the epidermis. The expression patterns of *CRR2* and *CRR4* still need to be determined.

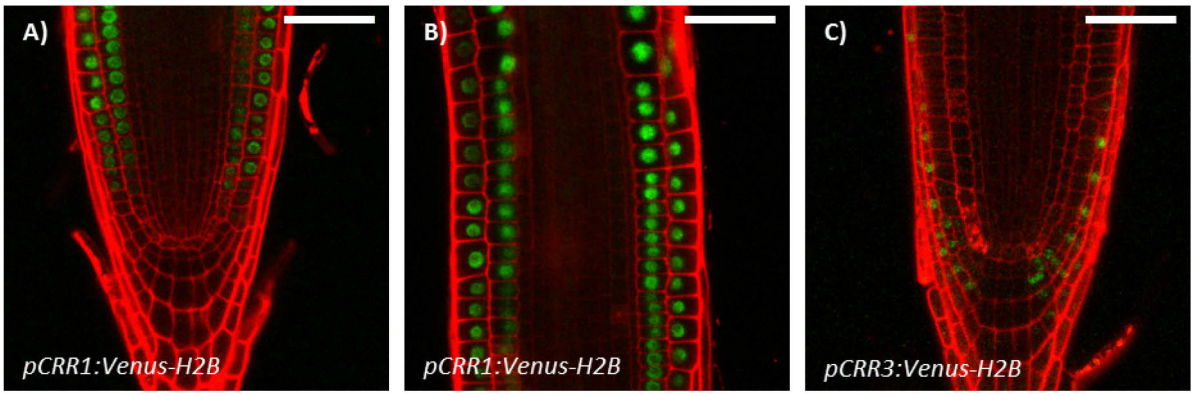

Figure 26 Expression of *pCRR1* and *pCRR3* in roots of *Arabidopsis thaliana*

A) Expression of *pCRR1:Venus H2B* in the root tip: *CRR1* is not expressed in the distal root meristem but the cortex and the epidermis.

B) Proximal expression of *pCRR1:Venus H2B*: *CRR1* is expressed in the cortex and the epidermis.

C) Expression of *pCRR3:Venus H2B*: expression was exclusively detected in LRC cells, and no other tissues.

Scale bar: 50µM.

5 Discussion

5.1 The function of ACR4 in the root meristem has evolved later in evolution than its epidermal function

Based on many molecular and classical phylogenic studies it is broadly accepted that the polyphyletic group of bryophytes (*Anthocerotophyta*, *Marchantiophyta* and *Bryophyta*) evolved earlier than vascular plants (Bennici, 2008; Graham, 1993; Renzaglia et al., 2000). Together they form the monophyletic group of land plants called *Embryophyta*. All extant sporophytes of vascular plants have roots which are connected to the vascular transportation system, whereas the gametophyt of bryophytes like *Physcomitrella patens* have rhizoids (Jones and Dolan, 2012). To identify orthologs of ACR4 in other plant species, a protein BLAST with the amino acid sequence of ACR4 was performed against the proteome of 17 species. The species were chosen based and their phylogenetic relationship (Figure 15). Among the 14 species, in which orthologs could be identified, *Arabidopsis lyrata* is the closest relative of *A. thaliana*, while *Physcomitrella patens*, a member of the *Bryophyta*, which have diverged from the vascular plants more than 400 million years ago, is the most distant relative. Orthologs of ACR4 could not be found in the *Chlorophyta* species *Clamydomonas reinhardtii* and *Volvox carteri*. Also in the draft genome of the *Charophyta* species *Klebsormidium flaccidum,* no ortholog could be found. Since *Klebsormidium flaccidum* is besides *Coleochaete* one of the closest related species to the *Embryophyta* sequenced so far, it seems plausible to assume that the *CRINKLY4* gene evolved in the *Embryophyta* (Hori et al., 2014). The observation that *ACR4* orthologs are only present in the *Embryophyta* is supported by a similar experiment performed in parallel to this thesis by Nikonorova et al. 2015 (Nikonorova et al., 2015). In *Populus trichocarpa*, two proteins with almost identical sequence identity (89.91 %) and similarity (93.06 %) were found, most likely the result of a recent genome duplication and therefore may be paralogos of each other (Tuskan et al., 2006). Also in *Physcomitrella patens*, an ortholog of ACR4 was found with striking similarity to *Arabidopsis thaliana* ACR4. This protein, named PpCR4, has all the typical features of AtACR4, including a signal sequence, 7 crinkly repeats with their characteristic CWG motif, a cysteine-rich region with similarity to the binding domain of mammalian tumor necrosis factors (TNFR), a transmembrane domain, a kinase and a C-terminal domain. Although just 9 of 10 Cystein positions in the TNFR domain are conserved, this domain is likely to bind peptides, as it was predicted for the TNFR domain of maize ZmCR4 and was genetically shown for the whole ACR4 protein (Stahl et al., 2009).

The observation, that the ACR4 protein with all its features is conserved in the moss *P. patens*, which do not have roots, points to a different role for PpCR4 in this species. As *CRINKLY4* (*CR4*) is involved in *A. thaliana* (*ACR4*), in *Zea mays* (*ZmCR4*) and in *Oryza sativa* (*OsCR4*) in regulation of epidermal identity, it is likely that *PpCR4* has a similar role in *P. patens* (Becraft et al., 1996; Jin et

al., 2000; Pu et al., 2012; Watanabe et al., 2004). Thus the epidermal function of *CR4* may have evolved earlier than its function in root meristem maintenance. This is in concert with the finding presented here that *CR4* orthologs can be found in the *Embryophyta* but not in aquatic green algae from the *Chlorophyta* (*C. reinhardtii* and *V. carteri*) and *Charophyta* (*K. flaccidum*). These three species (as all other algae) do not possess an epidermis with a functional cuticula (Raven et al., 2000). It was shown that the epidermis of *acr4* mutants is more permeable for toluidine blue and is thus not functioning as an effective barrier any more (Watanabe et al., 2004). In early land plants, an ancient version of the *CR4* gene could have helped to adapt to terrestrial life by supporting desiccation tolerance trough a functional tight epidermis. Later, when the vascular plants evolved roots, this genes function was recruited to root meristem maintenance. As there is evidence that roots have evolved twice in evolution, once in the *Lycopodiopsida* and once in all other plants ("*Euphyllophyta*") (Raven and Edwards, 2001), it will be interesting to see if the *CRINKLY4* gene was also recruited in the *Lycopodiopsida* to function in roots. Another interesting experiment, which would support the hypothesis that *CRINKLY4* evolved in the *Embryophyta,* is to search for orthologs in the genus *Chara*. These aquatic plants are believed to be the closest relatives to the *Embryophyta* (Renzaglia et al., 2000).

5.2 Expression of *ACR4* in the distal root meristem is conferred by an combination of two evolutionary conserved motifs

Many pathways and principles discovered in *Arabidopsis* are conserved in other plants, if the common ancestor of these plants and *Arabidopsis* already possessed this feature. For example, components of the CLAVATA pathway are conserved in several plant species such as *Zea mays*, *Antirrhinum*, *Oryza sativa* or *Petunia* (Chu et al., 2006; Cock and McCormick, 2001; Kieffer et al., 2006; Stuurman et al., 2002; Suzaki et al., 2009). Conservation of these genes most likely is not limited to gene/protein sequence and function, but also includes the mechanism of transcriptional regulation, *cis*-regulatory sequences and transcription factors binding to these. It is most likely that these binding sites are conserved because a mutation in these sites would prevent binding of the corresponding transcription factor. Hence these sequences are subjected to evolutionary pressure, which the surrounding sequences ("junk-DNA") do not exhibit, allowing them to be altered over time. Therefore it should be possible to detect these conserved motifs by computational methods. In this thesis the promoters of *ACR4* orthologs were analyzed with the MEME algorithm, under the presumption, that these orthologs are co-regulated. The MEME algorithm was shown to be a useful tool to identify *de novo* motifs, which are conserved across co-regulated genes (Bailey et al 2006). In four species from the *Brassicaceae* family (*Arabidopsis thaliana*, *Arabidopsis lyrata*, *Brassica rapa* and *Capsella rubella*) a pattern of conserved motifs was found which was not present in the promoters of other species tested (*Cucumis sativus*, *Brachypodium distachyon*, *Eucalyptus grandis*, *Glycine max*, *Medicago*

truncatula, *Physcomitrella patens*, *Populus trichocarpa*, *Sorghum bicolor*, *Vitis vinifera* and *Zea mays*). Deletion of parts of this motif pattern (*pACR4ΔX3* and *pACR4ΔX4*) led to a loss of *ACR4* expression in the distal root meristem of *A*. *thaliana* (see chapter 4.8). This shows that a small part, consisting of motif M6-1, M6-2 and M2 within a 106 bp long DNA region, but not the whole motif pattern is needed for distal expression in the root. This DNA region could be further narrowed down by a combinatorial deletion approach to two 15 bp long regions (motifs M6-1 and M2), which are redundantly required for distal *ACR4* expression in the RAM (see chapter 4.5). So far it is not clear if this motif combination also controls expression of the *CR4* orthologues in *Arabidopsis lyrata*, *Brassica rapa* and *Capsella rubella*, but this will be an interesting next step to analyze. The conservation of this pattern itself, as well as its conserved localization between -500bp to -600bp upstream of the transcriptional start site in *Arabidopsis thaliana, Arabidopsis lyrata* and *Capsella rubella*, do suggest that a similar mechanism, possibly with orthologous proteins, could regulate the *CR4* genes in these species on transcriptional level. In *Brassica rapa*, the motif pattern is located more than -1000bp away. This offers the possibility to test whether the distance of the pattern from the site of transcriptional initiation has an influence on gene expression. To this end element E7 of the *ACR4* promoter (150bp in size) and containing motifs M6-1 and M-2 were combined with a core *-60bp 35S CaMV* promoter (*E7-60bpCaMV:Venus-H2B*). As these few bp were sufficient to confer distal meristematic expression in roots, the distance of motifs M6-1 and M-2 to the transcriptional start site appears to have no influence on their functionality and transcription factors binding to these motifs are sufficient for initiation and/or activation of the preinitiation complex. Since M6-1 and M-2 act together and are separated by 66bp, it is not expected that a single transcription factor will bind to both of them. It is more likely that a protein complex is binding to them, in which each component recognizes one motif, or that both motifs are bound by two transcription factors individually. In either case, the motifs are acting redundantly and both motifs have to be deleted to disrupt distal *ACR4* expression. But these things still need to be tested.

Curiously, control of *ACR4* expression in the CSCs seems to be controlled in a different fashion. In contrast to wild type *ACR4* expression, expression of *E7-60bpCaMV:Venus-H2B* was significantly reduced in CSCs. Apparently, an additional motif to support *ACR4* expression in CSCs is necessary. Since the systematic deletion of the putative *ACR4* promotor did not yield any region that appeared to specifically alter *ACR4* expression in the CSCs, it is possible that an additional enhancer element somewhere else in the genome is responsible to control expression strength in the CSCs. Although such enhancers are only rarely described in *Arabidopsis*, an open chromatin signature based enhancer prediction system, utilizing DNaseI hypersensitive sites as indicator for DNA accessibility, suggests that there could be more than 10000 intergenic enhancers present in the *Arabidopsis* genome (Zhu et al., 2015). Also, additional DNA regions could be responsible for a fine-tuning of *ACR4* expression strength in the CSCs, or to modulate

ACR4 expression in a tissue specific manner, which could be at least partially independent of general expression initiation in the RAM.

5.3 The 5' untranslated region of *ACR4* is repressing *ACR4* expression

Besides transcriptional gene regulation, translation efficiency influences gene expression. Translation can be affected by specific sequences in the mRNA that can often be found in untranslated regions (UTRs), located up- and downstream of the main open reading frame (mORF). Another common motif repressing translation efficiency are upstream open reading frames (uORFs). uORFs are short protein coding regions in the 5' UTR an can be found in one-third of all known 5' UTRs of *A. thaliana* (Roy et al., 2010). They are overrepresented in 5' UTRs of transcription factors and protein kinases and have been shown to influence translation (Hanfrey et al., 2005; Kim et al., 2007; Roy et al., 2010). In most cases, the repressive activity is exerted through failure of translation re-initiation following a stop codon, but in some cases the translated peptide itself interacts with the ribosome and has an intrinsic repressive activity (Hanfrey et al., 2005; Rahmani et al., 2009). In contrast to most 5'UTRs with a median length of 82 to 88 bp, the 5' leader sequence of *ACR4* is exceptionally long, spanning 483 bp (Alexandrov et al., 2006). The 5'UTR of ACR4 contains 4 uORFs and deletion of the entire 5'UTR resulted in higher expression of *Venus-H2B* (see chapter 4.4). It is possible that transcription factors binding to this UTR are repressing transcription or, that one, or all of these uORFs, are influencing translation efficiency. To distinguish between transcriptional and translational repression, the start and stop codon of each upstream ORF could be mutated to an amino acid coding codon and the expression of the gene could then be measured by quantification of reporter expression. If the reporter expression is upregulated when a specific upstream ORF is not present anymore and the mRNA content measured by quantitative reverse transcription polymerase chain reaction (qRT-PCR) remains on wildtype level, this would show that the uORF is indeed influencing translation efficiency. The eukaryotic translation initiation factor 3 (eIF3) of *A. thaliana* is a big protein complex comprising 12 members (Burks et al., 2001). One of its members, the subunit "h" (eIF3h), is involved in translation re-initiation, and *eIF3h* mutants show pleiotropic defects associated with under-translation of mRNAs containing multiple uORFs (Kim et al., 2007; Kim et al., 2004). It will be interesting to investigate if this mutant also shows phenotypes linked to ACR4 function. Modifying ACR4 translation could add another layer of control to CSC maintenance. Furthermore, the promoter of *ACR4* contains a predicted binding site for bZIP transcription factors and the binding of AtbZIP02 to the minimal *ACR4* promoter p*PTA-Mini* could be shown in this thesis by a protoplast transactivation assay (see chapter 4.10). *AtbZIP02* contains a conserved uORF which leads to sucrose dependent repression of its translation (Wiese et al., 2004). If AtbZIP02 would indeed regulate *ACR4* expression, than *ACR4* expression could additionally be dependent on sucrose concentration.

5.4 The promoter of *ACR4* contains several known transcription factor binding sites

Transcription factors are proteins, which regulate gene expression, either by binding to specific sequences in *cis*-acting elements of genes, or by influencing to the activity of other proteins involved in the assembly and/or activation of the preinitiation complex. For many DNA binding transcription factors the target consensus sequence, often a small motif inside the 5' upstream regulating sequence of their target genes, has been identified. One resource to identify such known consensus sequences is the *Arabidopsis cis*-regulatory element database (*Atcis*DB). By employing this information resource, putative transcription factor binding sites were identified in the promoter of *ACR4* (see chapter 4.3.1). These binding sites have originally been identified in promoters of other genes, and are not necessarily functional in regulating *ACR4* transcription, but nevertheless they provide a good starting point for an initial analysis of *ACR4* transcriptional regulation. While most of the predicted transcription factor binding sites did not exhibit any activity in the assays described here (see chapter 4.3.2), a bZIP binding site, located -847bp upstream of the start codon, was shown to be able to drive gene expression in a protoplast transactivation assay when the bZIP transcription factors bZIP01, bZIP02, bZIP13 and bZIP23 were co-expressed (see chapter 4.10). That these transcription factors are indeed binding to the predicted bZIP binding will be addressed in further experiments.

One well studied example for a transcription factor family with a known motif are the WRKY transcription factors. They bind to the so-called *W-box*, consisting of "T/TGAC/C", a common motif in the genome of *A. thaliana* (Rushton et al., 1996). Consequently, not every *W-box* will have an impact on gene transcription. One *W-box* was identified in the putative promoter region of *ACR4* (see chapter 4.3.1). WRKY transcription factors are known to play important roles in transcriptional regulation of genes involved in biotic and abiotic stress. Thus, the *W-boxes* found in the promoter of *ACR4* could have an influence on *ACR4* expression under stress condition (Figure 9 A). Interestingly, *ACR4* was found to be more than 2 fold upregulated if grown on media with pH 4.6 compared to a control media with pH 5.7 according to cell specific microarray data (Iyer-Pascuzzi et al., 2011) (data accessed through eFP browser). In the same publication, the columella was furthermore identified as a response center for pH stress, and loss of CCs after 24h on medium with pH 4.6 was a phenotypic readout. It will be interesting to uncover the regulatory elements in the *ACR4* promoter needed for this transcriptional response, especially with a focus on the *W-box*. The promoter deletion variants constructed in this PhD thesis could be used to address this question of a possible role of ACR4 in stress-response. Also, new promoter versions could be cloned to analyze if WRKY transcription factors are involved in this pathway, thereby linking ACR4 to stress response.

5.5 The predicted WUS-binding site in element E7 is neither needed for expression nor it is a component of a complex ARE

Phytohormones control diverse developmental and physiological processes in plants, generally acting as long range signaling molecules. One major phytohormone is auxin, which is involved in several pathways, among them the initiation of the root meristem in the dermatogen stage of *Arabidopsis thaliana* embryogenesis (see chapter 1.4). In the early heart stage of embryogenesis an auxin maximum can be found in the developing RAM and at the sites of developing cotyledon primordia (Möller and Weijers, 2009). While this maximum overlaps with *WOX5* and *ACR4* expression in the QC, in the developing CCs it overlaps with *ACR4*, but not *WOX5* expression. If the WOX5 protein is moving from the QC position to the adjacent distal cell file (CSC position), as it was shown in post-embryonic development, is not known so far. Following germination, the auxin maximum in the root meristem is maintained, with the highest concentration in the cells of the QC (Petersson et al., 2009). Because of the overlap of *ACR4* expression with the auxin maximum in both, the developing embryo and the mature root, it has been hypothesized that *ACR4* expression in the root tip could be a direct result of the elevated auxin concentration. This idea is supported by the finding that *ACR4* expression is upregulated following treatment with exogenous auxin (Wink, 2013). In most known cases, the transcription of auxin-inducible genes is controlled by ARF transcription factors, which bind directly to short specific DNA sequences in the genes regulatory regions, called Auxin Responsive Elements (AREs). In the absence of auxin, these ARFs are prevented from binding to the AREs through interaction with IAA proteins (Hamann et al., 2002; Ulmasov et al., 1997a; Weijers et al., 2005). Auxin perception then leads to ubiquitination and subsequent degradation of the IAA proteins, therefore releasing the ARF and enabling it to bind to the ARE. It was shown that a single ARE alone is not sufficient to confer expression and that they have to be arranged at least in tandems (in direct repeats or as a palindrome) to be sufficient for auxin inducible expression (Ulmasov et al., 1997a; Ulmasov et al., 1995; Ulmasov et al., 1997b). Such repetitive motifs are called simple AREs, whereas complex AREs function through another mode of action: Complex AREs consist of a *cis*-acting element which function is repressed by a nearby ARE at low auxin concentrations (Guilfoyle et al., 1998). Thus, the function of such a coupled *cis*-acting element is controlled through auxin concentrations, thereby offering an additional mode of fine-tuning for gene expression. The AREs found in the promoter of *ACR4* do not match the criteria of simple AREs, as they are not close enough to each other but two AREs located between -832bp and -1039bp upstream of the start codon could act as a composite ARE, as they are flanking a predicted WUS-binding site (see chapter 4.3.1 and Figure 9 B). Therefore it was tested if these predicted *cis*-acting regulatory elements are indeed functional in terms of modulating the expression pattern of *ACR4*. However, with the methods used here, no obvious changes in *ACR4* expression were observed, leading us to conclude that the tested potential AREs and the WUS-binding site in the *ACR4* regulatory region have no influence on *ACR4* expression. It is to note, however, that there are

other potential AREs within the *pACR4* region that were not tested for their function. Albeit these AREs are isolated and it is unlikely that they are functional without any other elements, through loop formation of the DNA they might come close to each other to function as simple AREs. Another possibility is that they are functioning as part of complex AREs in concert with motifs not discovered or tested so far. Therefore it cannot be excluded, that these motifs might be necessary for auxin-dependent gene regulation. Since the DNA region that was identified in this work as important for distal *ACR4* expression (see chapter 4.5) comprises a region that is void of any AREs, it is more likely though that these additional AREs, should they be functional, would rather modify the expression than control it. The finding that the putative AREs do not appear to be functional does not exclude the possibility that auxin influences *ACR4* expression. It is possible that other elements than the predicted AREs are responsible for the observed *ACR4* upregulation following auxin treatment, or that the influence of auxin on *ACR4* expression is indirect.

5.6 The promoter of *ACR4* has modular organization

In post-embryonic development *ACR4* is expressed in the epidermis, QC, CSCs, CCs, LRC and the epidermis/LRC stem cells. In this thesis, a 150 bp region (element E7) within the promoter of *ACR4* was identified through a promoter deletion series, which is essential for expression of *ACR4* in the distal root meristem (QC, CSCs, CCs, LRC), but not in the epidermis. Furthermore, element E7 is also sufficient for distal expression, but expression strength in CSCs is drastically reduced (see chapter 4.6). This first observation indicates that different transcriptional regulators, binding to different motifs within the *ACR4 cis*-regulatory sequences, control *ACR4* expression in the distal meristem and the epidermis. It has been previously shown that the transcription factors ATML1 and PDF2 directly bind to a L1-box located at the end of element E9 in *pACR4* to control expression of *ACR4* in the epidermis (San-Bento et al., 2014). Real time quantitative reverse transcription PCR (qRT-PCR) data indicates that *ATML1* and *PDF2* are negative regulators of *ACR4*, since ACR4 mRNA levels are elevated in *pdf2 - atml1/+* (homozygous for *pdf2*, heterozygous for *atml1*) double mutants (San-Bento et al., 2014). On the other hand, *ACR4* reporters with mutations in the L1-box exhibited disturbed expression in the epidermis of the developing embryo at the heart stage, suggesting that the L1-box is needed for epidermal/protodermal expression during embryogenesis (San-Bento et al., 2014). In this thesis, expression in the epidermis was always present with promoter versions harboring the L1-box, but in a promoter version without the L1-box (*pACR4_P10*) expression of *ACR4* in the epidermis and the distal RAM was lost. It is to note however, that *pACR4_P10* comprises only the last 91 bp 5' of the transcriptional start site. Interestingly, the promoters of *ATML1* and *ACR4* share a similar motif combination close to the transcriptional start site: a WUS binding site (WUS-box) followed by a L1-box. Whereas in the *ATML1* promoter these two sites are separated by 15 bp

and both are on the 5' strand, in the *ACR4* promoter these motifs are overlapping and are located on opposite strands (Figure 27). As with ACR4, mutations in the L1 or WUS-box leads to reduced and disturbed expression of *ATML1* in the epidermis during embryogenesis (Takada and Jürgens, 2007). Because *WUS* and *WOX5* are not expressed in the epidermis, the reduced and disturbed expression in the L1 is likely due to other members of the WOX transcription factor family which are expressed there (Haecker et al., 2004). The WUS-boxes in the promoter of *ACR4* could provide binding sites for WOX transcription factors but not necessarily for WOX5. Because *WOX* genes are expressed in distinct patterns and play important roles during embryogenesis, the promoter versions cloned in this thesis could be used to study the expression pattern of *ACR4* during embryo development.

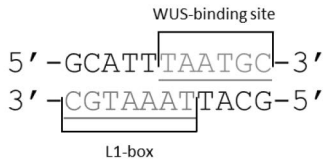

Figure 27 Composition of the L1-WUS-Box in pACR4
The L1-box (blue letters) located -117 bp upstream of the transcriptional start site is overlapping with a WUS-binding site (red letters) on the opposite strand. The Wus-box is located on the 5' strand and the L1-box on the 3' strand in reverse orientation.

The different expression patterns of the *ACR4* promoter versions are suggesting a modular organization of the *ACR4* promoter. Module 1 (including the L1 - box and the WUS - box) controls expression in the L1, module 2 (motif M6-1 and M2 in element E7) controls expression in the distal RAM, module 3 (exact location has to be determined) is enhancing *ACR4* expression in CSCs, and module 4 (uORFs in the 5' UTR) serves to fine-tune expression by influencing translation efficiency.

5.7 BINDING TO PROMOTER OF ACR4 is influencing *pACR4* activity in *N. benthamiana* epidermal cells

Having identified the DNA region needed and sufficient for distal *ACR4* expression (element E7), transcription factors binding to this region were identified through a protoplast transactivation assay (PTA). Four proteins belonging to the bZIP family of transcription factors bound to this region (*PTA-Mini*), from which it appears that the predicted bZIP-binding site found in the AtcisDB could be functional. As a control, the full-length *ACR4* promoter (*pACR4_P1*) was used in this screen, and 3 transcription factors were found to bind to it, including BIDING TO PROMOTER OF ACR4 (BTA). The proteins binding to *pACR4_P1 and* the promoter fragment *PTA-Mini* did not overlap. An explanation for this result could be that the bZIP-binding site in *PTA-Mini* was inaccessible on the full length promoter due to its conformation or that proteins expressed on

wild type level in the *A. thaliana* mesophyll protoplast were binding on the full length promoter and prevented that bZIP transcription factors were binding.

Zinc finger proteins like BTA potentially bind to many substrates, such as DNA, RNA, proteins and lipids (Krishna et al., 2003). It was shown here that a mutated version of BTA (*ind::BTA_ΔZincF-Cerulean*), lacking the DUF702-like domain, exhibited a speckled localization in the nucleus in contrast to the wild type protein. Additionally the mutated version of BTA was localized in chloroplasts, which did not occur with the wild type protein. Since proteasomes can be found in eukaryotes not only in the cytoplasm, but also in the nucleus, it is possible that the DUF702-like domain is necessary for protein stability and that the mutated version is degraded there (Kolodziejek et al., 2011). An alternative explanation is, that the DUF702-like domain of BTA confers binding to genomic DNA or that it is important for interaction with other proteins influencing BTA localization. To test, if BTA is capable of influencing *ACR4* expression, we employed a luciferase reporter assay. As it was found here that the *ACR4* promoter is active at a basal level in *N. benthamiana* epidermal cells and confers expression to reporter genes, a transient luciferase assay in *N. benthamiana* cells was used. With this assay, both up- and downregulation of reporter gene expression can be detected *in vivo*. Here, a CCD camera (NightOwl system, Berthold) was used to detect luciferase activity in the whole leaf, and the experiment was designed to avoid signal fluctuations between individual leafs by using one half of the infiltrated leaf as its own negative control. Using this experimental setup it was shown that BTA binds *pACR4 in vivo*, and that the predicted DUF702-like domain of BTA is necessary for downregulation of *pACR4* activity (see chapter 4.11). However, the exact DNA binding site in the *ACR4* promoter could not be determined. BTA is suspected to bind to element E9 and/or element E10 though since all promoter versions exhibiting altered expression contained this region. So far it is also not clear if BTA is a positive or negative regulator of *ACR4* expression in *Arabidopsis*. Overexpression of BTA in *Arabidopsis* mesophyll protoplasts resulted in an upregulation of *pACR4* activity, while overexpression of BTA in the heterologous organism *N. benthamiana* led to a downregulation of *pACR4*. It is to note here, that neither of these two systems accurately reflects the wild type situation: The mesophyll protoplasts are from *Arabidopsis*, the tissue however is not the tissue *BTA* is normally expressed in. The L1 layer epidermal cells of *N. benthamiana* on the other hand do reflect the correct tissue for BTA expression, but in a homologous expression system. Accordingly, both systems might lack essential co-factors for correct BTA activity. Nonetheless this system does confirm that BTA is capable of binding to the *ACR4* promotor and control its activity to drive gene expression.

5.8 *BINDING TO PROMOTER OF ACR4* is expressed in the distal root meristem

If it is to be assumed that BTA does regulate *ACR4* expression, an important prerequisite is that both genes are expressed in overlapping domains. To test this for the BTA-ACR4 combination, the expression pattern of *BTA* in the RAM of *A. thaliana* was analyzed. In the distal RAM *BTA* is expressed in all initial cells, young CCs and the LRC, whereas no expression could be seen in the QC, the most distal CCs and in border-like cells. In the proximal meristem *BTA* is predominantly expressed in the stele and, at lower levels, in the epidermis (see chapter 4.13). Because of this partially overlapping expression pattern with *ACR4* in the epidermis, CSCs, CCs, the LRC/epidermis initials and the LRC, and the results from the BTA - pACR4 interaction studies, it is likely that BTA is also binding to *pACR4* in its native expression domain. To understand the consequences of BTA – *pACR4* interaction, it will be interesting to analyze *ACR4* expression in *bta* mutants and in *BTA* overexpression lines. Also, it will be interesting to analyze if the potential regulation of *ACR4* is dependent on ACR4 itself. Because of the partially overlapping expression domains of *ACR4* and *BTA*, the function of BTA will not be restricted to regulate *ACR4* expression only. One promising approach to evaluate the function of BTA will be the analysis of *BTA* misexpression and the analysis of its mutant phenotype. Interestingly, *BTA* expression seems to be excluded from the QC, which could be an interesting observation in the context of BTAs role in the CSC-regulating ACR4-WOX5 module. Of course, it is possible that the promoter of *BTA* is simply not active in the QC, but it is also possible that *BTA* expression is actively repressed there. This was previously shown for *CDF4* which needs to be repressed in the QC and CSCs by WOX5, in order for maintaining the undifferentiated state of these cells (Pi et al., 2015). Therefore the phenotypic analysis of a *WOX5:BTA* construct or the analysis of *BTA* expression in *wox5* mutants will be of interest as well.

5.9 The direct WOX5 target *ZFP3* is binding to the promoters of *ACR4* and *WOX5*

In the context of this work, a Y1H-screen, optimized for transcription factors expressed in roots, was performed and several transcription factors could be identified that were able to bind to the 2000 bp 5' upstream regulating sequence of *WOX5* or to a 300 bp promoter fragment of *ACR4*. To narrow down and select the most interesting candidate genes, the data sets from the *WOX5* and *ACR4* screens were compared to each other. AT4G36930: SPATULA (SPT), AT5G25160: ZINC FINGER PROTEIN 3 (ZFP3), AT1G24625: ZINC FINGER PROTEIN 7 (ZFP7) were found to bind to both promoters. Since ZFP3 and ZFP7 are members of the same transcription factor family, there is a possibility that they may bind to the same *cis*-regulatory element. Both genes were shown to act redundantly in a repressive way to influence abscisic acid (ABA) signaling and have an impact on fertility (Joseph et al., 2014). Interestingly *ZFP3* was shown to be a direct target of WOX5 and is downregulated following *WOX5* overexpression (Pi et al., 2015). Thus, this gene could provide a link between *WOX5* and *ACR4* expression by binding to both promoters, while itself being a

target of WOX5. It is possible that ZFP3 provides a feedback to *WOX5* expression by upregulation of *WOX5* or that it is downstream of ACR4 signaling and is necessary for CLE40-mediated *WOX5* repression. Although ZFP3 was shown to be expressed in roots, according to a β-glucuronidase (GUS) reporter analysis it is not expressed in the root tip (Joseph et al., 2014). This should be tested by a more sophisticared analysis technique, e.g. using a fluorophore based reporter on a cellular level though. Another promising candidate for *WOX5* and *ACR4* regulation is the bHLH transcription factor SPT. SPT was initially described to be involved in carpel margin development but it is also involved in regulation of the root meristem size and the amount of QC cells (Heisler et al., 2001; Makkena and Lamb, 2013). Mutants of *spt* produce a larger root meristem with more QC cells compared to wild type *Col-0* roots, while the distal root meristem seems unaffected (Makkena and Lamb, 2013). To evaluate the roles of ZFP3, ZFP7 and SPT, binding of these genes to the *ACR4* and *WOX5* promoters should be confirmed and their expression pattern analyzed. Also the expression of *WOX5* and *ACR4* in mutant backgrounds of these genes in *Arabidopsis* is of interest.

5.10 ACR4 is involved in a CLE40-dependent auto regulatory feedback-loop

The CLE40 signaling module is involved in CSC maintenance through both, a WOX5-dependent and -independent pathway. In both pathways CLE40 acts through the receptor ACR4 to promote cell differentiation. While application of moderate concentrations of synthetic CLE40 peptide leads to differentiation of CSC, a high dosage leads to differentiation of cells in the QC position and to a shift of *WOX5* expression into a more proximal domain. CLE40 peptide treatment results in *ACR4* upregulation, which could be the consequence of an auto-regulatory feedback-loop. Alternatively, different receptors could perceive CLE40 and signaling to downregulate *ACR4*. Here, it is now shown that ACR4 is indeed necessary for the transcriptional upregulation of *ACR4,* since this upregulation was lost in *acr4-2* mutants following CLE40 peptide treatment. Interestingly, a translational reporter of ACR4 but without the intracellular kinase domain (*pACR4:ACR4ΔK-GFP*), expressed in *acr4-2* mutants still showed upregulation. This indicates that, while ACR4 is involved in this auto-regulatory feedback-loop, its kinase domain is not needed for upregulation of *ACR4* in the distal root meristem following CLE40 peptide treatment. Taken together, both results indicate that ACR4 most likely is interacting with other RLKs, which can complement the kinase function of ACR4 in the ACR4ΔK-GFP construct. The leucine-rich repeat receptor-like kinase CLV1 was shown to interact with ACR4 and ACR4-CLV1 complexes act together in the CLE40 pathway (Stahl et al., 2013). ACR4, as well as CLV1, can build homomeric complexes, and consequently three different receptor complexes can be found at the PM in the distal RAM (Bleckmann, 2010; Stahl et al., 2013): ACR4-ACR4 homomers, CLV1-CLV1 homomers and ACR4-CLV1 multimers. Since the upregulation of *acr4* mutants was lost, in can be concluded that the CLV1-CLV1 homomers are not sufficient for this signaling pathway. However, when the

ACR4ΔK-GFP variant was expressed in the *acr4* mutant, transcriptional upregulation of *ACR4* was restored. From this it can be concluded that the CLV1 kinase domain in the ACR4-CLV1 complexes is sufficient to signal into the cell and activate *ACR4* transcription. CLE40 peptide treatment is still able to upregulate *ACR4* in *clv1* mutants, confirming that first, ACR4-ACR4 homomers are sufficient for *ACR4* upregulation and that second, CLV1-CLV1 homomers are not involved in this upregulation (Stahl et al., 2013) (Figure 28).

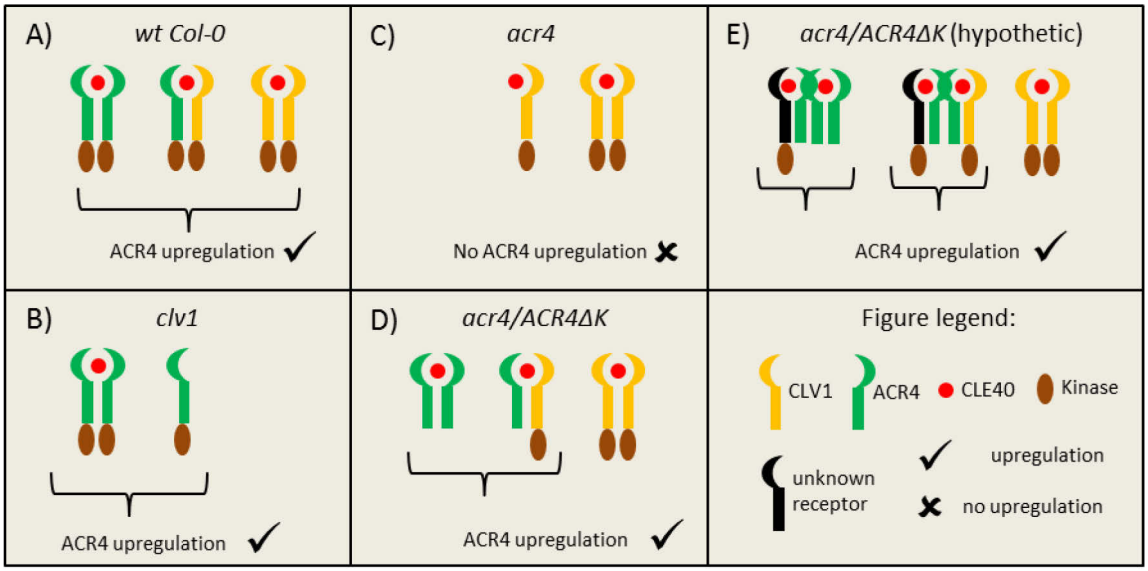

Figure 28 Importance of the ACR4 kinase domain in CLE40 dependent upregulation of *ACR4*

A) In Col-*0* wildtype ACR4-ACR4 (green receptors) homomers, CLV1-CLV1 homomers (yellow receptors) and ACR4-CLV1 multimers are formed in the RAM. CLV1, as well as ACR4, have signaling- active kinase domains (brown) (Cao et al., 2005; Stone et al., 1998). Application of CLE40 peptide (red dot) leads to upregulation (black check mark) of an *ACR4* reporter.

B) clv1 mutants are as well as wildtype plants (A) able to upregulate *ACR4* following CLE40 peptide treatment (Stahl et al., 2013).

C) In *acr4* mutants, CLE40 peptide treatment does not lead to an upregulation (black X) of the *ACR4* reporter.

D) *acr4* mutants complemented with an ACR4 variant lacking the kinase domain (*pACR4:ACR4ΔK-GFP*) are able to upregulate *ACR4* reporter expression.

E) CLE40/ACR4ΔK-dependent upregulation of *ACR4* could occur through signaling via the kinase-domains of interacting CLV1 receptors in the ACR4ΔK/CLV1 heteromeric complexes (as shown in D), or, a so far unknown ACR4-interacting RLK (black receptor) might signal from ACR4ΔK/RLK and ACR4ΔK/RLK/CLV1 complexes and substitute for the missing ACR4 kinase domain.

The role of the ACR4 kinase domain in ACR4-function in the epidermis is also not completely resolved. While it was shown that overexpression of a kinase dead version with a mutation in the putative ATP-binding site (codon 540 mutated from lysine to tryptophan) of ACR4 (*35S::ACR4KW*) is not able to rescue the phenotype of *acr4-1* and *acr4-5* mutants, a complementation construct with the wildtype promoter and a similar (codon 540 mutated from lysine to methionine) kinase dead version (*pACR4: KIN_NULL-GFP*) was able to complement the phenotype of *acr4-2* mutants back to the wild type phenotype (Gifford et al., 2005; Watanabe et al., 2004). In these two publications complementation was measured based on the seed abortion phenotype which is caused by malformed ovules and thereby is related to the epidermal phenotype of *ACR4*. The CSC phenotype in the RAM was not addressed in these experiments.

The ACR4 construct without the kinase domain that was used in this work, was not able to rescue the seed abortion phenotype (Gifford et al., 2005). Since this ACR4ΔK variant was able to restore the CLE40-dependent *ACR4* upregulation in the RAM, this observation indicates that ACR4 functions in different fashions, depending on the cellular context, potentially depending on the receptors with which the protein is interacting. This possibility should be further investigated. The transmembrane domain of ACR4 and its amino acid composition was identified to be the protein-interaction domain of ACR4, essential for both, homomerization and heteromerization with CLV1 (Stahl et al., 2013; Stokes and Gururaj Rao, 2008; Stokes and Rao, 2010). A recombinant ACR4 version with the transmembrane domain of BRI1-ASSOCIATED RECEPTOR KINASE 1 (BAK1) (ACR4_BAK1TM) is, accordingly, not able to build homomers and cannot interact with CLV1 anymore (Stahl et al., 2013). Since the rescue of *acr4* mutants with *pACR4:ACR4ΔK-GFP* might be dependent on its interaction with CLV1 or another RLK, it will be interesting to investigate if a *pACR4:ACR4_BAK1TM* or *pACR4:ACR4ΔK_BAK1TM* can also fulfil this. Additionally, the CSC phenotype of *acr4* mutants complemented with *pACR4:KIN_NULL-GFP* and *pACR4:ACR4ΔK-GFP* should be analyzed to investigate, if ACR4-signaling in these contexts is kinase-dependent or -independent.

5.11 Basal *ACR4* expression is independent of *ACR4*, *WOX5* and *CLE40*

Transcriptional pathways are often stabilized by negative feedback loops, if a stable gene expression level must be ensured. Such systems react on perturbations in signal strength by self-adjusting. One prominent example is the CLAVATA - WUSCHEL negative feedback loop in the SAM of *Arabidopsis*. Here, CLV3 signals from the stem cells through the receptors CLV1, CLV2 and CRN to repress the expression of the transcription factor *WUS* in the cells of the organizing center, thereby promoting cell differentiation. WUS, in turn, promotes stem cell fate and, thereby, *CLV3* expression, leading to its own transcriptional repression (see chapter 1.2 and Figure 3). Through this feedback loop the transcription rate of WUS is buffered to ensure a stable meristem size. In contrast to this concept, positive feedback loops are employed to rapidly amplify transcription of genes in response to a certain stimulus. One example for a system of this sort is described for the abscission of floral organs in *Arabidopsis*. Here, the final step in abscission is triggered by a peptide derived from INFLORESCENCE DEFICIENT IN ABSCISSION (IDA) which is perceived by the leucine-rich repeat-receptor-like kinases HAESA (HAE) and HAESA-LIKE2 (HSL2) (Butenko et al., 2003; Stenvik et al., 2008). Downstream of this IDA-signaling pathway, *HEA* itself is a target and its transcription gets derepressed, leading to an up to 27 fold increase in *HAE* transcription (Patharkar and Walker, 2015). This positive feedback loop shares some similarity with the CLE40-dependent auto-regulatory feedback loop of *ACR4*. Also here, a peptide ligand triggers the upregulation of its own receptor. However, in case of *ACR4*, the transcriptional upregulation is relatively moderate compared to *HAE*. This difference is probably

due to the distinct developmental contexts that these two pathways are active in: Whereas abscission is a final and unidirectional decision to shed organs, stem cell maintenance is a continuous process, and must therefore be balanced. If ACR4 receptor availability, however, correlates with CLE40 signaling activity, then other factors must restrict *ACR4* expression to prevent the system from overshooting. Alternatively, a possible scenario would be that CLE40-dependent *ACR4* auto-upregulation could be a mechanism to sequester an excess of CLE40 by deploying excess receptors to the membrane. In this model, only a certain amount of ACR4 receptors would bind CLE40 peptide, while a majority of receptors at the membrane will be unbound, and therefore signaling inactive. Since other proteins involved in signal transduction (be it other receptors or downstream-effectors) are less abundant, but will bind to all ACR4 proteins, with CLE40 or not, only a small fraction of the receptors at the membrane will form signaling active complexes. This could be tested in an *ACR4* overexpression experiment. If true, *ACR4* overexpression should lead to phenotypes resembling *cle40* mutants. To analyze the CLE40-ACR4 signaling network in more detail, and potentially uncover negative feedback-regulators of *ACR4* expression, the influence of *ACR4*, *CLE40* and *WOX5* on *ACR4* expression was analyzed in this thesis. In *wox5*, *acr4* and *cle40* mutant backgrounds, no change in *ACR4* expression could be found when compared to the Col-*0* wildtype. Accordingly, basal *ACR4* expression is independent of these genes. Ectopic WOX5 overexpression led to an upregulation of *ACR4* expression. Most likely, this is an indirect effect, since WOX5 promotes CSC fate and dedifferentiation of CCs, which could lead to changes in the *ACR4* expression levels (Bennett et al., 2014). There are WUS-binding sites within the *ACR4* promoter, but multiple lines of evidence are presented in this work that support the notion that WOX5 is not directly binding to the promoter of *ACR4* and that WOX5 is not directly regulating *ACR4* expression. First, *ACR4* transcription is not misregulated in *wox5-1* mutants in comparison to Col-*0* wildtype plants according to intensity quantifications of a nuclear localized *tandem-Tomato* fluorophore. Second, WOX5 was not found to bind to the full length *ACR4* promoter *pACR4_P1* in the protoplast transactivation assay, although *WOX5* is included in the transcription factor library used. Furthermore, protein localization studies of WOX5 are showing that WOX5 is localized to the QC, the initials of the stele and the CSCs, but never to the lateral root cap and to the columella cells. This means, that even if WOX5 is able to bind to the *ACR4* promoter and would alter the transcription rate, this would only affect *ACR4* expression in the QC and the CSCs, but not the whole *ACR4* expression domain. Finally, in the luciferase assay using *Nicotiana benthamiana* leaf epidermal cells, WOX5 was not able to bind to different *ACR4* promoter versions.

5.12 *CRR1* and *CRR3* are not expressed in the same expression pattern as *ACR4* and cannot be redundant in CSC maintenance

The receptor-like kinase ACR4 is involved in different developmental pathways like CSC maintenance, specification of epidermal tissues and lateral root development. During lateral root development *ACR4* is expressed in pericycle cells, which will undergo formative cell divisions to establish a lateral root primordium (De Smet et al., 2008). In *acr4* mutants more lateral root primordia per cm can be observed compared to the wildtype, and sometimes the primordia are very close together or even fused (De Smet et al., 2008). This phenotype is enhanced, when combinations with other mutants from the *CRINKLY* gene family are introduced, with triple mutant combinations, such as *acr4*/*crr1*/*crr2* or *acr4*/*crr1*/*crr3* displaying the most severe effects (De Smet et al., 2008). This additive, and thereby redundant, function of *ACR4* to repress supernumerary cell divisions was also observed in the distal root meristem (De Smet et al., 2008). One prerequisite for redundancy is that the *CRINKLY* genes are expressed in the same expression domain of *ACR4*. In this work it was shown that the expression patterns of *CRR1* and *CRR3* in the primary root meristem are different from those of *ACR4*. *CRR1* is not expressed in the distal root meristem, but in the epidermis and cortex (see chapter 4.15). *CRR3* expression was found exclusively in the lateral root cap. Because of this finding it can be excluded that CRR1 and CRR3 are acting redundantly with *ACR4* in CSC maintenance. However, it should not be excluded that ACR4 and CCR3 act in a common pathway in the lateral root cap, where both genes are expressed. So far, no function could be assigned to ACR4 in these cells, even though its expression there indicates that it does exert some function in these cell types as well.

5.13 Fluctuating CLE40 peptide levels and *CDF4* expression might shape the border between CSCs and recently divided daughter cells

Columella stem cell maintenance is a dynamic process in which CSCs divide and a new layer of daughter cells is produced which is not directly connected to the QC anymore. The proximal daughter cells retain CSC identity through their connection to the QC, whereas the distal daughter cells will undergo differentiation into columella cells. During a very short time, immediately following CSC division, the two new cell layers both consist of undifferentiated cells that do not divide. Because of this, the CLE40 signal, coming from the differentiated CCs, will be weaker in the QC-adjacent proximal daughter cells, than in the CC-adjacent distal daughter cells. Because of this, *WOX5* will be briefly derepressed in those cells, because of the reduced CLE40 concentration, leading to a stronger WOX5-dependent repression of *CDF4*. The distal daughter cells are separated by one cell layer from the QC and therefore receive less or no WOX5 protein anymore, but the normal concentration of CLE40 peptide, secreted from the adjacent CCs. This decrease of WOX5 protein leads to a derepression of *CDF4* and, accordingly, an increased CDF4 protein concentration. Eventually, this increase of CDF4 leads to the differentiation of the distal

daughter cells by derepression of a so far unknown gene. Following differentiation, the daughter cells start to produce CLE40, which diffuses to the CSCs, which are now in direct contact to differentiated CCs again. The CSCs are now exposed to elevated CLE40 levels, stop to express WOX5 (WOX5 is repressed through the CLE40 pathway) and consequently express more CDF4. Because, WOX5 still moves from the QC to the CSCs and represses *CDF4*, this intermediate CDF4 level is not high enough to cause differentiation. Later, the CSCs will divide again to give rise to a proximal and a distal daughter cell layer. Cell division and DNA replication are controlled by the cell cycle which functions as an internal clock. Each step of the cell cycle, is controlled by cyclin depended kinases (CDK) and cyclin (CYC) complexes. For example, the transition of the gap 1 (G1) to the synthesis (S) phase (G1/S) is controlled through reversible phosphorylation of RETINOBLASTOMA-RELATED (RBR) by complexes of CDK and D type cyclins (CYCD). Following CSC division, the distal daughter cells, which are destined to differentiated, must be barred from dividing again, while the proximal cells, that remain are undifferentiated, are allowed to re-enter cell division. At this point, the CLE40-WOX5-CDF4 module could be interconnected with the cell-cycle regulatory pathway to allow fine-tuning of both pathways. It has been shown previously that ectopic expression of CYCD3;3 in the QC induces aberrant cell divisions and disturbs quiescence (Forzani et al., 2014). In the wild type, depletion of CYCD3;3 from the QC is accomplished by WOX5, which directly binds to the promoter of CYCD3;3, thereby repressing its transcription. The elevated WOX5 levels in the proximal daughter cells following CSC division (reduced CLE40 peptide levels leads to derepression of WOX5) should, accordingly, result in a repression of *CYC3;3* during this intermediate developmental state of the CSC. Following differentiation of the distal daughter cells, WOX5 levels in the proximal cells will be reduced again due to the stronger CLE40 signal coming from the freshly differentiated CC, resulting in derepression of CYCD3;3. If CLE40 is also influencing the cell cycle independently of WOX5 remains to be studied.

The model for CSC maintenance presented here shows that a complex transcriptional network, interconnecting several different pathways is active in the distal root meristem. Cellular concentrations of transcription factors and signaling molecules are acting in cell specific and target specific manners to modulate transcription and protein activities. This demonstrates the limitations of experiments based on global gain or loss of functions analyses (mutants and 35S overexpression). The ability to modulate gene expression and protein concentrations in tissue-, cell- and time-dependent, specific fashion, followed by a combinatorial analysis of transcriptomes, translatomes and life-cell imaging will be a challenge, but also a necessity in the future.

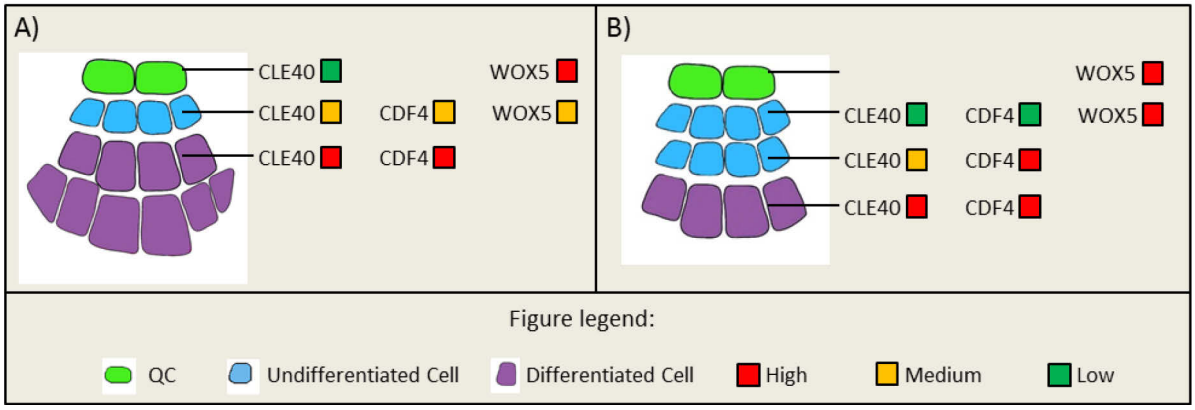

Figure 29 Estimated proteins concentrations of CLE40, CDF4 and WOX5 during different stages of columella development

Estimated protein concentrations in the QC (green cells), undifferentiated cells (cyan cells) and differentiated cells (violet cells).

A) Situation before a CSC division event or directly after differentiation of the distal daughter cells of a recent CSC division

B) Situation immediately after a CSC division event. Division gives rise to two layers (proximal and distal) of undifferentiated cells. The distal cells will differentiate, whereas the proximal cells stays undifferentiated.

6 Summary

The receptor-like kinase (RLK) ARABIDOPSIS CRINKLY 4 (ACR4) is involved in the specification of the epidermis and in columella stem cell (CSCs) homeostasis. These two functions of ACR4 seem to be separable and are controlled through different regulatory pathways, which is reflected in the two distinct expression domains of this gene: the epidermis and the distal root meristem (DRM). In this thesis, the 5' regulatory sequence (the putative promoter) of *ACR4* was analyzed with molecular and computational methods to identify specific sequence motifs that control gene expression in the *Arabidopsis* root. It is shown that the promoter of *ACR4* has a modular organization, comprising 4 modules, whereby each module is needed for a component of the total expression pattern. Module 1 is needed for epidermal expression and module 2 is needed for expression in the DRM. Module 3 is enhancing *ACR4* expression in CSCs and module 4 is a general enhancer of protein expression. Through a process of elimination the location of module 1 (epidermal expression) could be mapped to a 241 bp long region (elements E9 and E10) and module 4 consists of the 483 bp long 5' UTR. This UTR contains four upstream open reading frames (uORFs), which are likely inhibiting protein translation. While the exact location of module 3 (enhancing expression in CSCs) could not be determined, module 2 (needed for expression in the DRM) could be narrowed down to a combination of two evolutionary conserved motifs (M6-1 and M2), each 15 bp in length and spaced by 66 bp. These two motifs are acting redundantly and are necessary for robust expression of *ACR4* in the DRM. The 150 bp long element E7, containing these motifs, is sufficient for expression of *ACR4* in the DRM, when combined with a core 35S Cauliflower Mosaic Virus (35S CaMV) promoter. Since *ACR4* expression is upregulated in the RAM after synthetic CLE40-peptide treatment, it was investigated if the ACR4 RLK is involved in an auto-regulatory feedback loop. It could be shown that the RLK is needed for this process, but not necessarily its kinase domain. Thus, factors, which are directly regulating *ACR4* gene expression, can be both, upstream and downstream of *ACR4* signaling.

This potential auto-regulatory function was then examined in closer detail and also with regard to ACR4 expression strength in mutants of other known players in the CLE40-ACR4-WOX5 signaling module, namely *wox5-1*, *acr4-2* and *cle40-2.* Here it was found, that although ectopic overexpression of *WOX5* and global treatment with synthetic CLE40 peptide both lead to an upregulation of *ACR4* expression in the RAM, neither *WOX5* nor *CLE40* or *ACR4* are required for basal expression of *ACR4* in the DRM. Furthermore in this thesis, transcriptions factors were identified which were able to directly regulate *ACR4* expression, and a first analysis of the expression patterns of the ACR4-homologs *CRR1* and *CRR3* was performed to identify a potential overlap of the expression domain, which could hint to a functional redundancy between these CRINKLY family members.

Here, the previous observation that WOX5 is not a direct regulator of *ACR4* transcription is supported by the finding that WOX5 was not found as a protein binding to the *ACR4* promoter in a protoplast transactivation system (PTA). Additionally WOX5 was not influencing luciferase expression in *Nicotiana benthamiana* epidermal cells and a promoter version with a mutated *WUS* binding site gave rise to a wild type *ACR4* expression pattern. To find transcription factors, which are regulating *ACR4* expression, a PTA and a yeast-1-hybrid (Y1H) screen were combined. In these experiments several transcription factors were identified which were able to influence reporter expression. From those proteins, the ability to influence *ACR4* expression could be confirmed for a transcription factor, which was named BINDING TO THE PROMOTER OF ACR4 (BTA). In a luciferase assay in *N. benthamiana* BTA, a potential zinc-finger protein, was able to downregulate *ACR4* expression. The expression patterns of *ACR4* and *BTA* are partially overlapping in the root cap (CCs, LRC and their initials), which was shown with a promoter-reporter construct. Thus it seems likely that BTA may regulate *ACR4* expression in its native expression domain. In contrast to *BTA*, the expression domains of *CRR1* and *CRR3* are complementary to the expression domain *ACR4*. While *CRR1* is expressed in the epidermis and the cortex, the expression of *CRR3* is restricted to the LRC. Thus it seems unlikely that both genes are acting redundantly together with *ACR4* in regulating CSC homoeostasis. ACR4 orthologs exists in all land plant species examined but not in green algae. This suggest that the *ACR4* gene is an evolutionary innovation, which evolved after the transition step from aquatic living plants to land plants. As an ACR4 ortholog was also found in the moss *Physcomitrella patens*, which has no roots but rhizoids, it is postulated here that the epidermal function of *ACR4* evolved earlier than its function in roots and that *ACR4* was recruited later in evolution to be involved in CSC maintenance and in the initiation of lateral roots.

Finally, a revised model of the CLE40-ACR4-WOX5 signaling module to control CSCs homeostasis was illustrated.

7 Zusammenfassung

Bei ARABIDOPSIS CRINKLY 4 (ACR4) handelt es sich um eine Rezeptorkinase (RLK), welche in der Spezifizierung der Epidermis und in der Homöostase von Columella-Stammzellen (CSCs) im distalen Wurzelapikalmeristem (DRM) eine zentrale Rolle spielt. Diese zwei Funktion von ACR4 scheinen voneinander getrennt zu sein und werden durch zwei unterschiedliche Signalwege kontrolliert. Dies spiegelt sich auch in den unterschiedlichen Expressionsdomänen des Gens wieder. *ACR4* ist in der Epidermis und im distalen Wurzelapikalmeristem exprimiert, was darauf hindeutet, dass unterschiedliche Faktoren diese disjunkte Expression bedingen. Im Rahmen dieser Dissertation wurde die 5‘ gelegene regulative Sequenz (Promoter) von *ACR4* mittels bioinformatischer und molekularbiologischer Verfahren untersucht und die Expression von *ACR4* in den Mutanten von *wox5-1*, *acr4-2* und *cle40-2* quantifiziert. Ferner wurden Transkriptionsfaktoren identifiziert, welche die Expression von *ACR4* zu regulieren scheinen und die Expressionsmuster von zwei Mitgliedern der *ACR4*-Genfamilie wurden analysiert. Des Weiteren wurde die Notwendigkeit der ACR4-Rezeptorkinase in der vom CLE40-Peptid vermittelten Hochregulation der *ACR4*-Transkription untersucht.

Es konnte gezeigt werden, dass der *ACR4* Promoter modular aufgebaut ist und die vier einzelnen Module für jeweils einen Teil des Gesamtexpressionsmusters verantwortlich sind: Während Modul 1 für die epidermale Expression verantwortlich ist, wird Modul 2 für die Expression im distalen Wurzelapikalmeristem benötigt. Modul 3 verstärkt die Expression in Columella-Stammzellen, und Modul 4 scheint sich repressiv auf die gesamte Proteinexpression auszuwirken. Die physische Lokalisation von Modul 1 (epidermale Expression) konnte durch ein Ausschlussverfahren auf einen Bereich von 241 Basenpaare (bp) (Elemente E9 und E10) eingeengt werden und bei Modul 4 handelt es sich um einen 483 bp langen Abschnitt des 5‘ nicht-translatierten-Bereichs (5‘ UTR). Letzterer enthält 4 offene Leseraster (uORF), welche sich inhibierend auf die Proteintranslation auswirken könnten. Während die genaue Position von Modul 3 (verstärkt die Expression in Columella-Stammzellen) nicht bestimmt werden konnte, liegen für die Lokalisation von Modul 2 (Expression im distalem Wurzelapikalmeristem) genaue Daten vor. Es konnte gezeigt werden, dass zwei 15 bp lange und durch 66 bp voneinander getrennte evolutionär konservierte Motive (M6-1 und M2) für die Expression im distalen Wurzelapikalmeristem benötigt werden, und dass Element E7, welches diese zwei Motive enthält, in Kombination mit einem -60 bp 35S Kernpromoter hinreichend für die distale Expression ist. Da die Behandlung von Keimlingen mit synthetischem CLE40-Peptid zu einer Hochregulation der *ACR4*-Transkription führt wurde untersucht, ob die Regulation der *ACR4*-Expression ein Ziel des eigenen Signalweges ist. Es konnte gezeigt werden, dass diese Hypothese zutrifft und die Rezeptorkinase selbst essentiell für die eigene transkriptionelle Hochregulation

verantwortlich ist. Jedoch scheint die Kinasedomäne hierfür nicht benötigt zu werden. Dies lässt darauf schließen, dass die Kinasefunktion von ACR4 durch die Interaktion von ACR4 mit weiteren Proteinen mit Kinasefunktion redundant sein könnte.

Obwohl sowohl die Behandlung mit synthetischem CLE40-Peptid, also auch die ektopische Überexpression von *WOX5* zu einer Hochregulation der *ACR4*-Transkription führt, konnte in den mutanten Hintergründen von *cle40-2*, *wox5-1* und *acr4-2* keine Veränderung der Expression im Vergleich zum Wildtyp Col-*0* beobachtet werden. Dies deutet darauf hin, dass eine basale Expression von *ACR4* unabhängig von diesen drei Genen ist. Es scheint, dass WOX5 die *ACR4*-Expression nicht direkt reguliert, was zusätzlich durch folgende Befunde belegt werden konnte: Der Transkriptionsfaktor WOX5 war nicht in der Lage die *ACR4* Expression in Mesophyll-Protoplasten in einem Protoplasten-Transaktivierungs-Test (PTA) zu beeinflussen. Auch konnte die *ACR4*-Expression in epidermalen Zellen von *Nicotiana benthamiana* (Luciferase-Test) nicht durch eine Überexpression von *WOX5* beeinflusst werden. Des Weiteren führte eine Mutation einer *WUS*-bindestelle (an welcher WOX5 potentiell binden könnte) zu keiner Veränderung des wildtypischen Expressionsmusters von *ACR4* im distalen Wurzelapikalmeristem von *A*. *thaliana*.

Um Proteine zu identifizieren, die eine regulatorische Wirkung auf die *ACR4*-Expression haben, wurden eine Protoplasten-Transaktivierungs-Analyse (PTA, protoplast transactivation assay) und eine Hefe-1-Hybrid-Analyse (Y1H, yeast-1-hybrid screen) miteinander kombiniert. In diesen Analysen wurden einige Transkriptionsfaktoren identifiziert, welche die Promoteraktivität von *ACR4* positiv beeinflussen können. Die positive Wirkung auf die *ACR4*-Expression von einem dieser Transkriptionsfaktoren, welcher BINDING TO THE PROMOTER OF ACR4 (BTA) genannt wurde, konnte in einem Luciferase-Test bestätigt werden. Da gezeigt wurde, dass BTA in *A. thaliana* in der Wurzelhaube (Columella, laterale Wurzelhaube und deren Stammzellen) mit *ACR4* coexprimiert ist, wäre eine regulative Wirkung des Transkriptionsfaktors auf die *ACR4*-Expression also auch durch die gemeinsame Expressionsdomäne möglich. Die Expressionsmuster von *CRR1* und *CRR3* jedoch, zwei Mitglieder der CRR-Genfamilie, sind deutlich von *ACR4* zu unterscheiden. Da *CRR1*, in der Wurzel, nur in der Epidermis und im Cortex exprimiert ist und *CRR3* nur in der lateralen Wurzelhaube, ist es unwahrscheinlich, dass diese beiden Gene zusammen mit *ACR4* im Hinblick auf die CSCs-Homöostase redundant wirken. Orthologe Gene von *ACR4* konnten in allen in dieser Dissertation untersuchten Landpflanzen (Embryophyta) gefunden werden, nicht jedoch in aquatisch lebenden Algen. Dies deutet darauf hin, dass es sich bei *ACR4* um eine genetische Innovation handelt, welche beim Übergang zum Landleben evolvierte. Da ein Ortholog von *ACR4* auch in dem Laubmoos *Physcomitrella patens*, welches keine Wurzeln besitzt, gefunden werden konnte, wird postuliert, dass die epidermale Funktion von *ACR4* sich zuerst entwickelt hat und dass *ACR4* später rekrutiert wurde, um eine Funktion in der Wurzel zu erfüllen. Schließlich wurde ein erweitertes Modell des CLE40-ACR4-WOX5 Signalweges zur Regulation der Columella-Stammzellen-Homöostase erstellt.

8 Supplemental data

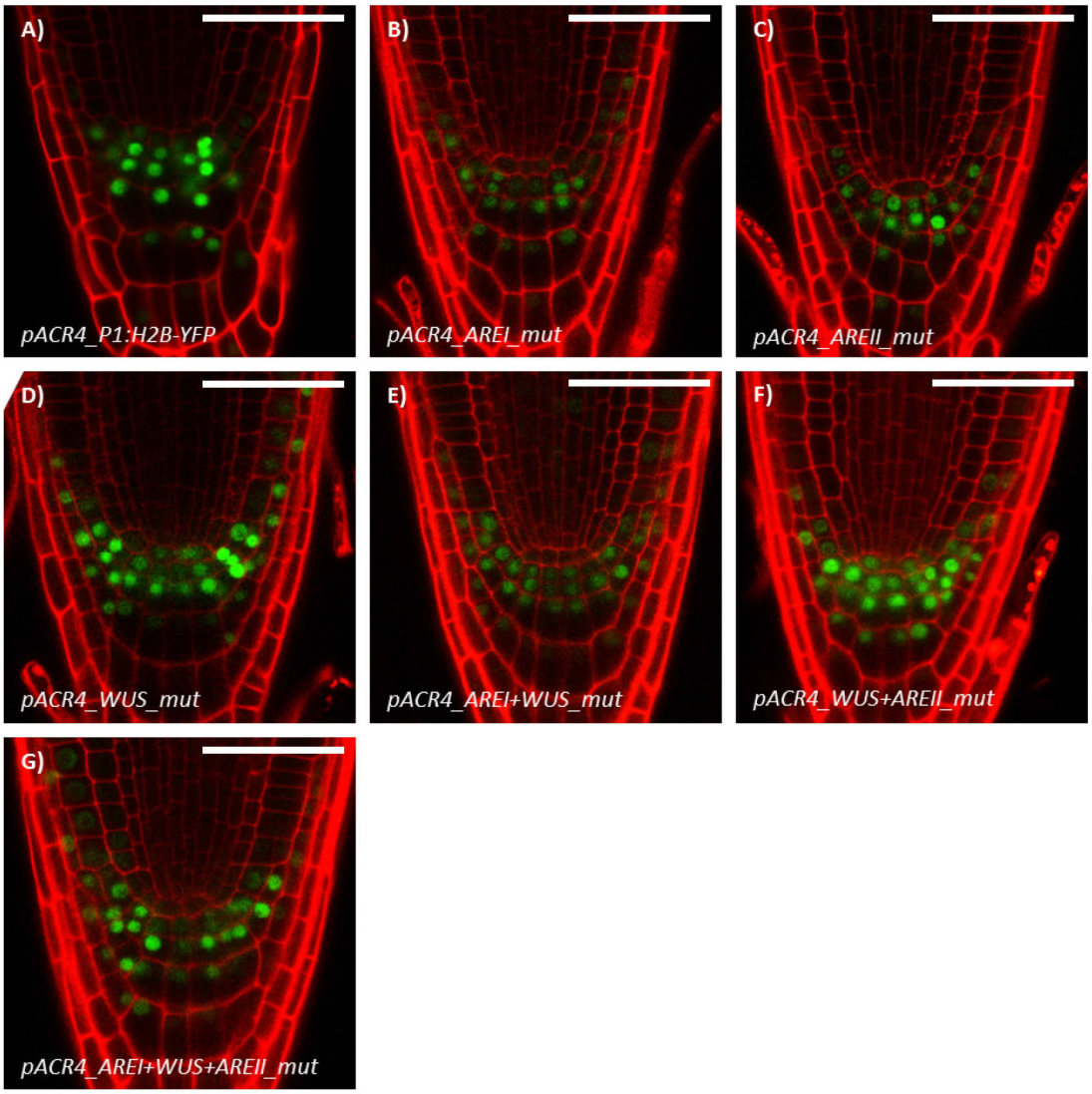

Figure S 1 The predicted WUS binding site and its adjacent AREs are not needed for ACR4 expression

Confocal images of root tips expressing wild type *pACR4_P1:H2B-YFP* and mutated *pACR4* versions conferring expression to *Venus-H2B*. No obvious differences in expression compared to *pACR4_P1* could be observed. Scale bar: 50 µM.

A) *pACR4_P1:H2B-YFP*; B) *pACR4_AREI_mut:Venus-H2B*; C) *pACR4_AREII_mut:Venus-H2B*; D*) pACR4_WUS_mut:Venus-H2B*; E) *pACR4_AREI+WUS_mut:Venus-H2B;* F) *pACR4_WUS+AREII_mut:Venus-H2B;* G) *pACR4_AREI+WUS+AREII_mut:Venus-H2B*

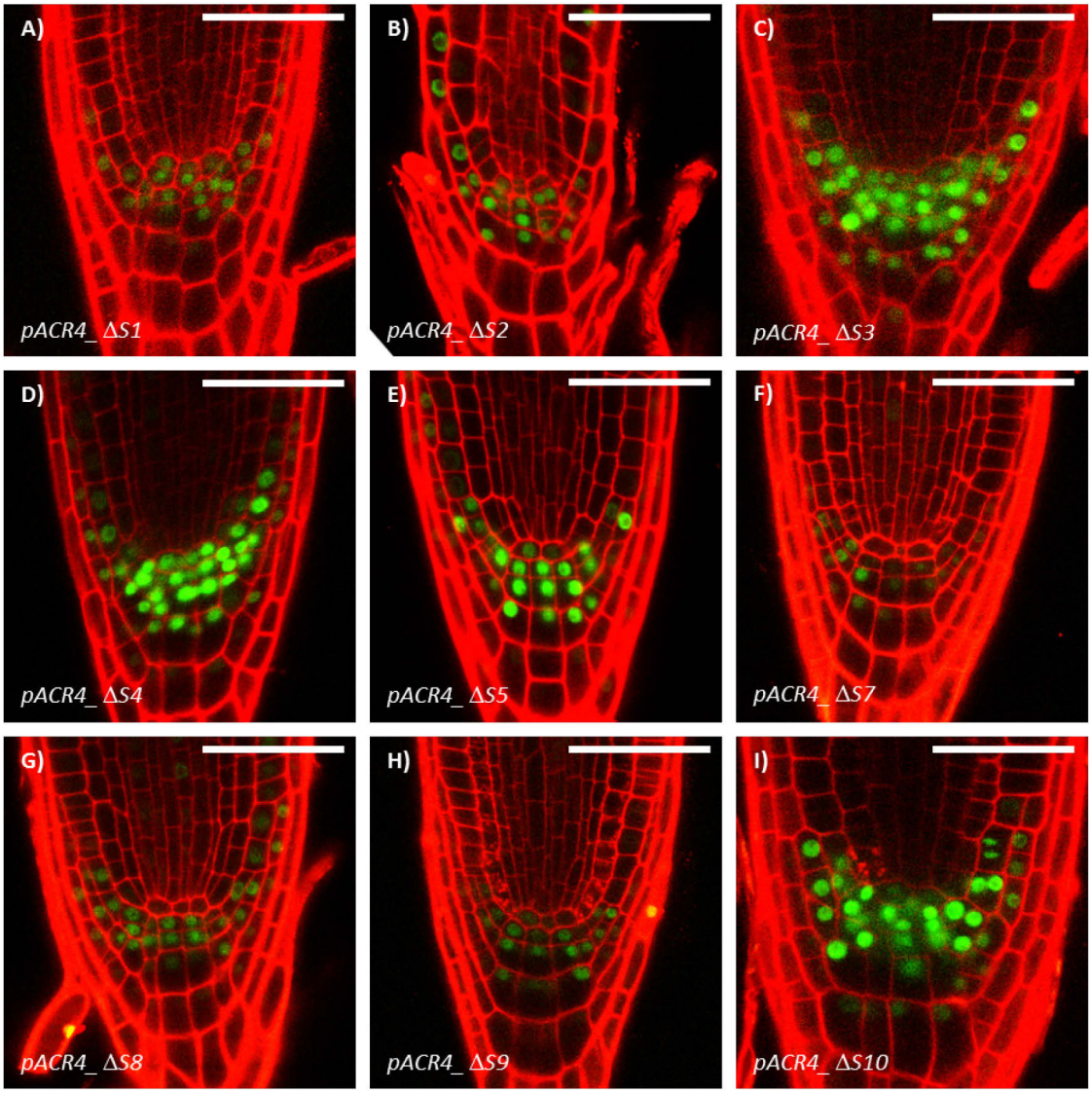

Figure S 2 Fine-mapping of element 7 for cis-acting elements necessary for distal expression of ACR4 in the root meristem

In this approach deletions of 15bp length were set in a systematic way covering the whole element 7.

All promoter derivatives showed the wild type expression pattern of ACR4. For pACR4_ΔS6 no T1 transformants could be selected. Scale bar: 50 µM.

AAATCGAGCGATTGAGAGCACTTCGCAAAATCAGAGCGACAAAAAAAAATAAAAACCAATCCTTTCGATTCCAAATTTTTTGT
TACTCACTCGCACGAGTTTTATTTGGTCGTTAGTTATCTCTTTCGTTGAATAACGGTTTTAATTTAAACCGTTACTTTTTATC
AATGGCGACTTCGTCACCGTCTCTGAGTAACAATGGTCTTTCCTCCGTCGTCACGCCTCCCAAAACTCTCCGTGGTCTCAATA
AGCCTAAGTGTATTCAATGCGGCAATGTAGCTCGCTCCAGGTATTGCTTCTACGCATTGTTTCATCGAAGGACTTAGGTTTTT
TACATCTGGGGTTTCGATTTATGGATTGTTCTTGGGTTTTTGATCTGAAAGGATTCGAATTTGTCTTGTATAGTACTTTTTCG
TTTTGATTTAGGGTTCATAGGTTTGTGGGTTTGGGTTTTTATTCATGATTTGGTGATTAATCTGTTGGAGATTGTTTAAAGTT
TTGAGCTTTAGTATCGAAAGATCAGTTTTTTGAGATTATTGGTGAAGTAATTGTAATTGTATTGCTTGGATTTGATAAATGCA
GGTGCCCTTTTCAATCTTGTAAGGGTTGTTGTTCAAGAGCAGAGAATCCCTGCCCGATTCACGGTATGTTTGCCCTGTCAAAT
CTCAACTTCATAATTAGCTAAAGTGATCAGTTTTAGAGTTTAGTGTTGATAACTTTGATTGGAGAGTTCTATTCTTTCACTTG
GTAAGTTTAGAGTTTAGTATTCTTGACTTCTATAGGGTTCGTTTGGTTGTCTCGGGACAAAAAAACCTATAAAGAACCATAAG
ACTGATTCTTGGAATGTGCTTGTGATTAGCTGAGAGATATAGAGATGTTATCATGGACTGTTTTGTGTTTCTTCTTATGTGTT
TTATTTCGCTGCAGTTCTTAAAGTAGCTTCAACGTCTGGTGAGAAGACGCAGGCGCCAAGTACTCCATCTTCAGAGCAGAAAG
CAACCGAGGGCACTCCCGGGTACATATATATAAACTAATTTTCTGTTTTGTTTGTGCTTCCATGGGCAAGTGAATCTTAGATG
ATAAACCGGTGTTTGCTTACTAATACTTTGATAGGAGATTCTTCAGCTTTCTTGTTTTATTGCACGTAGTTGATAGTGAGATG
ATATATTGGTCTTGTGGAACTAAAATATGGCGCTTTATGTTGACGTTTTCTTCTTTTGGAAATTGTTTCAGGAGTACCACTAG
AGTTTCGTCAATCCGGCAACTTTCTAGCAACTTTGCTCAGTTTAATAACCTGAATGCTTCTTCCCGCCAGAGAAAACCTTTGA
CGATAAAGGTATACTAATTAAGACGTCTTTCATTGACTTTAGTACTCTATGAAAAATCTCCATTTAGTTGTTTTCCTCTTATC
AGTTTTTGTTCTGTCTATATTCTATAGGATGCTCAAGCTTTAAACGAGTGGCGGTTTACAAAGCTAAAAGAGTACAGAGACAG
AAACATTGAAGTAGAAAATGAAGCTTTTGATCGGTACATGAGTAATGTGAATTTACTCGAAGAAGCATTTTCATTTACATCTG
TTCCTGATGAAGAGAGTCATGGAACAGCAGCTCCTGAGCAAAACAAAGAGGAAAATATTGTTTCAGAGCTTAAACTGAGGCTG
AGATCGAACTCTGCAAGAACAGAGAGCTTTAAGAAGCGGATCGCGGAGACAGTCAAAGCCGGTTTGGTGAAGCTTAAGAGACT
GGATTTAGGCAGTTCTTCAGATGATCAAGATGATATCAAAAGGCGGGTCAAAAGAAAGAAATGGGAAGAGAAAGGTTCAGCTT
TGAATGAAATAATCGATAAACTGAACAAAGCAAGAACCGAAGAGGATCTCAAATCTTGCTTAGAGATGAAATCAAAGCTCTGT
GGTCAAGTTTCTCCCACTGCTGCTTCCGAGAAGAACAAGATCTTTCCGGGTGTAGTCCGAAAAGTTGAGATGAGTGAAGAAGC
ACTTCAAAAAATCGCTGAGAATCTCCAATCTTTTGACAAAGTTGGAATGTTGTGAAGTCGAGAACATCCTGTGGATGAACTGA
AAAGTTTGAGTGGCAAGAAAATTTCTAGATCCTTCGTGACCACGGTATTGTACAATGATCAAACATCCCTCAAAACTGATCCT
GAAGACTCCAAAGACTCAAGAGATTCTTGTAAAGTAGTGTTGAGCATCATTTAGATATTAGAACTCAGCCATGGATAAAGCTG
TTGATTCTATCTCATTGGATTTTTTTCACTGTGTGTTGTTGCTTTGTTAGATTTGAAATTGCTCATTGGATTACCTTTGACTT
AATAAATAGTTGGTTTGGTTTGGT

Cyan:5'UTR Violet:Exon Green:Intron Red:3'UTR

Figure S 3 DNA Sequence of *BTA*

Five exons (violet) and 4 introns (green) can be found in the DNA sequence of *BTA* according to data from "The Arabidopsis Information Resource". The 5' UTR (Cyan) is 167 bp long and the 3' UTR (red) is 301 bp long.

Thanks for using the 'AtSubP' web server.

Your prediction results are as under:

Seven different scores corresponding to each seven localizations are displayed for each of the query sequence. The final location is the corresponding highest score sorted within the seven locations. Please note: if all the scores are negative, the query sequence is predicted to be "Unknown" category i.e. NOT (Chloroplast, Cytoplasm, Golgi apparatus, Mitochondrion, Extracellular, Nucleus or Cell membrane protein).

Prediction approach followed	Amino acid composition-based
Number of sequences entered	1
Predicted on	Wed Dec 23 05:52:51 2015

Sequence ID	Seq length	Chloro	Cyto	Golgi	Mito	Extracl	Nucl	Celmemb	PREDICTION
AT1G32730	326	-1.6993116	-1.6035549	-1.8008901	-1.4046573	-1.7245603	1.70074	-1.5326456	Nucleus

Figure S 4 AtSupP predicts a nuclear localization of BTA

According to the Arabidopsis Subcellular Localization Prediction Server (AtSupP) BINDING TO PROMOTER OF ACR4 (BTA) is a nuclear localized protein. Screenshot.

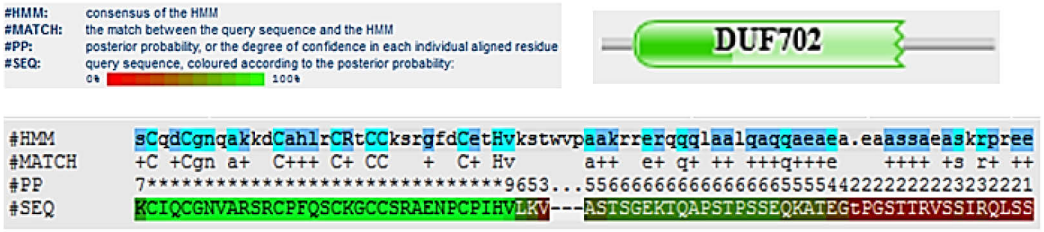

Figure S 5 Comparison of the protein sequence of BTA with the Pfam B database

BTA has a DUF702-like domain, which is only found in the SHORT INTERNODES (SHI) family of transcription factors. While the N-terminal part of this domain is conserved, the C-terminal part is less conserved. Screenshot.

TF binding to *pWOX5_Y1H*	TF binding to *pACR4_Y1H-Min*	TF binding to both constructs
AT5G52020	AT3G45610	AT4G36930
AT2G38340	AT4G34680	AT1G24625
AT1G21910	AT1G33240	AT5G25160
AT5G05410	AT3G61630	
AT5G44210	AT4G39070	
AT3G25730	AT5G25160	
AT5G18560	AT4G34610	
AT1G01260	AT2G44840	
AT5G62610	AT1G07640	
AT5G54680	AT1G24625	
AT4G36930	AT4G36930	
AT3G19290	AT1G67910	
AT2G35530	AT3G58070	
AT2G40950	AT1G68360	
AT4G36620	AT1G04880	
AT2G18380	AT1G51700	
AT3G60530	AT3G22760	
AT4G32890	AT5G60200	
AT5G25160	AT1G16530	
AT1G66140	AT1G31320	
AT1G67030	AT4G00940	
AT1G24625		
AT2G22900		
AT3G53340		
AT1G47870		
AT1G61730		
AT2G22840		
AT4G34610		
AT4G12350		
AT4G37260		
AT3G50060		
AT3G49690		
AT2G44730		
AT1G54060		
AT4G26640		
AT2G04880		
AT2G02540		

Figure S 6 Transcription factors binding pWOX5_Y1H and pACR4_Y1H-Min

Listed are the transcription factors binding to *pWOX5_Y1H* and *pACR4_Y1H-Min* in the Y1H done. Three transcription factors bound to both constructs.

9 Literature

Abas, L., Benjamins, R., Malenica, N., Paciorek, T., Wišniewska, J., Moulinier–Anzola, J. C., Sieberer, T., Friml, J. and Luschnig, C. (2006). Intracellular trafficking and proteolysis of the Arabidopsis auxin-efflux facilitator PIN2 are involved in root gravitropism. *Nature Cell Biology* **8**, 249-256.

Aida, M., Beis, D., Heidstra, R., Willemsen, V., Blilou, I., Galinha, C., Nussaume, L., Noh, Y.-S., Amasino, R. and Scheres, B. (2004). The PLETHORA genes mediate patterning of the Arabidopsis root stem cell niche. *Cell* **119**, 109-120.

Alexandrov, N. N., Troukhan, M. E., Brover, V. V., Tatarinova, T., Flavell, R. B. and Feldmann, K. A. (2006). Features of Arabidopsis genes and genome discovered using full-length cDNAs. *Plant Molecular Biology* **60**, 69-85.

Araya, T., Miyamoto, M., Wibowo, J., Suzuki, A., Kojima, S., Tsuchiya, Y. N., Sawa, S., Fukuda, H., von Wirén, N. and Takahashi, H. (2014). CLE-CLAVATA1 peptide-receptor signaling module regulates the expansion of plant root systems in a nitrogen-dependent manner. *Proceedings of the National Academy of Sciences* **111.5**, 2029-2034.

Ausubel, F. M., Brent, R., Kingston, R. E., Moore, D. D., Seidman, J. G., Smith, J. A. and Struhl, K. E. (1987). *Current Protocols in Molecular Biology*. 1.1-10.16.

Bailey, T. L., Williams, N., Misleh, C. and Li, W. W. (2006). MEME: discovering and analyzing DNA and protein sequence motifs. *Nucleic acids research* **34**, W369-W373.

Barton, M. (2010). Twenty years on: the inner workings of the shoot apical meristem, a developmental dynamo. *Developmental biology* **341**, 95-113.

Barton, M. K. and Poethig, R. S. (1993). Formation of the shoot apical meristem in Arabidopsis thaliana: an analysis of development in the wild type and in the shoot meristemless mutant. *Development* **119**, 823-831.

Becraft, P. W., Stinard, P. S. and McCarty, D. R. (1996). CRINKLY4: a TNFR-like receptor kinase involved in maize epidermal differentiation. *Science* **273**, 1406-1409.

Benfey, P. N., Ren, L. and Chua, N.-H. (1989). The CaMV 35S enhancer contains at least two domains which can confer different developmental and tissue-specific expression patterns. *The EMBO Journal* **8**, 2195.

Bengough, A. and McKenzie, B. (1997). Sloughing of root cap cells decreases the frictional resistance to maize (Zea mays L.) root growth. *Journal of Experimental Botany* **48**, 885-893.

Bennett, T., van den Toorn, A., Sanchez-Perez, G. F., Campilho, A., Willemsen, V., Snel, B. and Scheres, B. (2010). SOMBRERO, BEARSKIN1, and BEARSKIN2 regulate root cap maturation in Arabidopsis. *The Plant Cell* **22**, 640-654.

Bennett, T., van den Toorn, A., Willemsen, V. and Scheres, B. (2014). Precise control of plant stem cell activity through parallel regulatory inputs. *Development* **141**, 4055-4064.

Bennici, A. (2008). Origin and early evolution of land plants: Problems and considerations. *Communicative & integrative biology* **1**, 212-218.

Blancaflor, E. B., Fasano, J. M. and Gilroy, S. (1998). Mapping the functional roles of cap cells in the response of Arabidopsis primary roots to gravity. *Plant Physiology* **116**, 213-222.

Bleckmann, A. (2010). Untersuchungen zur Stammzellregulation im Sprossapikalmeristem von Arabidopsis thaliana. Doctoral thesis. Heinrich-Heine-Universität Düsseldorf.

Boer, D. R., Freire-Rios, A., van den Berg, W. A., Saaki, T., Manfield, I. W., Kepinski, S., López-Vidrieo, I., Franco-Zorrilla, J. M., de Vries, S. C. and Solano, R. (2014). Structural basis for DNA binding specificity by the auxin-dependent ARF transcription factors. *Cell* **156**, 577-589.

Brady, S. M., Orlando, D. A., Lee, J.-Y., Wang, J. Y., Koch, J., Dinneny, J. R., Mace, D., Ohler, U. and Benfey, P. N. (2007). A high-resolution root spatiotemporal map reveals dominant expression patterns. *Science* **318**, 801-806.

Brand, U., Fletcher, J. C., Hobe, M., Meyerowitz, E. M. and Simon, R. (2000). Dependence of stem cell fate in Arabidopsis on a feedback loop regulated by CLV3 activity. *Science* **289**, 617-619.

Burks, E. A., Bezerra, P. P., Le, H., Gallie, D. R. and Browning, K. S. (2001). Plant initiation factor 3 subunit composition resembles mammalian initiation factor 3 and has a novel subunit. *Journal of Biological Chemistry* **276**, 2122-2131.

Butenko, M. A., Patterson, S. E., Grini, P. E., Stenvik, G.-E., Amundsen, S. S., Mandal, A. and Aalen, R. B. (2003). Inflorescence deficient in abscission controls floral organ abscission in Arabidopsis and identifies a novel family of putative ligands in plants. *The Plant Cell* **15**, 2296-2307.

Cao, X., Li, K., Suh, S. G., Guo, T. and Becraft, P. W. (2005). Molecular analysis of the CRINKLY4 gene family in Arabidopsis thaliana. *Planta* **220**, 645-657.

Chu, H., Qian, Q., Liang, W., Yin, C., Tan, H., Yao, X., Yuan, Z., Yang, J., Huang, H. and Luo, D. (2006). The FLORAL ORGAN NUMBER4 gene encoding a putative ortholog of Arabidopsis CLAVATA3 regulates apical meristem size in rice. *Plant Physiology* **142**, 1039-1052.

Clough, S. J. and Bent, A. F. (2000). Vapor-phase sterilization of Arabidopsis seed. http://www.plantpath.wisc.edu/fac/afb/vapster.html

Clough, S. J. and Bent, A. F. (1998). Floral dip: a simplified method forAgrobacterium-mediated transformation ofArabidopsis thaliana. *The Plant Journal* **16**, 735-743.

Cock, J. M. and McCormick, S. (2001). A large family of genes that share homology with CLAVATA3. *Plant Physiology* **126**, 939-942.

Colette, A., Lu, K.-J. and Weijers, D. (2015). Building a plant: cell fate specification in the early Arabidopsis embryo. *Development* **142**, 420-430.

Crawford, B. C., Sewell, J., Golembeski, G., Roshan, C., Long, J. A. and Yanofsky, M. F. (2015). Genetic control of distal stem cell fate within root and embryonic meristems. *Science* **347**, 655-659.

Cruz-Ramírez, A., Díaz-Triviño, S., Wachsman, G., Du, Y., Arteága-Vázquez, M., Zhang, H., Benjamins, R., Blilou, I., Neef, A. B. and Chandler, V. (2013). A SCARECROW-RETINOBLASTOMA protein network controls protective quiescence in the Arabidopsis root stem cell organizer. PLoS Biol **11**, e1001724

Darwin, C. and Darwin, F. (1880). *The Power of Movement in Plants*. Publisher: John Murray, London.

Daum, G., Medzihradszky, A., Suzaki, T. and Lohmann, J. U. (2014). A mechanistic framework for noncell autonomous stem cell induction in Arabidopsis. *Proceedings of the National Academy of Sciences* **111**, 14619-14624.

De Smet, I., Vassileva, V., De Rybel, B., Levesque, M. P., Grunewald, W., Van Damme, D., Van Noorden, G., Naudts, M., Van Isterdael, G., De Clercq, R., et al. (2008). Receptor-like kinase ACR4 restricts formative cell divisions in the Arabidopsis root. *Science* **322**, 594-597.

Dellaporta, S. L., Wood, J. and Hicks, J. B. (1983). A plant DNA minipreparation: version II. *Plant Molecular Biology Reporter* **1**, 19-21.

Deplancke, B., Vermeirssen, V., Arda, H. E., Martinez, N. J. and Walhout, A. J. (2006). Gateway-compatible yeast one-hybrid screens. *Cold Spring Harbor Protocols* **5**, pdb-prot4590.

Ding, Z. and Friml, J. (2010). Auxin regulates distal stem cell differentiation in Arabidopsis roots. *Proceedings of the National Academy of Sciences* **107**, 12046-12051.

Dolan, L., Janmaat, K., Willemsen, V., Linstead, P., Poethig, S., Roberts, K. and Scheres, B. (1993). Cellular organisation of the Arabidopsis thaliana root. *Development* **119**, 71-84.

Forzani, C., Aichinger, E., Sornay, E., Willemsen, V., Laux, T., Dewitte, W. and Murray, J. A. (2014). WOX5 suppresses CYCLIN D activity to establish quiescence at the center of the root stem cell niche. *Current Biology* **24**, 1939-1944.

Fridborg, I., Kuusk, S., Robertson, M. and Sundberg, E. (2001). The Arabidopsis protein SHI represses gibberellin responses in Arabidopsis and barley. *Plant Physiology* **127**, 937-948.

Gaudinier, A., Zhang, L., Reece-Hoyes, J. S., Taylor-Teeples, M., Pu, L., Liu, Z., Breton, G., Pruneda-Paz, J. L., Kim, D. and Kay, S. A. (2011). Enhanced Y1H assays for Arabidopsis. *Nature Methods* **8**, 1053-1055.

Gifford, M. L., Dean, S. and Ingram, G. C. (2003). The Arabidopsis ACR4 gene plays a role in cell layer organisation during ovule integument and sepal margin development. *Development* **130**, 4249-4258.

Gifford, M. L., Robertson, F. C., Soares, D. C. and Ingram, G. C. (2005). ARABIDOPSIS CRINKLY4 function, internalization, and turnover are dependent on the extracellular crinkly repeat domain. *Plant Cell* **17**, 1154-1166.

Graham, L. E. (1993). *Origin of Land Plants*: John Wiley & Sons, Inc. ISBN: 0471615277

Guilfoyle, T., Hagen, G., Ulmasov, T. and Murfett, J. (1998). How does auxin turn on genes? *Plant Physiology* **118**, 341-347.

Haecker, A., Groß-Hardt, R., Geiges, B., Sarkar, A., Breuninger, H., Herrmann, M. and Laux, T. (2004). Expression dynamics of WOX genes mark cell fate decisions during early embryonic patterning in Arabidopsis thaliana. *Development* **131**, 657-668.

Hamann, T., Benkova, E., Bäurle, I., Kientz, M. and Jürgens, G. (2002). The Arabidopsis BODENLOS gene encodes an auxin response protein inhibiting MONOPTEROS-mediated embryo patterning. *Genes & Development* **16**, 1610-1615.

Han, P., Li, Q. and Zhu, Y.-X. (2008). Mutation of Arabidopsis BARD1 causes meristem defects by failing to confine WUSCHEL expression to the organizing center. *The Plant Cell* **20**, 1482-1493.

Hanfrey, C., Elliott, K. A., Franceschetti, M., Mayer, M. J., Illingworth, C. and Michael, A. J. (2005). A dual upstream open reading frame-based autoregulatory circuit controlling polyamine-responsive translation. *Journal of Biological Chemistry* **280**, 39229-39237.

Hawes, M. C., Smith, L. Y. and Stephenson, M. (1991). Root organogenesis from single cells released from the root cap of Medicago sp. *Plant cell, Tissue and Organ culture* **27**, 303-308.

Heisler, M. G., Atkinson, A., Bylstra, Y. H., Walsh, R. and Smyth, D. R. (2001). SPATULA, a gene that controls development of carpel margin tissues in Arabidopsis, encodes a bHLH protein. *Development* **128**, 1089-1098.

Hellens, R. P., Allan, A. C., Friel, E. N., Bolitho, K., Grafton, K., Templeton, M. D., Karunairetnam, S., Gleave, A. P. and Laing, W. A. (2005). Transient expression vectors for functional genomics, quantification of promoter activity and RNA silencing in plants. *Plant methods* **1**, 13.

Höfgen, R. and Willmitzer, L. (1988). Storage of competent cells for Agrobacterium transformation. *Nucleic Acids Research* **16**, 9877.

Hori, K., Maruyama, F., Fujisawa, T., Togashi, T., Yamamoto, N., Seo, M., Sato, S., Yamada, T., Mori, H. and Tajima, N. (2014). Klebsormidium flaccidum genome reveals primary factors for plant terrestrial adaptation. *Nature communications* **5**, *3978.*

Hülsewede, A. (2010). Über Peptid gesteuerte Signaltransduktion In der Entwicklung von Arabidopsis thaliana. Diploma thesis. Heinrich-Heine-Universität Düsseldorf.

Ikeda, M., Mitsuda, N. and Ohme-Takagi, M. (2009). Arabidopsis WUSCHEL is a bifunctional transcription factor that acts as a repressor in stem cell regulation and as an activator in floral patterning. *The Plant Cell* **21**, 3493-3505.

Iyer-Pascuzzi, A. S., Jackson, T., Cui, H., Petricka, J. J., Busch, W., Tsukagoshi, H. and Benfey, P. N. (2011). Cell identity regulators link development and stress responses in the Arabidopsis root. *Developmental cell* **21**, 770-782.

Jin, P., Guo, T. and Becraft, P. W. (2000). The maize CR4 receptor-like kinase mediates a growth factor-like differentiation response. *Genesis* **27**, 104-116.

Jones, V. A. and Dolan, L. (2012). The evolution of root hairs and rhizoids. *Annals of Botany* **110**, 205-212.

Joseph, M. P., Papdi, C., Kozma-Bognár, L., Nagy, I., López-Carbonell, M., Rigó, G., Koncz, C. and Szabados, L. (2014). The Arabidopsis ZINC FINGER PROTEIN3 interferes with abscisic acid and light signaling in seed germination and plant development. *Plant Physiology* **165**, 1203-1220.

Jürgens, G., Ruiz, R. A. T., Laux, T., Mayer, U. and Berleth, T. (1994). Early events in apical-basal pattern formation in Arabidopsis. *Plant Molecular Biology*, 95-103. ISBN: 978 3 642 78854 3.

Kadereit, J. W., Körner, C., Kost, B. and Sonnewald, U. (2014). *Strasburger– Lehrbuch der Pflanzenwissenschaften*. ISBN: 978 3642544347

Kaundal, R., Saini, R. and Zhao, P. X. (2010). Combining machine learning and homology-based approaches to accurately predict subcellular localization in Arabidopsis. *Plant Physiology* **154**, 36-54.

Kenrick, P. and Strullu-Derrien, C. (2014). The origin and early evolution of roots. *Plant Physiology* **166**, 570-580.

Kieffer, M., Stern, Y., Cook, H., Clerici, E., Maulbetsch, C., Laux, T. and Davies, B. (2006). Analysis of the transcription factor WUSCHEL and its functional homologue in Antirrhinum reveals a potential mechanism for their roles in meristem maintenance. *The Plant Cell* **18**, 560-573.

Kim, B.-H., Cai, X., Vaughn, J. N. and von Arnim, A. G. (2007). On the functions of the h subunit of eukaryotic initiation factor 3 in late stages of translation initiation. *Genome Biol* **8**, R60.

Kim, T.-H., Kim, B.-H., Yahalom, A., Chamovitz, D. A. and von Arnim, A. G. (2004). Translational regulation via 5′ mRNA leader sequences revealed by mutational analysis of the Arabidopsis translation initiation factor subunit eIF3h. *The Plant Cell* **16**, 3341-3356.

Kolodziejek, I., Misas-Villamil, J. C., Kaschani, F., Clerc, J., Gu, C., Krahn, D., Niessen, S., Verdoes, M., Willems, L. I. and Overkleeft, H. S. (2011). Proteasome activity imaging and profiling characterizes bacterial effector syringolin A. *Plant Physiology* **155**, 477-489.

Koncz, C. and Schell, J. (1986). The promoter of TL-DNA gene 5 controls the tissue-specific expression of chimaeric genes carried by a novel type of Agrobacterium binary vector. *Molecular and General Genetics* **204**, 383-396.

Krishna, S. S., Majumdar, I. and Grishin, N. V. (2003). Structural classification of zinc fingers SURVEY AND SUMMARY. *Nucleic acids research* **31**, 532-550.

Leyser, H. O. and Furner, I. (1992). Characterisation of three shoot apical meristem mutants of Arabidopsis thaliana. *Development* **116**, 397-403.

Lin, J.-r. and Hu, J. (2013). SeqNLS: nuclear localization signal prediction based on frequent pattern mining and linear motif scoring. PLoS one **10,** e76864

Makkena, S. and Lamb, R. S. (2013). The bHLH transcription factor SPATULA regulates root growth by controlling the size of the root meristem. *BMC Plant Biology* **13.1**, 1

Mansfield, S. and Briarty, L. (1991). Early embryogenesis in Arabidopsis thaliana. II. The developing embryo. *Canadian Journal of Botany* **69**, 461-476.

Massa, G. D. and Gilroy, S. (2003). Touch modulates gravity sensing to regulate the growth of primary roots of Arabidopsis thaliana. *The Plant Journal* **33**, 435-445.

Mayer, K. F., Schoof, H., Haecker, A., Lenhard, M., Jürgens, G. and Laux, T. (1998). Role of WUSCHEL in regulating stem cell fate in the Arabidopsis shoot meristem. *Cell* **95**, 805-815.

Mendes, M. A., Guerra, R. F., Berns, M. C., Manzo, C., Masiero, S., Finzi, L., Kater, M. M. and Colombo, L. (2013). MADS domain transcription factors mediate short-range DNA looping that is essential for target gene expression in Arabidopsis. *The Plant Cell* **25**, 2560-2572.

Meyer, M. R., Shah, S., Zhang, J., Rohrs, H. and Rao, A. G. (2015). Evidence for Intermolecular Interactions between the Intracellular Domains of the Arabidopsis Receptor-Like Kinase ACR4, Its Homologs and the Wox5 Transcription Factor. *PloS one* **10.3**, e0118861

Möller, B. and Weijers, D. (2009). Auxin control of embryo patterning. *Cold Spring Harbor Perspectives in Biology* **1**, a001545.

Müller, R., Borghi, L., Kwiatkowska, D., Laufs, P. and Simon, R. (2006). Dynamic and compensatory responses of Arabidopsis shoot and floral meristems to CLV3 signaling. *The Plant Cell* **18**, 1188-1198.

Nagata, T. and Takebe, I. (1971). Plating of isolated tobacco mesophyll protoplasts on agar medium. *Planta* **99**, 12-20.

Nägeli, C., Schwendener, S. and Leitgeb, H. (1858). *Beiträge zur wissenschaftlichen Botanik: Das Wachsthum des Stammes und der Wurzel bei den Gefässpflanzen und die Anordnung der Gefässstränge im Stengel*.

Nikonorova, N., Vu, L. D., Czyzewicz, N., Gevaert, K. and De Smet, I. (2015). A phylogenetic approach to study the origin and evolution of the CRINKLY4 family. *Frontiers in Plant Science* **6**, 880

Ohyama, K., Shinohara, H., Ogawa-Ohnishi, M. and Matsubayashi, Y. (2009). A glycopeptide regulating stem cell fate in Arabidopsis thaliana. *Nature Chemical Biology* **5**, 578-580.

Patharkar, O. R. and Walker, J. C. (2015). Floral organ abscission is regulated by a positive feedback loop. *Proceedings of the National Academy of Sciences* **112**, 2906-2911.

Petersson, S. V., Johansson, A. I., Kowalczyk, M., Makoveychuk, A., Wang, J. Y., Moritz, T., Grebe, M., Benfey, P. N., Sandberg, G. and Ljung, K. (2009). An auxin gradient and maximum in the Arabidopsis root apex shown by high-resolution cell-specific analysis of IAA distribution and synthesis. *The Plant Cell* **21**, 1659-1668.

Pi, L., Aichinger, E., van der Graaff, E., Llavata-Peris, C. I., Weijers, D., Hennig, L., Groot, E. and Laux, T. (2015). Organizer-Derived WOX5 Signal Maintains Root Columella Stem Cells through Chromatin-Mediated Repression of CDF4 Expression. *Developmental Cell* **33.5**, 576-588.

Pu, C. X., Ma, Y., Wang, J., Zhang, Y. C., Jiao, X. W., Hu, Y. H., Wang, L. L., Zhu, Z. G., Sun, D. and Sun, Y. (2012). Crinkly4 receptor-like kinase is required to maintain the interlocking of the palea and lemma, and fertility in rice, by promoting epidermal cell differentiation. *The Plant Journal* **70**, 940-953.

Rahmani, F., Hummel, M., Schuurmans, J., Wiese-Klinkenberg, A., Smeekens, S. and Hanson, J. (2009). Sucrose control of translation mediated by an upstream open reading frame-encoded peptide. *Plant Physiology* **150**, 1356-1367.

Raven, J. and Edwards, D. (2001). Roots: evolutionary origins and biogeochemical significance. *Journal of Experimental Botany* **52**, 381-401.

Raven, P. H., Evert, R. F. and Eichhorn, S. E. (2000). *Biologie der Pflanzen*. ISBN: 978 3110154627.

Reddy, G. V. and Meyerowitz, E. M. (2005). Stem-cell homeostasis and growth dynamics can be uncoupled in the Arabidopsis shoot apex. *Science* **310**, 663-667.

Renzaglia, K. S., Duff, R. J., Nickrent, D. L. and Garbary, D. J. (2000). Vegetative and reproductive innovations of early land plants: implications for a unified phylogeny. *Philosophical Transactions of the Royal Society B: Biological Sciences* **355**, 769-793.

Richards, S., Wink, R. H. and Simon, R. (2015). Mathematical modelling of WOX5-and CLE40-mediated columella stem cell homeostasis in Arabidopsis. *Journal of Experimental Botany* **66.1**, 5375.

Roeder, A. H., Chickarmane, V., Cunha, A., Obara, B., Manjunath, B. and Meyerowitz, E. M. (2010). Variability in the control of cell division underlies sepal epidermal patterning in Arabidopsis thaliana. *PLoS Biol* **8**, e1000367.

Roeder, A. H., Cunha, A., Ohno, C. K. and Meyerowitz, E. M. (2012). Cell cycle regulates cell type in the Arabidopsis sepal. *Development* **139**, 4416-4427.

Roy, B., Vaughn, J. N., Kim, B.-H., Zhou, F., Gilchrist, M. A. and Von Arnim, A. G. (2010). The h subunit of eIF3 promotes reinitiation competence during translation of mRNAs harboring upstream open reading frames. *RNA* **16**, 748-761.

Rushton, P. J., Torres, J. T., Parniske, M., Wernert, P., Hahlbrock, K. and Somssich, I. (1996). Interaction of elicitor-induced DNA-binding proteins with elicitor response elements in the promoters of parsley PR1 genes. *The EMBO Journal* **15**, 5690.

Sabatini, S., Heidstra, R., Wildwater, M. and Scheres, B. (2003). SCARECROW is involved in positioning the stem cell niche in the Arabidopsis root meristem. *Genes & Development* **17**, 354-358.

Sambrook, J., Fritsch, E. F. and Maniatis, T. (1989). *Molecular cloning*. ISBN: 1936113422

San-Bento, R., Farcot, E., Galletti, R., Creff, A. and Ingram, G. (2014). Epidermal identity is maintained by cell-cell communication via a universally active feedback loop in Arabidopsis thaliana. *Plant J* **77**, 46-58.

Sarkar, A. K., Luijten, M., Miyashima, S., Lenhard, M., Hashimoto, T., Nakajima, K., Scheres, B., Heidstra, R. and Laux, T. (2007). Conserved factors regulate signalling in Arabidopsis thaliana shoot and root stem cell organizers. *Nature* **446**, 811-814.

Satina, S., Blakeslee, A. and Avery, A. G. (1940). Demonstration of the three germ layers in the shoot apex of Datura by means of induced polyploidy in periclinal chimeras. *American Journal of Botany*, 895-905.

Satoh, R., Fujita, Y., Nakashima, K., Shinozaki, K. and Yamaguchi-Shinozaki, K. (2004). A novel subgroup of bZIP proteins functions as transcriptional activators in hypoosmolarity-responsive expression of the ProDH gene in Arabidopsis. *Plant and Cell Physiology* **45**, 309-317.

Schmidt, A. (1924). Histologische Studien an phanerogamen Vegetationspunkten. *Bot. Archiv* **8**, 345-404.

Schofield, R. (1977). The relationship between the spleen colony-forming cell and the haemopoietic stem cell. *Blood cells* **4**, 7-25.

Sharma, V. K., Ramirez, J. and Fletcher, J. C. (2003). The Arabidopsis CLV3-like (CLE) genes are expressed in diverse tissues and encode secreted proteins. *Plant Molecular Biology* **51**, 415-425.

Stahl, Y., Grabowski, S., Bleckmann, A., Kuhnemuth, R., Weidtkamp-Peters, S., Pinto, K. G., Kirschner, G. K., Schmid, J. B., Wink, R. H., Hulsewede, A., et al. (2013). Moderation of Arabidopsis root stemness by CLAVATA1 and ARABIDOPSIS CRINKLY4 receptor kinase complexes. *Current Biology* **23**, 362-371.

Stahl, Y. and Simon, R. (2005). Plant stem cell niches. *International Journal of Developmental Biology* **49**, 479.

Stahl, Y. and Simon, R. (2009). Is the Arabidopsis root niche protected by sequestration of the CLE40 signal by its putative receptor ACR4? *Plant Signal Behav* **4**, 634-635.

Stahl, Y., Wink, R. H., Ingram, G. C. and Simon, R. (2009). A signaling module controlling the stem cell niche in Arabidopsis root meristems. *Current Biology* **19**, 909-914.

Stenvik, G.-E., Tandstad, N. M., Guo, Y., Shi, C.-L., Kristiansen, W., Holmgren, A., Clark, S. E., Aalen, R. B. and Butenko, M. A. (2008). The EPIP peptide of INFLORESCENCE DEFICIENT IN ABSCISSION is sufficient to induce abscission in Arabidopsis through the receptor-like kinases HAESA and HAESA-LIKE2. *The Plant Cell* **20**, 1805-1817.

Steward, F., Mapes, M. O. and Mears, K. (1958). Growth and organized development of cultured cells. II. Organization in cultures grown from freely suspended cells. *American Journal of Botany*, 705-708.

Stokes, K. D. and Rao, A. G. (2008). Dimerization properties of the transmembrane domains of Arabidopsis CRINKLY4 receptor-like kinase and homologs. *Arch Biochem Biophys* **477**, 219-226.

Stokes, K. D. and Rao, A. G. (2010). The role of individual amino acids in the dimerization of CR4 and ACR4 transmembrane domains. *Arch Biochem Biophys* **502**, 104-111.

Stone, J. M., Trotochaud, A. E., Walker, J. C. and Clark, S. E. (1998). Control of meristem development by CLAVATA1 receptor kinase and kinase-associated protein phosphatase interactions. *Plant Physiology* **117**, 1217-1225.

Stothard, P. (2000). The sequence manipulation suite: JavaScript programs for analyzing and formatting protein and DNA sequences. *Biotechniques* **28.6**, 1102-1104.

Stuurman, J., Jäggi, F. and Kuhlemeier, C. (2002). Shoot meristem maintenance is controlled by a GRAS-gene mediated signal from differentiating cells. *Genes & Development* **16**, 2213-2218.

Suzaki, T., Ohneda, M., Toriba, T., Yoshida, A. and Hirano, H.-Y. (2009). FON2 SPARE1 redundantly regulates floral meristem maintenance with FLORAL ORGAN NUMBER2 in rice. *PLoS Genet* **5**, e1000693.

Takada, S. and Jürgens, G. (2007). Transcriptional regulation of epidermal cell fate in the Arabidopsis embryo. *Development* **134**, 1141-1150.

Tamura, K., Shimada, T., Ono, E., Tanaka, Y., Nagatani, A., Higashi, S. i., Watanabe, M., Nishimura, M. and Hara-Nishimura, I. (2003). Why green fluorescent fusion proteins have not been observed in the vacuoles of higher plants. *The Plant Journal* **35**, 545-555.

Tanaka, H., Watanabe, M., Watanabe, D., Tanaka, T., Machida, C. and Machida, Y. (2002). ACR4, a putative receptor kinase gene of Arabidopsis thaliana, that is expressed in the outer cell layers of embryos and plants, is involved in proper embryogenesis. *Plant Cell Physiol* **43**, 419-428.

Tuskan, G. A., Difazio, S., Jansson, S., Bohlmann, J., Grigoriev, I., Hellsten, U., Putnam, N., Ralph, S., Rombauts, S. and Salamov, A. (2006). The genome of black cottonwood, Populus trichocarpa (Torr. & Gray). *Science* **313**, 1596-1604.

Ulmasov, T., Hagen, G. and Guilfoyle, T. J. (1997a). ARF1, a transcription factor that binds to auxin response elements. *Science* **276**, 1865-1868.

Ulmasov, T., Liu, Z.-B., Hagen, G. and Guilfoyle, T. J. (1995). Composite structure of auxin response elements. *The Plant Cell* **7**, 1611-1623.

Ulmasov, T., Murfett, J., Hagen, G. and Guilfoyle, T. J. (1997b). Aux/IAA proteins repress expression of reporter genes containing natural and highly active synthetic auxin response elements. *The Plant Cell* **9**, 1963-1971.

Van den Berg, C., Willemsen, V., Hage, W., Weisbeek, P. and Scheres, B. (1995). Cell fate in the Arabidopsis root meristem determined by directional signalling. *Nature* **378**, 62-65

Van den Berg, C., Willemsen, V., Hendriks, G., Weisbeek, P. and Scheres, B. (1997). Short-range control of cell differentiation in the Arabidopsis root meristem. *Nature* **390**, 287-289.

Watanabe, M., Tanaka, H., Watanabe, D., Machida, C. and Machida, Y. (2004). The ACR4 receptor-like kinase is required for surface formation of epidermis-related tissues in Arabidopsis thaliana. *Plant J* **39**, 298-308.

Wehner, N., Hartmann, L., Ehlert, A., Böttner, S., Oñate-Sánchez, L. and Dröge-Laser, W. (2011). High-throughput protoplast transactivation (PTA) system for the analysis of Arabidopsis transcription factor function. *The Plant Journal* **68**, 560-569.

Weijers, D., Benkova, E., Jäger, K. E., Schlereth, A., Hamann, T., Kientz, M., Wilmoth, J. C., Reed, J. W. and Jürgens, G. (2005). Developmental specificity of auxin response by pairs of ARF and Aux/IAA transcriptional regulators. *The EMBO journal* **24**, 1874-1885.

Wiese, A., Elzinga, N., Wobbes, B. and Smeekens, S. (2004). A conserved upstream open reading frame mediates sucrose-induced repression of translation. *The Plant Cell* **16**, 1717-1729.

Willemsen, V., Bauch, M., Bennett, T., Campilho, A., Wolkenfelt, H., Xu, J., Haseloff, J. and Scheres, B. (2008). The NAC domain transcription factors FEZ and SOMBRERO control the orientation of cell division plane in Arabidopsis root stem cells. *Developmental Cell* **15**, 913-922.

Wink, R. (2013). On the function of peptide signaling pathways in the root meristem of Arabidopsis thaliana. Doctoral thesis. Heinrich-Heine-Universität.

Yadav, S. R. and Helariutta, Y. (2014). Programmed cell death: new role in trimming the root tips. *Current Biology* **24**, R374-R376.

Yoshida, S., de Reuille, P. B., Lane, B., Bassel, G. W., Prusinkiewicz, P., Smith, R. S. and Weijers, D. (2014). Genetic control of plant development by overriding a geometric division rule. *Developmental cell* **29**, 75-87.

Zhang, Y., Jiao, Y., Liu, Z. and Zhu, Y.-X. (2015). ROW1 maintains quiescent centre identity by confining WOX5 expression to specific cells. *Nature Communications* **6**, 1–8.

Zhao, P., Zhou, X., Zhang, L., Wang, W., Ma, L., Yang, L., Peng, X., Bozhkov, P. V. and Sun, M. (2013). A bipartite molecular module controls cell death activation in the basal cell lineage of plant embryos. *PLoS Biology* **11.9**, e1001655.

Zhu, B., Zhang, W., Zhang, T., Liu, B. and Jiang, J. (2015). Genome-Wide Prediction and Validation of Intergenic Enhancers in Arabidopsis Using Open Chromatin Signatures. *The Plant Cell* **27**, 2415-2426.

Zuo, J., Niu, Q. W. and Chua, N. H. (2000). An estrogen receptor-based transactivator XVE mediates highly inducible gene expression in transgenic plants. *The Plant Journal* **24**, 265-273.

10 Appendix

10.1 Abbreviations

A. thaliana	Arabidopsis thaliana
A. tumefaciens	Agrobacterium tumefaciens
aa	amino acid
ACR4	ARABIDOPSIS CRINKLY4
AGRIS	Arabidopsis Gene Regulatory Information Server
ARE	AUXIN RESPONSE ELEMENT
ARF	AUXIN RESPONSE FACTOR
ARF10	AUXIN RESPONSE FACTOR 10
ARF16	AUXIN RESPONSE FACTOR 16
ARF5	AUXIN RESPONSE FACTOR 5
At	Arabidopsis thaliana
AtcisBD	Arabidopsis cis-regulatory element database
AtML1	ARABIDOPSIS THALIANA MERISTEM LAYER1
AtSupP	Arabidopsis Subcellular Localization Prediction Server
AUX/IAA	AUXIN/INDOLE-3-ACETIC ACID-protein
BAK1	BRI1 ASSOCIATED RECEPTOR KINASE1
BARD1	BRCA1-ASSOCIATED RING DOMAIN 1
BDL	BODENLOS
bHLH	Basic helix-loop-helix
BLAST	basic local alignment search tool
bp	base pair
BTA	BINDING TO PROMOTER OF ACR4
bZIP	Basic Leucine Zipper
CaMV	cauliflower mosaic virus
CC(s)	columella cell(s)
CCD	charge-coupled device
CDF4	CYCLIN DOF FACTOR 4
cDNA	complementary DNA
CDS	coding sequence
CLE	CLAVATA3/EMBRYO-SURROUNDING REGION-related
CLE40	CLAVATA3/EMBRYO-SURROUNDING REGION-related 40
CLSM	confocal laser scanning microscope
CLV	CLAVATA
CLV1	CLAVATA1
CLV2	CLAVATA2
CLV3	CLAVATA 3
cm	centimeter
Col-0	Columbia-0 (ecotype of Arabidopsis thaliana)

CR4	CRINKLY4
CR4	CRINKLY4
CRN	CORYNE
CRN	CORYNE
CRR	CR4-RELATED PROTEIN
CRR1	CRINKLY4 RELATED 1
CRR2	CRINKLY4 RELATED 2
CRR3	CRINKLY4 RELATED 3
CRR4	CRINKLY4 RELATED 4
CSC(s)	columella stem cell(s)
CYCD3;3	CYCLIN D3;3
dag	days after germination
DEX	dexamethasone
DNA	deoxyribonucleic acid
DRM	distal root meristem
DUF702	domain of unknown function 702
DYT	double yeast tryptone
DZ	differentiation zone
E.coli	Escherichia coli
e.g.	exempli gratia
eIF3	translation initiation factor 3
g	gram
gDNA	genomic DNA
GFP	green fluorescent protein
GM	Growth Media
GR	glucocorticoid receptor
GUS	β-glucuronidase
H2B	Histone 2 B
H3K4me4	histone H3 lysine 4 tri-methylation
HAE	HAESA
HSL2	HAESA-LIKE2
Hyp	Proline hydroxylation
i.e.	id est
IDA	INFLORESCENCE DEFICIENT IN ABSCISSION
ind	inducible
kb	kilobase pairs
l	litre
L1	Layer-1
L2	Layer-2
L3	Layer-3
LB	Lysogeny Broth
Ler	Landsberg erecta
LRC	lateral root cap

LRP1	LATERAL ROOT PROMODRIUM 1
LRR	leucine-rich repeats
M	molar
MADS	MCM1, AGAMOUS, DEFICIENS, SRF
MEME	Multiple Em for Motif Elicitation
MES	2-(N-morpholino)ethanesulfonic acid
min	minutes
mM	millimolar
mORF	main open reading frame
MP	MONOPTEROS
mRNA	messenger RNA
NAC	NO APICAL MERISTEM; ARABIDOPSIS TRANSCRIPTION ACTIVATION FACTOR 1/2; CUP-SHAPED COTYLEDON 2
NaCl	sodium chloride
N. benthamiana	*Nicotiana benthamiana*
NCBI	National Center for Biotechnology Information
NTT	NO TRANSMITTING TRACT
OC	organizing center
ORF	open reading frame
pAH	plasmid Adrian Hülsewede
PCR	polymerase chain reaction
PDF2	PROTODERMAL FACTOR2
Pfam	Protein Families Database
PIN	PIN-FORMED
PLT	PLETHORA
PLT 1	PLETHORA 1
PLT 2	PLETHORA 2
PRM	proximal root meristem
PTA	protoplast transactivation assay
QC	quiescent center
qRT-PCR	Real time quantitative reverse transcription PCR
RAM	root apical meristem
RLK	receptor-like kinase
RNA	ribonucleic acid
ROW1	REPRESSOR OF WUSCHEL 1
RPK2	RECEPTOR-LIKE PROTEIN KINASE 2
S	Svedberg
SAM	shoot apical meristem
SCR	SCARECROW
SEP3	SEPALLATA3
seqNLS	Sequential Pattern Mining Algorithm for Nuclear Localization Signals
SHI	SHORT INTERNODES
SHR	SHORTROOT

SMB	SOMBRERO
SPT	SPATULA
SRS3	SHI RELATED SEQUENCE 3
STK	SEEDSTICK
STY	STYLIS
TAIR	The Arabidopsis Information Resource
T-DNA	transfer-DNA
tdTomato	tandem-Tomato
TMO6	TARGET OF MONOPTEROS 6
TMO7	TARGET OF MONOPTEROS 7
TNFR	TUMOR NECROSIS FACTOR
TPL	TOPLESS
TPR	TOPLESS-RELATED
uORF	upstream open reading frame
UTR	untranslated region
VDD	VDDVERDANDI
WOX	WUSCHEL RELATED HOMEOBOX
WOX5	WUSCHEL-RELATED HOMEOBOX 5
WP4	WIP DOMAIN Protein 4
WP5	WIP DOMAIN Protein 5
wt	wild type
WUS	WUSCHEL
Y1H	yeast-one-hybrid
YFP	yellow fluorescent protein
ZFP3	ZINC FINGER PROTEIN 3
ZFP7	ZINC FINGER PROTEIN 7
(v/v)	volume per volume
(w/v)	weight per volume
Δ	delta
%	percent
°C	degree Celsius

10.2 Plasmid maps

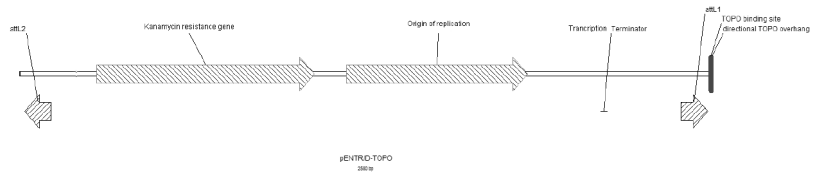

Figure 30 Plasmid map of pENTR/D-Topo
This linearized plasmid was used for cloning of entry vectors with the "pENTR™/SD/D-TOPO® Cloning Kit".

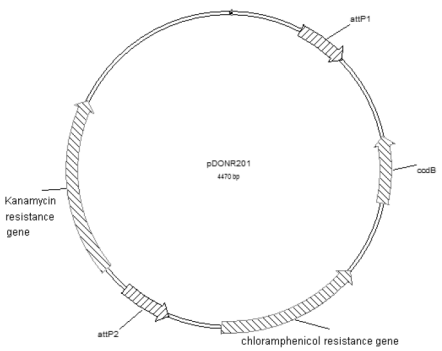

Figure 31 Plasmid map of *pDONR 201*

This plasmids was used for cloning of entry vectors in a gateway BP reaction. Between the two gateway attP sites (attP1 and attP2), the gene CONTROL OF CELL DEATH B (ccdB) and a gene conferring resistance to chloramphenicol is located.

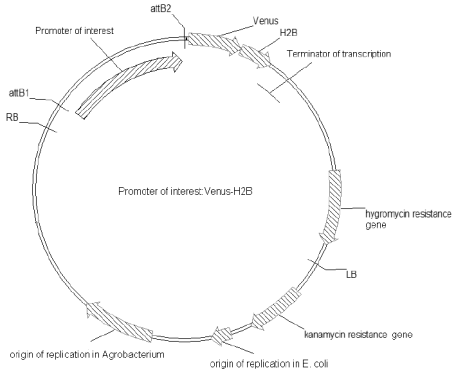

Figure 32 Plasmid map of expression vectors using *Venus-H2B* as a reporter
This type of expression vector was used for analysis of transcriptional expression. The promoter of interest (located between the two Gateway sites "attB1" and "attB2") is conferring expression to a *Venus-H2B* reporter. The T-DNA is located between the right border (RB) and the left border (LB). The plasmid contains two origins of replication: one for the replication in *E. coli* and one for the replication in *Agrobacterium*.

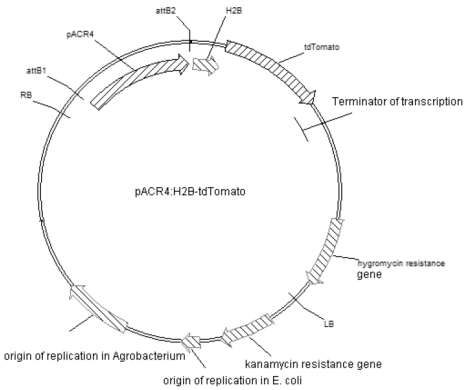

Figure 33 Plasmid map of *pACR4:H2B-tdTomato*
This expression vector was used to transform plants. The full length *ACR4* promoter (*pACR4*) is located between two Gateway sites (attB1 and attB2) and confers expression to *H2B-tdTomato*. The T-DNA is located between the right border (RB) and the left border (LB). The plasmid contains two origins of replication: one for the replication in *E. coli* and one for the replication in *Agrobacterium*.

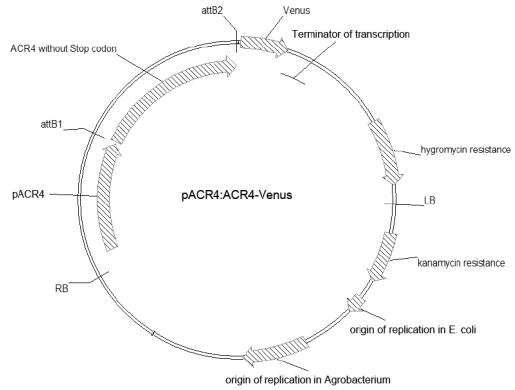

Figure 34 Plasmid map of *pACR4:ACR4-Venus*
This type of expression vector was used for analysis of ACR4 protein localization. The CDS of ACR4 is located between two Gateway sites (attB1 and attB2) and is in frame with a Venus reporter. Different versions of the *ACR4* promoter (*pACR4*) were cloned 5' to the *ACR4* gene. The T-DNA is located between the right border (RB) and the left border (LB). The plasmid contains two origins of replication: one for the replication in *E. coli* and one for the replication in *Agrobacterium*.

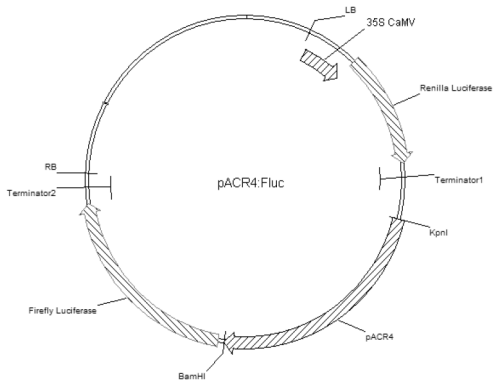

Figure 35 Plasmid map of *pACR4:Fluc*

This type of expression vectors were used for analysis of *pACR4* activity in luciferase assays in *N*. *benthamiana* epidermal cells. The vector backbone is *pGreen 0800 Luc* (Hellens et al., 2005). Different types of *ACR4* promoters were cloned 5' to the *firefly luciferase* gene with restriction endonucleases KpnI and BamHI.

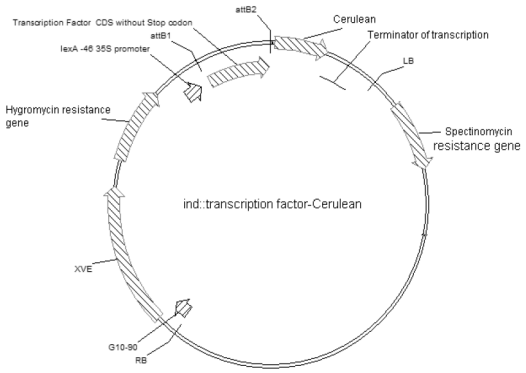

Figure 36 Plasmid map of inducible transcription factors used in the luciferase assay

This estradiol inducible expression vector was used to express transcription factors of choice in *N*. *benthamiana*. The CDS of the transcription factors were cloned by gateway LR recombination 3' to a minimal lexA -46 35S promoter.

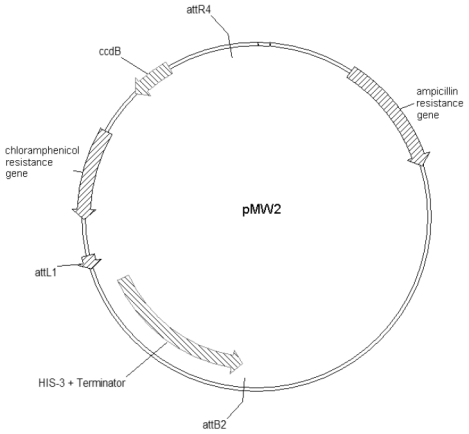

Figure 37 Plasmid map of *pMW2*

The destination vector *pMW2* was used for re-combinations with entry vectors containing the promoter of interest for the Y1H screen.

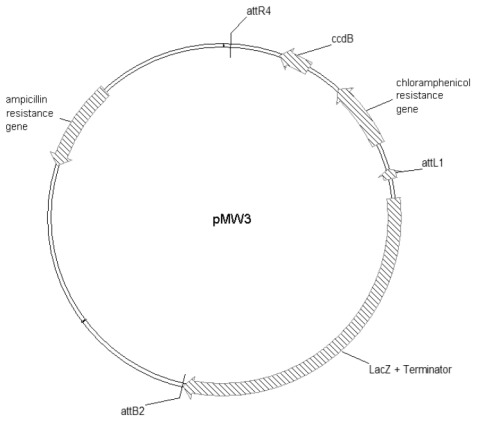

Figure 38 Plasmid map of *pMW3*

The destination vector *pMW3* was used for re-combinations with entry vectors containing the promoter of interest for the Y1H screen.

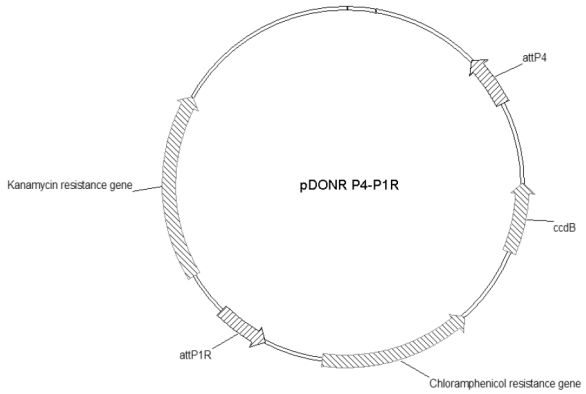

Figure 39 Plasmid map of *pDONR P4-P1R*

This donor vector was used to clone entry vectors used in LR re-combinations with *pMW2* and *pMW3*.

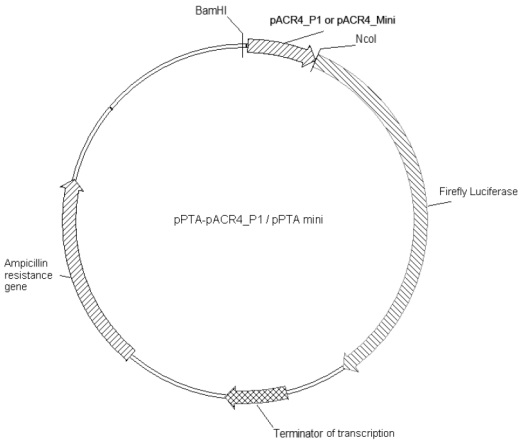

Figure 40 Plasmid map of expression vectors used in the PTA

For the PTA the full length *ACR4* promoter or a minimal *ACR4* promoter were cloned 5' to a firefly luciferase gene. The vector backbone is *pBT10*.

10.3 List of figures

10.4 List of supplementary figures

10.5 List of tables

11 Eidesstattliche Erklärung

Eidesstattliche Erklärung zur Dissertation mit dem Titel:

„**Functional characterization and analysis of the *ARABIDOPSIS CRINKLY 4* promoter in *Arabidopsis thaliana***"

Hiermit erkläre ich, dass ich diese Dissertation selbstständig verfasst und keine anderen als die angegebenen Hilfsmittel genutzt habe. Alle wörtlich oder inhaltlich übernommenen Stellen habe ich als solche gekennzeichnet.

Ich versichere außerdem, dass ich diese Dissertation nur in diesem und keinem anderen Promotionsverfahren eingereicht habe und, dass diesem Promotionsverfahren kein gescheitertes Promotionsverfahren vorausgegangen ist.

Ort, Datum Unterschrift

12 Acknowledgements

Ich möchte mich bei meinem Doktorvater Prof. Dr. Rüdiger Simon bedanken, welcher es mir ermöglich hat, in seinem Institut für Entwicklungsgenetik, an meiner Dissertation zu arbeiten. Vielen Dank für die gute Betreuung, die Unterstützung und Diskussionen welche wir geführt haben. In diesem Zusammenhang möchte ich mich auch bei Prof. Dr. Michael Feldbrügge bedanken, welcher zusammen mit meinem Doktorvater an der Entwicklung der Ideen dieser Arbeit mitgewirkt hat und sich bereit erklärt hat das Zweitgutachten für diese Dissertation zu übernehmen.

Ich hatte die Möglichkeit, finanziert durch ein Stipendium des i-GRAD plant, ein halbes Jahr in den USA zu arbeiten und zu leben. Deshalb möchte ich mich auch bei Dr. Sigrun Wegener-Feldbrügge, der ehemaligen Koordinatorin des iGRAD-plant und bei Prof. Dr. Eva Farre, bei der ich in den USA arbeiten durfte, bedanken.

Bei Barbara, Yvonne und Marc möchte ich mich für das Korrekturlesen dieser Arbeit bedanken. Insbesondere bei dir Marc, möchte ich mich für deine konstruktiven Anregungen bedanken, welche mir sehr geholfen haben. Ich wünsche dir und Madlen viel Erfolg und vor allem alles Gute bei eurem neuen Abenteuer in Australien.

Bei Cornelia, Carin und Silke möchte ich mich für all die Hilfe bei der täglichen Laborarbeit bedanken. Ich danke auch allen Weggefährten während meiner Zeit in der AG Simon, die ich hier nicht alle aufzählen möchte, da ich garantiert jemand vergessen werde.

Zum Schluss möchte ich noch meinen Eltern und meinem Lebensgefährten danken, dafür, dass ihr immer für mich da wahrt.